

=====  
Università degli Studi di Napoli Federico II  
Facoltà di Ingegneria  
=====



*Filomena Dato*

AN ITERATIVE MODEL FOR  
VULNERABILITY CURVES (PGA)  
GENERATION OF MASONRY BUILDINGS.

Tesi di Dottorato  
XXX ciclo

Il Coordinatore  
*Prof. Ing. Luciano Rosati*

Tutor  
*Prof. Arch. Giulio Zuccaro*

Co-Tutor  
*Arch. Francesco Cacace*  
*Ing. Daniela De Gregorio*

Dottorato di Ricerca in Ingegneria Strutturale, geotecnica  
e rischio sismico

*On the front cover:*

Vulnerability Curves of masonry buildings.

AN ITERATIVE MODEL FOR VULNERABILITY CURVES (PGA)  
GENERATION OF MASONRY BUILDINGS

---

Copyright © 2018 Università degli Studi di Napoli Federico II – P.le Tecchio 80, 80136  
Napoli, Italy – web: [www.unina.it](http://www.unina.it)

Proprietà letteraria, tutti i diritti riservati. La struttura ed il contenuto del presente volume non possono essere riprodotti, neppure parzialmente, salvo espressa autorizzazione. Non ne è altresì consentita la memorizzazione su qualsiasi supporto (magnetico, magnetico-ottico, ottico, cartaceo, etc.).

Benché l'autore abbia curato con la massima attenzione la preparazione del presente volume, Egli declina ogni responsabilità per possibili errori ed omissioni, nonché per eventuali danni dall'uso delle informazione ivi contenute.

Finito di stampare il 20/2/2018

*To Enzo and  
Giuseppe*



# TABLE OF CONTENTS

Table of contents .....	1
List of Figures.....	3
List of Tables .....	9
Introduction.....	11
Summary.....	15
1 Seismic vulnerability .....	17
1.1 Seismic risk assessment .....	17
1.2 Buildings seismic vulnerability.....	21
1.2.1 Seismic hazard measures .....	23
1.2.2 Vulnerability classes.....	24
1.2.3 “SAVE” methodology.....	25
1.2.4 The damage level.....	28
1.3 Seismic vulnerability assessment approaches.....	31
1.3.1 Observed vulnerability - Statistical approach.....	32
1.3.2 Calculated Vulnerability - Mechanical approach. ....	34
1.3.3 Hybrid Method.....	35
1.4 Seismic vulnerability assessment tools .....	36
1.4.1 Damage Probability Matrices (DPM).....	36
1.4.2 Vulnerability Index Method .....	40
1.4.3 Vulnerability Curves .....	42
2 The masonry structure .....	49
2.1 Introduction .....	49
2.2 Masonry structure.....	51
2.3 Mechanical models of masonry structure .....	54
2.4 The constitutive model.....	56
3 No-tension material (NTM) .....	59
3.1 The constitutive model of no-tension material.....	62
3.1.1 Simplified uniaxial models .....	62
3.1.2 Approach formulated by G. Del Piero (1989) .....	64
3.1.3 Approach formulated by A. Baratta et al. (1991, 2005)....	66
3.1.4 Approach formulated by D. Addessi et al. (2014) .....	69
4 Collapse mechanisms of masonry structures .....	73
4.1 Introduction .....	73
4.2 Theory of Masonry Structures.....	75

4.2.1	Elastic analysis .....	75
4.2.2	Limit analysis .....	75
4.3	Collapse mechanisms classification .....	77
4.4	Global collapse mechanisms .....	79
4.5	In-plane collapse mechanisms .....	81
4.5.1	Shear crack .....	83
4.5.2	Failure by slip .....	88
4.5.3	Buckling failure .....	91
4.6	Out-of-plane collapse mechanism .....	94
4.6.1	Simple overturning .....	97
4.6.2	Vertical bending .....	101
4.6.3	Horizontal bending .....	106
4.7	Analysis of the mechanisms of collapse: the case study of Fonte del Campo .....	112
4.7.1	Earthquake central Italy .....	112
4.7.2	Impact on the buildings .....	114
4.7.3	Analysis of Fonte del Campo .....	119
5	Research steps: the iterative model .....	133
5.1	Statistical analysis of existing masonry buildings .....	134
5.2	Iterative model generation .....	136
5.3	Seismic Vulnerability classification by “SAVE” method. ....	138
5.4	Collapse Mechanisms calculation. ....	141
5.5	Vulnerability curves assessment .....	144
6	Research results: the vulnerability curves .....	145
6.1	Damage vulnerability curves .....	150
6.2	Comparison with alternative strategies .....	152
7	Conclusions .....	161
8	References .....	163

## LIST OF FIGURES

Fig. 1 The seismic activity map recorded by INGV National Seismic Network in 2016 (Iside, <a href="http://iside.rm.ingv.it">http://iside.rm.ingv.it</a> ). .....	17
Fig. 2 The seismic hazard map made by INGV National Seismic Network in 2016 ( <a href="http://zonesismiche.mi.ingv.it/">http://zonesismiche.mi.ingv.it/</a> ). .....	19
Fig. 3 Classification of structures (buildings) into vulnerability classes according to EMS 98 (Grünthal, 1998). .....	25
Fig. 4 Save Methodology (Zuccaro et al. 2006). .....	27
Fig. 5 Difference between SPD <sub>v</sub> function of EMS'98 and SPDP modified by vulnerability parameters. ....	27
Fig. 6 Classification of damage to masonry buildings according to EMS 98 (Grünthal, 1998). ....	29
Fig. 7 Classification of damage to buildings of reinforced concrete according to EMS 98 (Grünthal, 1998). ....	30
Fig. 8 The vulnerability assessment method; the bold path shows a traditional assessment method. (Calvi, 2006). ....	32
Fig. 9 Vulnerability functions to relate damage factor ( $d$ ) and peak ground acceleration (PGA) for different values of vulnerability index ( $I_v$ ) (adapted from Guagenti and Petrini(1989)) .....	42
Fig. 10 Lognormal cumulative distribution function. ....	44
Fig. 11 Vulnerability curves produced by Spence et al. (1992).D1 to D5 relate to damage states in the MSK scale. ....	45
Fig. 12 Simulated (thick line) and observed (thin line) vulnerability functions for MSK intensity VII (Barbat et al., 1996). ....	47
Fig. 13 Components of unreinforced brick (left) and unreinforced concrete block (right) walls. FEMA P-774 (2009). ....	49
Fig. 14 Reinforced brick wall (FEMA 1994). ....	50
Fig. 15 Breakdown of fatalities attributed to earthquake by cause (Period 1900-1999) Navaratnarajah, Sathiparan (2015). ....	51
Fig. 16 General classification of rubble masonry: (a) coursed masonry, (b) un-coursed masonry, (c) dry masonry, (d) “composite” masonry. ....	53
Fig. 17 General classification of ashlar masonry: (e) Fine masonry, (f) Rought masonry, (g) Chamfered masonry. ....	54

Fig. 18 Modeling method for masonry structures: (a) masonry sample, (b) detail micro-mechanical model, (c) simplified micro-mechanical model, (d) macro-mechanical model (Laurenço et al., 1995). .....	55
Fig. 19 Qualitative stress-strain diagram in uniaxial tension and compression (Ricamato et al, 2007). .....	56
Fig. 20 Stress - strain masonry curve (Ricamato et al, 2007). .....	57
Fig. 21 NTM model: yield surface in $\sigma_x, \sigma_y, \tau_{xy}$ stress space (Zuccaro and Papa, 1996).....	61
Fig. 22: (a) model <i>zero</i> , (b) model <i>one</i> , (c) model <i>two</i> , (Angelillo, 2014)..	62
Fig. 23 No-tension plastic admissible stresses: normality rule of the fracture and crushing tensors. (D. Addessi, S. Marfia, E. Sacco and J. Toti , 2014) .....	72
Fig. 24 Typical earthquake damage of masonry structures due to different direction of shaking (Pitta, 2000). .....	74
Fig. 25 MEDEA: Global Collapse Mechanisms (masonry). (Zuccaro et al. 2010). .....	78
Fig. 26 MEDEA: Local Collapse Mechanisms (masonry) (Zuccaro et al. 2010). .....	79
Fig. 27 Out-of-plane (left) and in-plane (right) behaviour of a single wall. ....	79
Fig. 28 In-plane collapse mechanisms: failure modes in unreinforced masonry walls (a ) Shear crack, (b) Failure by slip, (c) Buckling failure..	81
Fig. 29 Macro-Element model of the masonry structure. ....	82
Fig. 30 Diagonal shear cracks due to earthquake Central Italy- Amatrice 2016.....	84
Fig. 31 Diagonal shear cracks due to earthquake Central Italy- Arquata del Tronto 2016.....	84
Fig. 32 Diagonal shear cracks due to earthquake Central Italy- Illica (Accumuoli) 2016.....	85
Fig. 33 Shear crack mechanism.....	86
Fig. 34 Mohr's circle for shear crack stress. ....	87
Fig. 35 Failure by slip due to earthquake Central Italy- Pescara del Tronto 2016.....	89
Fig. 36 Failure by slip due to earthquake Central Italy- Illica (Accumuli) 2016.....	90
Fig. 37 Failure by slip .....	90
Fig. 38 Buckling failure of a masonry wall.....	91



Fig. 39 Buckling failure due to earthquake Central Italy- Accumuli, 2016 .....	92
Fig. 40 Buckling ultimate limit state .....	92
Fig. 41 Out-of-plane failure mechanisms of the FaMIVE method (D'Ayala and Speranza 2003) .....	95
Fig. 42 Simple overturning due to earthquake Central Italy, Accumuli, 2016 .....	98
Fig. 43 Vertical crack patterns between the wall and the orthogonal lateral walls, Illica, 2016 .....	98
Fig. 44 Simple overturning due to earthquake Central Italy, Amatrice, 2016 .....	99
Fig. 45 Simple overturning failure, vertical section of the wall .....	101
Fig. 46 Vertical bending of masonry wall due to earthquake Central Italy, Fonte del Campo, 2016 .....	102
Fig. 47 Vertical bending of masonry wall due to earthquake Central Italy, Illica, 2016 .....	102
Fig. 48 Vertical bending failure, vertical section of the wall .....	103
Fig. 49 Horizontal bending of a masonry wall (Borri, 2004) .....	107
Fig. 50 Horizontal bending due to earthquake Central Italy, Pescara del Tronto, 2016 .....	108
Fig. 51 Horizontal bending, horizontal section of the wall. ....	111
Fig. 52 Shake Map on 24 August in the Rieti, Ascoli and Perugia provinces. Source: INGV .....	112
Fig. 53 The seismic sequence started on 24th August in the Rieti, Ascoli and Perugia provinces (updated 16 September 2016). Source: INGV ..	113
Fig. 54 Towns analysed by visual surveys on October 2016. ....	114
Fig. 55 Coursed rubble masonry, Illica October 2016. ....	115
Fig. 56 Un-coursed rubble masonry, Fonte del Campo October 2016 ..	115
Fig. 57 Out-of-plane collapse mechanisms, Accumoli October 2016. .	116
Fig. 58 In-plane collapse mechanisms, Illica October 2016. ....	116
Fig. 59 Masonry building with RC roof, Accumoli October 2017. ....	117
Fig. 60 Masonry building renovated with mortar injection (on the left) and old collapsed masonry building (on the right), Saletta, October 2017..	118
Fig. 61 Old masonry building with steel ties, Accumoli October 2017..	118
Fig. 62 Planimetry of Fonte del Campo. ....	119
Fig. 63 Classification of Fonte del Campo buildings. ....	120
Fig. 64 AeDes form: sections 3 and 4 .....	121
Fig. 65 MEDEA survey form. ....	122

Fig. 66 Analysis of the Vulnerability class of the buildings of Fonte del Campo. ....	126
Fig. 67 Distribution of the Vulnerability classes of the buildings of Fonte del Campo. ....	127
Fig. 68 Levels of damage distribution on Fonte del Campo map. ....	128
Fig. 69 Damage state probability (D0, D1, D2, D3, D4, D5) observed on the vulnerability class of buildings of Fonte del Campo. ....	129
Fig. 70 Damage state probability observed for each mechanisms of collapse on the vulnerability classes of buildings of Fonte del Campo. ....	130
Fig. 71 Damage state probability observed for in-plane and out of plane mechanisms of collapse on the vulnerability classes of buildings of Fonte del Campo. ....	130
Fig. 72 Before and after the 24th August 2016 earthquake. Damage level 4 on vulnerability class A building in Fonte del Campo. ....	131
Fig. 73 Before and after the 24th August 2016 earthquake. Damage level 3 on vulnerability class B building in Fonte del Campo. ....	132
Fig. 74 Research methodology, Zuccaro at al. (2012). ....	133
Fig. 75 Earthquakes investigated in the Plinivs Study Centre Database. ....	135
Fig. 76 Lognormal distribution curves for buildings vulnerability class A as functions of trigger acceleration of each Collapse Mechanism (PGA) vs the Damage State probability ....	147
Fig. 77 Lognormal distribution curves for buildings vulnerability class B as functions of trigger acceleration of each Collapse Mechanism (PGA) vs the Damage State probability ....	148
Fig. 78 Lognormal distribution curves for buildings vulnerability class C as functions of trigger acceleration of each Collapse Mechanism (PGA) vs the Damage State probability ....	148
Fig. 79 Lognormal distribution curves for buildings vulnerability class D as functions of trigger acceleration of each Collapse Mechanism (PGA) vs the Damage State probability ....	149
Fig. 80 Mechanism type activating probability for each vulnerability class (A, B, C, D) ....	150
Fig. 81 Damage Vulnerability Curves for each vulnerability Class (A, B, C, D). ....	151
Fig. 82 Damage Vulnerability Curves for each vulnerability Class (A, B, C, D). ....	152

Fig. 83 Comparison between damage Vulnerability Curves of vulnerability Class B and the one obtained by Cattari et al (2014) .....	153
Fig. 84 Comparison between damage Vulnerability Curves of vulnerability Class B and the one obtained by Cattari et al, 2014. ....	153
Fig. 85 Comparison between the In-plane mechanisms vulnerability curves and vulnerability curves derived from DPM [Zuccaro and De Gregorio, 2015] for vulnerability class A.....	155
Fig. 86 Comparison between the out of plane mechanisms vulnerability curves and vulnerability curves derived from DPM [Zuccaro and De Gregorio, 2015] for vulnerability class A.....	155
Fig. 87 Comparison between the In-plane mechanisms vulnerability curves and vulnerability curves derived from DPM [Zuccaro and De Gregorio, 2015] for vulnerability class B.....	156
Fig. 88 Comparison between the out of plane mechanisms vulnerability curves and vulnerability curves derived from DPM [Zuccaro and De Gregorio, 2015] for vulnerability class B.....	156
Fig. 89 Comparison between the In-plane mechanisms vulnerability curves and vulnerability curves derived from DPM [Zuccaro and De Gregorio, 2015] for vulnerability class C.....	157
Fig. 90 Comparison between the out of plane mechanisms vulnerability curves and vulnerability curves derived from DPM [Zuccaro and De Gregorio, 2015] for vulnerability class C.....	158
Fig. 91 Comparison between the In-plane mechanisms vulnerability curves and vulnerability curves derived from DPM [Zuccaro and De Gregorio, 2015] for vulnerability class D.....	158
Fig. 92 Comparison between the out of plane mechanisms vulnerability curves and vulnerability curves derived from DPM [Zuccaro and De Gregorio, 2015] for vulnerability class D.....	159



## LIST OF TABLES

Table 1 SPD range assigned for each vulnerability class of the buildings. ....	26
Table 2 Classification of damage according to the European Macroseismic Scale, EMS. ....	31
Table 3 Format of the Damage Probability Matrix Proposed by Whitman et al. (1973).....	37
Table 4 Damage Probability Matrix, class A (Braga et al., 1982, 1985)..	37
Table 5 Damage Probability Matrix, class B (Braga et al., 1982, 1985)...	38
Table 6 Damage Probability Matrix, class C (Braga et al., 1982, 1985)...	38
Table 7 DPM obtained through a statistical analysis of the data collected about the observed damages due to earthquakes occurred in Italy since 1980 (Zuccaro et al. , 2015). ....	39
Table 8 Typology of masonry components .....	51
Table 9 A sample of the information collected by AeDES and MEDEA forms.....	123
Table 10 Typological characteristics identified on buildings of Fonte del Campo. ....	124
Table 11 A sample of the Seismic Vulnerability classification of the buildings of Fonte del Campo.....	125
Table 12 Probability of combination between the typology of vertical structure of the buildings and other features (typology of horizontal structure, number of floors and percentage of openings). ....	135
Table 13 Main typological characteristics identified on existing masonry buildings and assigned to the virtual buildings by a random procedure. ....	136
Table 14 Dataset of virtual buildings generated by a random procedure. (Sample of the first 13 occurrences of the computed dataset).....	137
Table 15 Seismic vulnerability classification of the virtual buildings (Sample of the first 13 occurrences of the computed dataset).....	139
Table 16 Percentage of the virtual buildings, classified in vulnerability class buildings, calculated for each structural characteristics. ....	140
Table 17 Main typological characteristics identified on the virtual buildings classified in vulnerability classes. ....	141

Table 18 Value of the trigger acceleration ( $a_g$ ) corresponding to the considered collapse mechanisms (sample of the first 8 occurrences of the computed dataset)..... 143

Table 19 Data computed in order to plot the normal distribution curves (arithmetic mean and standard deviation) and the lognormal distribution curves (logarithmic arithmetic mean and logarithmic standard deviation). ..... 145

## INTRODUCTION

In the last ten years, a large number of losses have been caused by earthquakes occurred in Italy (Abruzzo 2009, Emilia Romagna 2012, central Italy earthquake 2016). The collapse of masonry buildings is the primary cause for loss of life during an earthquake (Coburn & Spence, 2002), thus the strong interest to assess the seismic vulnerability of existing buildings to prepare seismic risk mitigation plans.

A good semantic definition of vulnerability is given by Sandi [1986]: “the seismic vulnerability of a building is its behaviour described by a cause-effect law, where the cause is the earthquake and the effect is the damage”, however beside this a quantitative definition within the framework of the decision theory can be given: Vulnerability is the probability that an element at risk of a given typological class (i.e. A, B, C, ..... ) can accuse a level of damage (i.e. D1, D2, D3,.....) consequent to the action of a given level of hazard intensity (i.e. V, VI, VII,.....).

In order to perform vulnerability assessments of masonry buildings, several approaches, each one related to a different level of approximation, are available in the literature (Calvi et al., 2006). For the reader's convenience, such strategies can be grouped in two categories:

- Observed vulnerability /Statistical approach.

The vulnerability is derived from the synthetic analysis of the formal and structural characteristics of the building.

A restricted number of building categories, called "vulnerability classes", are identified as a function of the typological and structural characteristics. Each class is then associated to an expected behaviour under seismic action, this behaviour is described by a vulnerability function that generally is calibrated by analyzing the damage observed during past events.

Applications of this method, using the Damage Probability Matrices (DPM), were originally proposed by Whitman et al. (1973), who analyzed the damages observed in more than 1600 buildings after the 1971 San Fernando earthquake, by Braga et al (1982,1986) after the 1980 south-Italia earthquake and by Zuccaro et al (2000), Bernardini et al (2007a, 2007b).

The validity of this approach is reliable on a large number of buildings having characteristics to be included in specific vulnerability classes, obviously it is not reliable for single buildings. On the other hand it has the undeniable advantage of demanding both little information and rapid processing. Furthermore, it is derived from observations of the actual performance of assets in real earthquakes. For this reason it is useful for investigating a wide range of buildings (urban scale or wider). The research in this context aims to achieve a greater reliability of results while maintaining an acceptable agility of the investigation.

- Calculated Vulnerability/ Mechanical approach.

The vulnerability evaluation is the result of accurate computations using simplified limit state analysis on predefined categories of Structural Mechanics.

The damage evaluation is formulated on the basis of analytical calculations to determine the seismic response of the building, the stress and corresponding strain state are derived.

In this way, the problem of seismic vulnerability of masonry structures is developed in structural engineering terms. Vulnerability is computed as a direct function of construction characteristics, structural response to seismic actions and damage effects. Applications of this method can be seen in the work of Giuffrè (1991), Singhal and Kiremidjian (1996), Park and Ang (1985), Masi (2003), Rossetto and Elnashai (2005), Dumova-Jovanoska (2004), D'Ayala et al. (2015).

This approach provides assessments certainly more reliable on single buildings, but it requires detailed knowledge of technical features of the buildings and the development of time consuming structural calculations. Therefore it is difficult to implement at large scale.

Despite its robustness, the mechanical approach requires a detailed knowledge of structural features of the analyzed buildings and high computational efforts in computing the structural responses and, for these reasons, it is hardly implemented at a large scale.

In order to overcome the drawbacks of both these strategies, hybrid methodologies, aiming at combining the results of a simplified mechanical model with the vulnerability evaluations of a statistical approach, have been recently proposed. Their main philosophy consists in enriching a limited dataset, which is statistically analyzed, by the computation of



simulated mechanical data or, alternatively, to introduce probabilistic corrections, derived by observed dataset, in a mechanical model, see, e.g., Cavalieri et al. (2017).

Following a hybrid approach, the procedure presented in this dissertation aims to develop collapse probability distribution for a set of building classes suitable for the Italian structural typologies. In particular, the statistical data derived by the survey of about 250,000 buildings is adopted to randomly generate a virtual set of mechanical models where each instance is characterized by mechanical properties relevant to a typological class according to the vulnerability assessment method proposed by Zuccaro et al. (2012). The structural models are analyzed by means of simplified limit state analysis procedures in order to evaluate their seismic response and to compute the vulnerability probability curves, expressed in terms of seismic acceleration for each typological class.

In particular, the adopted hybrid methodology, aiming to determine the vulnerability curves as functions of the structural typology and of the seismic acceleration, can be described in the following steps both statistical and mechanical nature:

- i. *Statistical analysis of existing masonry buildings.* The analysis, pursued thanks to the PLINIVS Study Centre<sup>1</sup> Database, is based on the survey performed all along the Italian peninsula. About 250,000 of the residential masonry buildings (ISTAT Census 2011) have been surveyed distributed on about 600 municipalities. This analysis has allowed to investigate the geometrical and structural characteristics of Italian masonry buildings and identify the recurring combinations of these characteristics. The probability of combination between a particular characteristic (e.g. type of vertical structure) and other features (e.g. type of horizontal structure, presence of ties, etc.) have been then evaluated.
- ii. *Iterative model generation.* An iterative procedure has been implemented by an ad-hoc software developed in order to generate virtual model of buildings (about 100,000). The program adopts a random assignment procedure of the structural

---

<sup>1</sup> PLINIVS Study Centre for Hydrogeological, Volcanic and Seismic Engineering. University of Naples, Italy. Centre of competence of Italian Civil Protection. [www.plinivs.it](http://www.plinivs.it)

- characteristics whose probability distributions are known from previous step.
- iii. *Seismic Vulnerability classification by "SAVE" method<sup>2</sup>*. The generated virtual buildings have been classified in vulnerability classes (A, B, C, D) according to the assignment procedure based on the criteria defined in the "SAVE" project (Zuccaro et al. 2015).
  - iv. *Collapse Mechanisms calculation*. For each virtual building the trigger acceleration (ag) responsible of the relevant Collapse Mechanisms have been computed. The mechanisms considered, assumed with reference to the classification adopted in the MEDEA methodology (Zuccaro and Papa, 2002), are: in-plane (shear crack, failure by slip and buckling failure) and out-of-plane (simple overturning, vertical bending and horizontal bending) collapse mechanisms.
  - iv. *Vulnerability curves assessment*. Collecting the obtained results, for each typological class (A, B, C, D), vulnerability curves are built, expressing the collapse probability as a function of the ground acceleration (ag).

The approach adopted constitutes a preliminary study to understand the basic seismic behaviour of the ordinary masonry buildings. Further developments of this research will include additional improvements also in dynamic state, able to identify a more accurate evaluation of collapse accelerations (Boothby, 2001; De Jong, 2009), considering micromechanical modelling of failure (effects of deformations in the mortar joints, detailed properties of the material, irregularity in the panels, etc.) and more detailed sensitivity analyses on the observed data used and on their reliability.

---

<sup>2</sup> "SAVE" - Updated Tools for the Seismic Vulnerability Evaluation of the Italian Real Estate and of Urban Systems. National Research project funded by Italian Government

## SUMMARY

This dissertation includes a detailed analysis of the seismic vulnerability assessment of the masonry buildings. Chapter 1 starts from the definition of the seismic risk assessment and reviews the relevant literature for the buildings seismic vulnerability assessment. In particular, this study discusses the current state of the buildings seismic vulnerability approaches (observed vulnerability, calculated vulnerability and hybrid approach) and their assessment tools (damage probability matrices, vulnerability index method, vulnerability curves).

Moreover Chapter 2 includes details about the mechanical characteristics of the masonry structure and its constitutive models. Chapter 3 includes an analysis of the no-tension material (NTM) according to Heyman (Heyman, 1966; Heyman, 1969) assumptions. In particular the chapter reviews some formulations of the constitutive problem of no-tension material, all based on the use of mathematical algorithmic (Del Piero (1989), Baratta et al. (1991, 2005), Addessi (2014)).

Chapter 4 analysed the collapse mechanisms (in-plane and out-of-plane) potentially triggered in masonry buildings by the seismic action. This work, based on Heyman's general principles of limit analysis (Heyman 1966, 1995, 1998), examines the collapse mechanisms of masonry structures in response to horizontal ground accelerations. The masonry structure is analyzed using rigid block or “macro-elements” analysis based on equilibrium and making work calculations in order to verify the stability of the structure and determine the critical collapse mechanism. In particular in paragraph 8.7 the study of the mechanisms of collapse is used to analyze the seismic damage caused by the earthquake that hit the central Apennines on 24th August, 2016. In particular, among all towns, it is investigated the case study of Fonte del Campo.

The hybrid vulnerability approach presented in this dissertation is analysed in Chapter 5, which also summarizes the iterative procedure adopted in this research based on a Montecarlo simulation analysis.

Numerical results are presented by discussing the failure probability curves relevant to each collapse mechanism, and by computing the vulnerability curves of each structural typology, shown in Chapter 6.

The presented results are compared with alternative strategies, such as the approach proposed by Cattari et al., (2014) and the procedure presented by Zuccaro et al. (2015). A brief discussion on such comparisons and on the robustness of the proposed algorithm is reported in paragraph 6.2; Finally, conclusions and future work are summarized in Chapter 7.

# 1 SEISMIC VULNERABILITY

## 1.1 SEISMIC RISK ASSESSMENT

Every year, from 1700 to 2500 earthquakes equal to or greater than magnitude 2.5 occurred in Italy (INGV database) (Fig. 1). These earthquakes range from very small events felt by only a few individuals to great earthquakes that destroy entire cities.

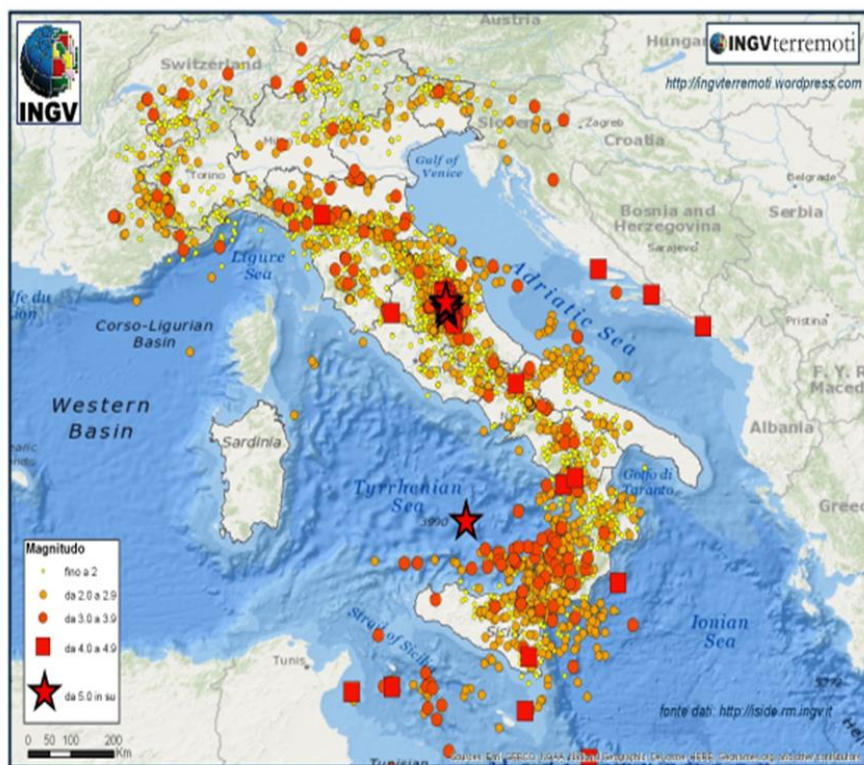


Fig. 1 The seismic activity map recorded by INGV National Seismic Network in 2016 (Iside, <http://iside.rm.ingv.it>).

The number of lives, lost and the amount of economic losses that result from an earthquake depend on the size, depth and location of the earthquake, the intensity of the ground shaking and related effects on the

building inventory, and the vulnerability of that building inventory to damage.

The seismic risk assessment has a fundamental role for the society because provides all the information for each community or organizations to support the risk mitigation decision-making.

The seismic risk can generally be defined as the measurement of the damage expected in a given interval of time, based on the type of seismicity, the resistance of buildings and the nature, quality and quantity of assets exposed.

The seismic risk is determined by the convolution of three parameters: hazard, exposure and vulnerability. They can be defined as:

- Seismic hazard is defined as the probability in a given area and in a certain interval of time of an earthquake occurring that exceeds a certain threshold of intensity, magnitude or peak ground acceleration (PGA).

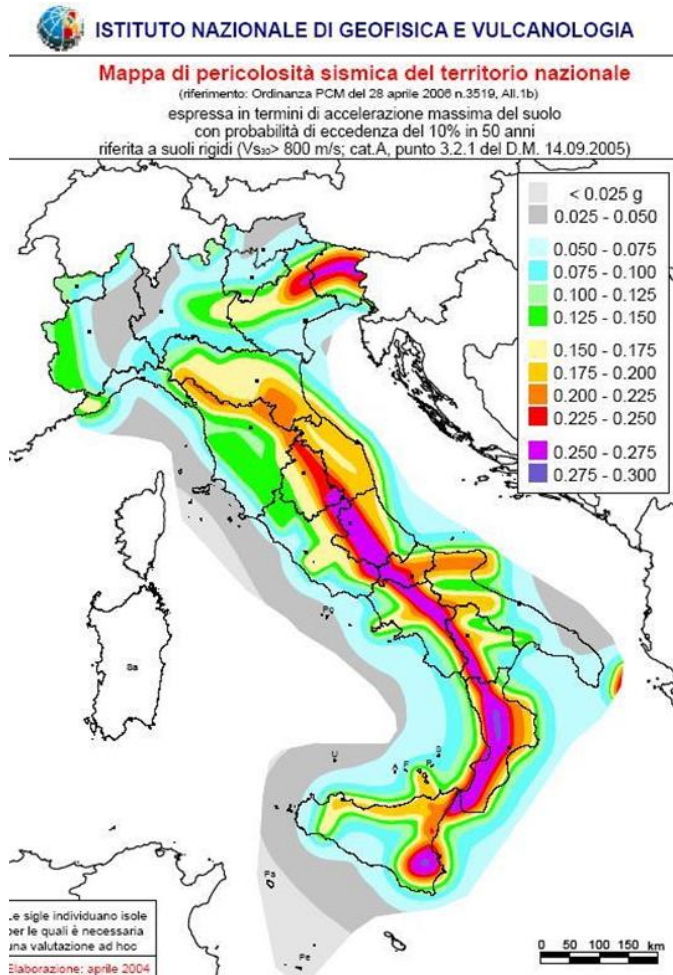
It can be evaluated from instrumental, historical, and geological observations and is quantified by two parameters: a level of hazard and its recurrence interval or frequency: for example, an M7.5 earthquake with a recurrence interval of 500 years, and peak ground acceleration (PGA) of 0.3g with a return period of 1,000 years.

Two major approaches – deterministic and probabilistic – are worldwide used at present for seismic hazard assessment.

The deterministic approach is based on the study of damage observed during seismic events in the past at a given site, reconstructing the damage scenarios to determine the frequency of repetition of earthquakes of the same intensity.

In the probabilistic approach, initiated with the work of Cornell (1968), the seismic hazard is estimated in terms of a ground motion parameter – macroseismic intensity, peak ground acceleration – and its annual probability of return period at a site. The method yields regional seismic probability maps, displaying contours of maximum ground motion (macroseismic intensity, PGA) of equal – specified – return period.

In Italy there are numerous studies and documents regarding the seismic hazard of the peninsula, representing by a seismic hazard map (**Fig. 2**)



**Fig. 2** The seismic hazard map made by INGV National Seismic Network in 2016 (<http://zonesismiche.mi.ingv.it/>).

It is clear that although seismic hazard and risk have often been used interchangeably, they are fundamentally different concepts. High seismic hazard does not necessarily mean high seismic risk, and vice versa. For example, there are high seismic hazards in the California deserts, but low seismic risk because there are few exposures (people or buildings).

- In a seismic risk assessment the exposure is defined as a quality and quantity analysis of assets (people, buildings, infrastructure and activities) exposed. The first objective for a general risk mitigation project is safeguarding human life. For this reason it is very important to assess the number of people involved, dead and/or injured using calculations based on the number of collapsed or damaged buildings.
- Seismic vulnerability can be defined as the probability that exposed assets (people, buildings, infrastructure and activities) have a given level of damage due to a seismic event of a given intensity. One of the main causes of death during an earthquake is building collapse. The kind of building damage depends on: the duration and intensity of the earthquake, the structure of the building, its age, materials, location, vicinity to other buildings and non-structural elements.

In order to estimate seismic risk, we have to assume a model (distribution) for the probability of earthquake occurrence in time. One commonly used distribution is the Poisson model (Cornell, 1968).

The methodology of the risk analysis, including hazard, vulnerability and exposed assets, depends on the geographical scale of the task (national scale, regional scale or local studies of urban areas).

The studies on the Italian peninsula show that Italy has high seismic risk, in terms of victims, damage to buildings and direct and indirect costs expected after an earthquake. It has a medium-high seismic hazard (due to the frequency and intensity of phenomena), very high vulnerability (due to the fragility of building, infrastructural, industrial, production and service assets) and an extremely high exposure (due to population density and its historical, artistic and monumental heritage that is one of its kind in the world).

In order to reduce the seismic risk, it is useful to reduce the vulnerability of the exposed assets.

Most of the loss of lives and casualties during an earthquake are caused by the collapse of structures and buildings thus it is fundamental to assess the seismic vulnerability status of existing buildings and include the results of this assessment in the planning of seismic risk mitigation.



This study includes a detailed analysis of the seismic vulnerability of the buildings and its assessment methodologies.

## 1.2 BUILDINGS SEISMIC VULNERABILITY

The seismic vulnerability in the study is considered exclusively in the structural sense, implying the ability of buildings and structures to resist damage from earthquakes.

A good definition of vulnerability is given by Sandi (1986): “the seismic vulnerability of a building is its behavior described by a cause- effect law, where the cause is the earthquake and the effect is the damage”.

There are different factors that affect the overall vulnerability of a structure besides construction type. These factors, described by Grünthal (1998) in EMS 98, are generally applicable to all types of structures:

- *Quality of the materials and workmanship.*  
A building that is well-built will be stronger than one that is badly built. The use of good quality materials and good construction techniques is crucial to improving the seismic behavior of the building. In the case of materials, the quality of the mortar is particularly important, and even rubble masonry can produce a reasonably strong building if the mortar is of high quality. Poor workmanship can include both carelessness and cost-cutting measures, such as a failure to tie in properly parts of the structure. In cases of poorly built engineered structures, it may be that the finished structure actually fails to meet the provisions of the appropriate seismic building code.
- *State of preservation and strengthening of the buildings.*  
A good state of preservation allows to have a performance of the building in accordance with its expected strength from other factors. A building which has been allowed to decay may be significantly weaker. In cases of abandoned or derelict buildings, and also in cases where there is an evident lack of maintenance some measures must be taken to retrofit buildings in order to improve their seismic behaviour.
- *Regularity in plan and in elevation.*

It is often possible to observe in damaged buildings how the irregularity contributed to the bad seismic behavior. The ideal building would be a cube in which all internal variations in stiffness (like stairwells) were symmetrically arranged. Regularity should be considered in a global sense in plan and elevation. In some cases, especially old masonry buildings, buildings that previously had a good level of regularity may be adversely affected by subsequent modifications

- *Ductility.*

Ductility is defined as the ability of the structure or parts of it to sustain large deformations beyond the yield point without breaking. It depending on the construction type and structural system. In the field of applied seismic engineering, the ductility is expressed in terms of demand and availability. The ductility demand is the maximum ductility level that the structure can reach during a seismic action, which is a function of both the structure and the earthquake. The available ductility is the maximum ductility that the structure can sustain without damage and it is an ability of the structure. In buildings designed against earthquakes, the parameters of the building determining dynamic characteristics will be controlled.

- *Position of the building.*

The position of a building with respect to other buildings in the vicinity can affect its behavior in an earthquake. In the case of a houses anchored to a neighbor causing an irregularity in the overall stiffness of the structure which will lead to increased damage. Severe damage can be the result of two tall buildings of different natural periods that are situated too close to one another. During an earthquake they may sway at different frequencies and smash into each other, causing an effect known as pounding.

The aim of a vulnerability assessment is to obtain the probability of a specific level of damage caused by a scenario earthquake to a given building type.

In order to assess a seismic vulnerability of an urban area it is not always possible to analyze the characteristics of each single building. It is recommended to group the buildings that have similar seismic behavior in typological classes also known as vulnerability buildings classes.

In summary, a seismic vulnerability assessment take in to account three elements:

- i. The measures of the earthquake.
- ii. The vulnerability class of the buildings.
- iii. The damage level.

### **1.2.1 Seismic hazard measures**

A vulnerability assessment needs a particular characterization of the ground motion, which will represent the seismic demand of the earthquake on the building.

Traditionally, the measures of the earthquake is expressed in macroseismic intensity scales (Modified Mercalli Intensity, MMI, EMS 98) and instrumental quantities (peak ground acceleration, PGA).

Macroseismic intensity scales are based on how strongly the ground shaking is experienced in an area, as well as observations of building damage. This means that macroseismic scales include information about building fragility in the areas in which they have been calibrated. This should be taken into account when applying a macroseismic scale outside the area in which it was originally developed – for example, using the European Macroseismic Scale (EMS) outside Europe.

The Macroseismic intensity scales have this characteristics:

- They are discrete rather than continuous and often Roman numerals are used to reflect this.
- They are monotonic (in the sense that VII generally relates to a stronger ground shaking than VI, for example), but nonlinear (each increment does not necessarily represent a constant increase in ground shaking).

Instrumental intensity measures are based on quantities that are calculated from strong ground motion recordings. The most commonly used instrumental measure in the vulnerability literature is peak ground acceleration (PGA). Compared with macroseismic scales, instrumental measures may be less correlated with damage.

More recent proposals have linked the seismic vulnerability of the buildings to response spectra obtained from the ground motions.

### 1.2.2 Vulnerability classes

A vulnerability classes express a different ways that buildings respond to earthquake shaking.

Grünthal (1998) gives a general description of the vulnerability class: “If two groups of buildings are subjected to exactly the same earthquake shaking, and one group performs better than the other, then it can be said that the buildings that were less damaged had lower earthquake vulnerability than the ones that were more damaged, or it can be stated that the buildings that were less damaged are more earthquake resistant, and vice versa”.

The most common scale used to classify the buildings vulnerability is the EMS scale (Grünthal, 1998).

The EMS 98 defined four groups of buildings structure (masonry, RC, steel and wood) and six classes of decreasing vulnerability (A-F) (**Fig. 3**):

The A, B and C classes represent the strength of an adobe house, brick building and reinforced concrete (RC) structure. They should be compatible with building classes A-C in the MSK-64 and MSK-81 scales. Classes D and E are intended to represent an improved level of earthquake resistant buildings as reinforced or confined masonry and steel structures, which are well-known to be resistant to earthquake shaking. Class F is intended to represent the vulnerability of a structure with a high level of earthquake resistant design.

Type of Structure		Vulnerability Class					
		A	B	C	D	E	F
MASONRY	rubble stone, fieldstone	○					
	adobe (earth brick)	○	—				
	simple stone	—	○				
	massive stone		—	○	—		
	unreinforced, with manufactured stone units	—	○	—			
	unreinforced, with RC floors		—	○	—		
	reinforced or confined			—	○	—	
REINFORCED CONCRETE (RC)	frame without earthquake-resistant design (ERD)	—	—	○	—		
	frame with moderate level of ERD		—	—	○	—	
	frame with high level of ERD			—	—	○	—
	walls without ERD		—	○	—		
	walls with moderate level of ERD			—	○	—	
	walls with high level of ERD				—	○	—
STEEL	steel structures			—	—	○	—
WOOD	timber structures		—	—	○	—	

○ most likely vulnerability class; — probable range;  
 - - - - - range of less probable, exceptional cases

Fig. 3 Classification of structures (buildings) into vulnerability classes according to EMS 98 (Grünthal, 1998).

In some cases, the EMS 98 vulnerability scale has high level of uncertainty: the “probable range” may be large and this can falsify the planning of seismic risk mitigation.

### 1.2.3 “SAVE” methodology

Zuccaro et al. (2006, 2009, 2015) made a reformulation of EMS 98 vulnerability classes assignment. This procedure, defined as “SAVE” methodology (Strumenti di Analisi di Vulnerabilità degli Edifici esistenti), classifies the buildings taking into account not only the vertical structure of the buildings as in EMS 98 but also the typological-structural characteristics of the buildings or “vulnerability factors”.

The vulnerability factors are defined as the most recurrent structural characteristics responsible of the seismic behavior of the buildings (pushing roofs, floor stiffness etc.).

This typological characteristics are identified through the analysis of the observed damages due to previous earthquakes and parameterized through the Synthetic Parameter of Damage (SPD).

The SAVE assignment procedure can be synthetically defined in these steps (**Fig. 4**):

- i. Each building is classify according to EMS 98 vulnerability scale.
- ii. The  $SPD_v$  is obtained calculating the average value of SPD corresponding to the EMS 98 class of the building. The table (**Table 1**) shows the range of SPD values assigned for each vulnerability class of the buildings. The values of the SPD range is the result of a statistical analysis of the average behavior of buildings with same characteristics.

**Table 1 SPD range assigned for each vulnerability class of the buildings.**

Vulnerability class				
A	B	C	D	E
-	2.0	1.7	1.4	1.0
2.0	1.7	1.4	1.0	-

- iii. The typological-structural characteristics of the building (vulnerability factors) are analysed and parameterized in coefficients of influence (positive or negative) “ $P_s(1,2,3\dots)$ ”.
- iv. The results thus obtained is summed with the value of the  $SPD_v$  to obtain a new value defined as  $SPDP$ . If the  $SPDP$  is bigger than  $SPD_v$  this means that the building structure has a lower resistance than that evaluated by the EMS 98 and vice versa (**Fig. 5**).
- v. A new vulnerability class, corresponding to the value of  $SPDP$ , is assigned to the building.

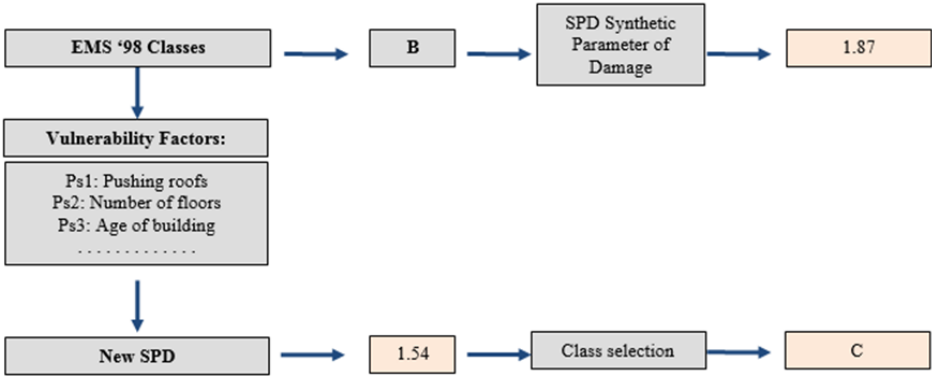


Fig. 4 Save Methodology (Zuccaro et al. 2006).

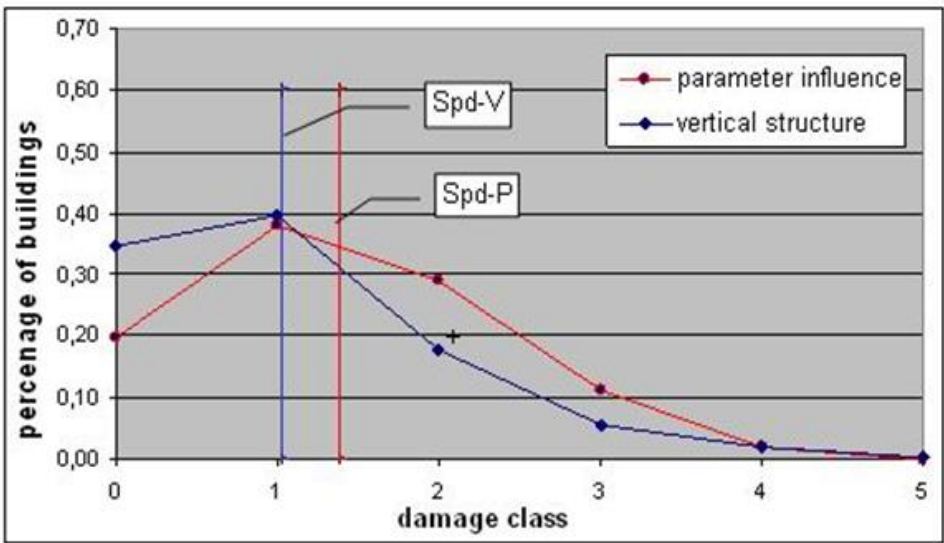


Fig. 5 Difference between SPDv function of EMS'98 and SPDP modified by vulnerability parameters.

#### 1.2.4 The damage level

Each vulnerability assessment method models the level of damage on a discrete damage scale according to the MSK scale (Medvedev and Sponheuer, 1969), the Modified Mercalli scale (Wood and Neumann, 1931) or the EMS98 scale (Grünthal, 1998).

The most frequently used method is the classification according to European Macroseismic Scale (EMS) 1998, which includes a low level of damage (Level 0, Level 1, Level 2), a substantial to heavy damage state (Level 3), very heavy damage state (Level 4), and destruction damage state (Level 5).

The way in which a building deforms under earthquake shaking depends on the building type.

EMS 98 analyzed the classification of damage in two categories: masonry buildings (**Fig. 6**) and buildings of reinforced concrete (**Fig. 7**).

In both categorizes is it possible to distinguish the damage to the primary (load bearing/ structural) system and damage to secondary (non-structural) elements (like infill or curtain walls).








Classification of damage to masonry buildings	
	Grade 1: Negligible to slight damage (no structural damage, slight non-structural damage) Hair-line cracks in very few walls. Fall of small pieces of plaster only. Fall of loose stones from upper parts of buildings in very few cases.
	Grade 2: Moderate damage (slight structural damage, moderate non-structural damage) Cracks in many walls. Fall of fairly large pieces of plaster. Partial collapse of chimneys.
	Grade 3: Substantial to heavy damage (moderate structural damage, heavy non-structural damage) Large and extensive cracks in most walls. Roof tiles detach. Chimneys fracture at the roof line; failure of individual non-structural elements (partitions, gable walls).
	Grade 4: Very heavy damage (heavy structural damage, very heavy non-structural damage) Serious failure of walls; partial structural failure of roofs and floors.
	Grade 5: Destruction (very heavy structural damage) Total or near total collapse.

Fig. 6 Classification of damage to masonry buildings according to EMS 98 (Grünthal, 1998).


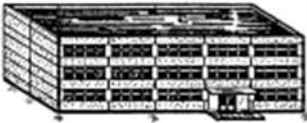



Classification of damage to buildings of reinforced concrete	
	<p><b>Grade 1: Negligible to slight damage</b> (no structural damage, slight non-structural damage)</p> <p>Fine cracks in plaster over frame members or in walls at the base.</p> <p>Fine cracks in partitions and infills.</p>
	<p><b>Grade 2: Moderate damage</b> (slight structural damage, moderate non-structural damage)</p> <p>Cracks in columns and beams of frames and in structural walls.</p> <p>Cracks in partition and infill walls; fall of brittle cladding and plaster. Falling mortar from the joints of wall panels.</p>
	<p><b>Grade 3: Substantial to heavy damage</b> (moderate structural damage, heavy non-structural damage)</p> <p>Cracks in columns and beam column joints of frames at the base and at joints of coupled walls. Spalling of concrete cover, buckling of reinforced rods.</p> <p>Large cracks in partition and infill walls, failure of individual infill panels.</p>
	<p><b>Grade 4: Very heavy damage</b> (heavy structural damage, very heavy non-structural damage)</p> <p>Large cracks in structural elements with compression failure of concrete and fracture of rebars; bond failure of beam reinforced bars; tilting of columns.</p> <p>Collapse of a few columns or of a single upper floor.</p>
	<p><b>Grade 5: Destruction</b> (very heavy structural damage)</p> <p>Collapse of ground floor or parts (e. g. wings) of buildings.</p>

Fig. 7 Classification of damage to buildings of reinforced concrete according to EMS 98 (Grünthal, 1998).

In summary, the table (Table 2) shows the general descriptions of damage level of the buildings:

**Table 2 Classification of damage according to the European Macroseismic Scale, EMS.**

<b>Damage Level</b>	<b>Description</b>
D0	No damage
D1	Cracking of non-structural elements, such as dry walls. Brick or stucco external cladding
D2	Major damage to the non-structural elements, such as collapse of a whole masonry infill wall; minor damage to load bearing elements
D3	Significant damage to load-bearing elements, but no collapse
D4	Partial structural collapse (individual floor or portion of building)
D5	Full collapse

### **1.3 SEISMIC VULNERABILITY ASSESSMENT APPROACHES**

The various approaches for vulnerability assessment that have been proposed in the last 30 years and used in loss estimation can be divided into two main categories: statistical or empirical approach and mechanical or analytical approach, both of which can be used in hybrid approaches. (Fig. 8).

The choice of the most suitable procedure is highly dependent on the resources available and the scale and aim of the study. Statistical approach can be used for large scale studies to define damage scenarios, however if the purpose of the study is to identify within a district or urban center specific buildings in need of strengthening, so as to increase their seismic resilience, then a suitable mechanical procedure should be preferred.

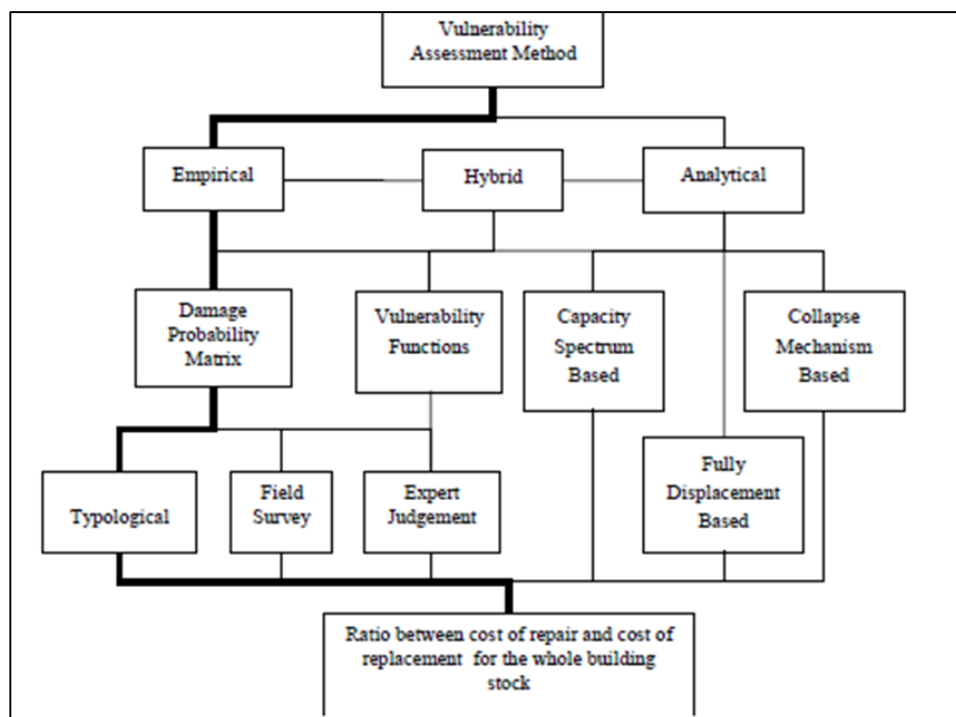


Fig. 8 The vulnerability assessment method; the bold path shows a traditional assessment method. (Calvi, 2006).

### 1.3.1 Observed vulnerability - Statistical approach.

This method constitutes the only reasonable and possible approach that could be initially employed in seismic risk analyses at a large scale.

It has been first carried out in the early 70's and calibrated as a function of macroseismic intensities. Applications of this method, using the Damage Probability Matrices (DPM), were originally proposed by Whitman et al. (1973), who analyzed the damages observed in more than 1600 buildings after the 1971 San Fernando earthquake, by Braga et al (1982,1986) after the 1980 south-Italia earthquake and by Zuccaro et al (2000), Bernardini et al (2007a, 2007b).

The statistical assessment method classifies the vulnerability of the buildings based on damage observed in previous earthquakes to the same kind of buildings.

This method is generally the most desirable from a risk management viewpoint because it is derived wholly from observations of the actual performance of assets in real earthquakes.

Although this method is an observational method and hence of good affordability, in practice there are several uncertainties about the way in which the data are acquired.

To produce such statistical analysis, large sets of data are needed to cover the whole range of performances of a given building typology to the whole range of possible seismic intensity considered, and multiple observations of building performance for the same level of intensity.

However, it has been seen that it is not always possible to require damage data from past earthquakes and that the damage data available today are inadequate, especially for intensities greater than MMVII.

In general, any procedure for the statistical prediction of damage consists basically of three steps: collecting observations after an earthquake, grouping the results by buildings characteristics and performing a statistical analysis of the data.

First the observations of previous earthquakes are collected recording:

$x_i$  = intensity of the earthquake at each building  $i$

$y_i$  = damage of the building  $i$

$c_i$  = attributes of the building  $i$  (structural material, lateral force resisting system, height, age, etc.)

Second the results are analyzed and grouped by one or more attributes of the buildings or by vulnerability classes of the building. At last, for each group of the data a statistical analysis (average, standard deviation, regression analysis...) is made.

There are three main types of statistical tools used in statistical approach for the seismic vulnerability assessment of buildings: damage probability matrices (DPM), Vulnerability Index Method and vulnerability functions.

### 1.3.2 Calculated Vulnerability - Mechanical approach.

The mechanical approach determines the response of a particular building, representative of a typology, by using structural analysis techniques and numerical tools. Applications of this method can be seen in the work of Giuffrè (1991), Singhal and Kiremidjian (1996), Park and Ang (1985), Masi (2003), Rossetto and Elnashai (2005), Dumova-Jovanoska (2004), D'Ayala et al. (2015).

This approach is particularly useful when studying a single building or a single typology of building or when assessing the improved performance due to strengthening and retrofit.

The reliability of the results is affected by the simulated models that reproduce the main characteristics of the buildings and their structural behavior. It is also dependent on the numerical tools available and by the ability of the assessor to interpret the results.

Mechanical methods, which use numerical simulations to analyze the structural behavior of buildings, are more sophisticated approaches than statistical methods. The data required for these approaches can be extracted from construction drawings and/or laboratory tests.

These approaches present the advantage of framing the problem of seismic vulnerability of masonry structures in structural engineering terms, defining their vulnerability as a direct function of construction characteristics, structural response to seismic actions and damage effects. However the following should be noted in applying these methods:

- Mechanical methods are suitable to identify structural damage states, through structural analysis. They are less useful in quantifying the likely damage to content and non-structural elements.
- Many of the different mechanical approaches that exist are specific to particular types of structure, and have diverse data requirements and computational burdens.
- When comparing results from different mechanical methods it should be borne in mind that output in terms of vulnerability are dependent on different assumptions on the representative intensity measures chosen and representative response measures chosen.

According to "Norme Tecniche per le Costruzioni" (DM 14-1-2008) mechanical methods used to predict the seismic performance of a building are:

- Linear static analysis.
- Linear dynamic analysis.

- Nonlinear static analysis. (Pushover analysis)
- Nonlinear dynamic analysis (NDA).

The last two are considered the most accurate methods for predicting Reinforced Concrete building response to earthquake ground motion.

The most used seismic analysis of unreinforced masonry structures is based on mechanical approach. Mechanical method is based on the application of kinematics models, which identify lateral collapse load multipliers of a given configuration of macro-elements and loads by imposing either energy balance or equilibrium equations. These methods present the advantage of requiring few input parameters to estimate the vulnerability and to identify the occurrence of possible in-plane or out of plane mechanisms for a given building.

### **1.3.3 Hybrid Method**

Hybrid methods combine post-earthquake damage statistics with simulated, analytical damage statistics from a mathematical model of the building typology. Applications of this method can be seen in the work of Kappos et al. (1995, 1998), Barbat et al. (1996), Zuccaro et al. (2012), Cavalieri et al. (2017).

These methods are useful when there is a lack of damage data at certain intensity levels for the geographical area under consideration and they also allow calibration of the analytical methods.

Kappos et al. (1995, 1998) have derived damage probability matrices using a hybrid procedure. The DPMs for each intensity level were constructed using the available data from past earthquakes and the results of nonlinear dynamic analysis of models that simulated the behaviour of each building class. Intensity and PGA were correlated using empirical relationships.

Barbat et al. (1996) made a hybrid vulnerability assessment of Spanish urban areas. A post-earthquake study was initially performed for two earthquakes with a maximum intensity of VII on the MSK scale.

Statistical analyses were then performed to obtain the vulnerability function for the MSK intensity level VII. A computer simulation process was subsequently used to obtain the vulnerability functions at other intensity levels.

The main difficulty in the use of hybrid methods is that the two vulnerability curves, statistical and mechanical, include different sources

of uncertainty and are thus not directly comparable. In the mechanical curves the sources of uncertainty are clearly defined during the generation of the curves whilst the specific sources and levels of variability in the statistical data are not quantifiable. The method used to calibrate the mechanical vulnerability curves using statistical data should include the additional uncertainty present in the statistical data which is not accounted for in the mechanical data.

## 1.4 SEISMIC VULNERABILITY ASSESSMENT TOOLS

Regardless of the assessment method used, there are three main types of statistical tools using for the seismic vulnerability assessment of buildings: damage probability matrices (DPM), Vulnerability Index Method and vulnerability functions.

### 1.4.1 Damage Probability Matrices (DPM)

The Damage Probability Matrices (DPM), traditionally derived using observed damage data, express in a discrete form the probability that a building obtaining a damage level  $j$ , due to a ground motion of intensity  $i$  (1):

$$P [D = j | i] \quad (1)$$

The concept of a DPM is that a given structural typology will have the same probability of being in a given damage state for a given earthquake intensity.

The general form of DPM suggested by Whitman et al. (1973) is compiled for various structural typologies according to the damaged sustained in over 1600 buildings after the 1971 San Fernando earthquake (Table 3).

Damage to buildings is described by a series of damage states (DS), while the intensity of the earthquake is described by the modified Mercalli intensity (MMI) scale. In a particular column, each number PDSI in the matrix is the probability that a particular state of damage will occur, given that a level of earthquake intensity is experienced. The sum of the probabilities in each column is 100%.



**Table 3 Format of the Damage Probability Matrix Proposed by Whitman et al. (1973).**

Damage State	Structural Damage	Non-Structural Damage	Damage Ratio (%)	Intensity of Earthquake				
				V	VI	VII	VIII	IX
0	None	None	0-0.05	95	79	33	6	0
1	None	Minor	0.05-0.3	5	18	34	19	2
2	None	Localized	0.3-1.25	0	3	20	44	18
3	Not Noticeable	Widespread	1.25-3.5	0	0	10	13	30
4	Minor	Substantial	3.5-7.5	0	0	3	6	20
5	Substantial	Extensive	7.5-20	0	0	0	12	10
6	Major	Nearly Total	20-65	0	0	0	0	7
7	Building Condemned		100	0	0	0	0	8
8	Collapse		100	0	0	0	0	5

One of the first European versions of a damage probability matrix was produced by Braga et al. (1982) (Table 4, Table 5, Table 6), which was based on the damage data of Italian buildings after the 1980 Irpinia earthquake. The damage distributions of any class buildings for different seismic intensities was described by a binomial distribution which has the advantage of needing one parameter only which ranges between 0 and 1. The buildings were separated into three vulnerability classes (A, B and C) and a DPM based on the MSK scale was evaluated for each class.

**Table 4 Damage Probability Matrix, class A (Braga et al., 1982, 1985).**

Intensity of Earthquake	Class A					
	Damage State					
	0	1	2	3	4	5
VI	0.188	0.373	0.296	0.117	0.023	0.002
VII	0.064	0.234	0.344	0.252	0.092	0.014
VIII	0.002	0.020	0.108	0.287	0.381	0.202
IX	0.0	0.001	0.017	0.111	0.372	0.489
X	0.0	0.0	0.002	0.030	0.234	0.734

**Table 5 Damage Probability Matrix, class B (Braga et al., 1982, 1985).**

Intensity of Earthquake	Class B					
	Damage State					
	0	1	2	3	4	5
VI	0.36	0.408	0.185	0.042	0.005	0.0
VII	0.188	0.373	0.296	0.117	0.023	0.002
VIII	0.031	0.155	0.312	0.313	0.157	0.032
IX	0.002	0.022	0.114	0.293	0.376	0.193
X	0.0	0.001	0.017	0.111	0.372	0.498

**Table 6 Damage Probability Matrix, class C (Braga et al., 1982, 1985).**

Intensity of Earthquake	Class C					
	Damage State					
	0	1	2	3	4	5
VI	0.715	0.248	0.035	0.002	0.0	0.0
VII	0.401	0.402	0.161	0.032	0.003	0.0
VIII	0.131	0.329	0.330	0.165	0.041	0.004
IX	0.050	0.206	0.337	0.276	0.113	0.018
X	0.005	0.049	0.181	0.336	0.312	0.116

Later, an additional vulnerability class D has been included, using the EMS98 scale (Grüntal, 1998), to account for the buildings that have been constructed since 1980. These buildings should have a lower vulnerability as they have either been retrofitted or designed to comply with recent seismic codes.

An example of Damage Probability Matrices (DPM) which take in to account the EMS98 scale are exposed by Zuccaro et al. (2015) (**Table 7**). The DPM are obtained by a statistical analysis, made thanks to the PLINIVS Study Centre Database, which is based on the data collected on the observed damages due to previous earthquakes taken place in Italy since 1980.

About 4% of the 6.903.982 residential masonry Italian buildings (ISTAT 2011) belonging to about 550 municipalities was investigated.

**Table 7 DPM obtained through a statistical analysis of the data collected about the observed damages due to earthquakes occurred in Italy since 1980 (Zuccaro et al. , 2015).**

Class	Intensity of Earthquake	Damage State					
		D0	D1	D2	D3	D4	D5
A	V	0,3487	0,4089	0,1919	0,0450	0,0053	0,0002
B		0,5277	0,3598	0,0981	0,0134	0,0009	0,0000
C		0,6591	0,2866	0,0498	0,0043	0,0002	0,0000
D		0,8587	0,1328	0,0082	0,0003	0,0000	0,0000
A	VI	0,2887	0,4072	0,2297	0,0648	0,0091	0,0005
B		0,4437	0,3915	0,1382	0,0244	0,0022	0,0001
C		0,5905	0,3281	0,0729	0,0081	0,0005	0,0000
D		0,7738	0,2036	0,0214	0,0011	0,0000	0,0000
A	VII	0,1935	0,3762	0,2926	0,1138	0,0221	0,0017
B		0,3487	0,4089	0,1919	0,0450	0,0053	0,0002
C		0,5277	0,3598	0,0981	0,0134	0,0009	0,0000
D		0,6591	0,2866	0,0498	0,0043	0,0002	0,0000
A	VIII	0,0656	0,2376	0,3442	0,2492	0,0902	0,0131
B		0,2219	0,3898	0,2739	0,0962	0,0169	0,0012
C		0,4182	0,3983	0,1517	0,0289	0,0028	0,0001
D		0,5584	0,3451	0,0853	0,0105	0,0007	0,0000
A	IX	0,0102	0,0768	0,2304	0,3456	0,2592	0,0778
B		0,1074	0,3020	0,3397	0,1911	0,0537	0,0060
C		0,3077	0,4090	0,2174	0,0578	0,0077	0,0004
D		0,4437	0,3915	0,1382	0,0244	0,0022	0,0001
A	X	0,0017	0,0221	0,1138	0,2926	0,3762	0,1935
B		0,0313	0,1563	0,3125	0,3125	0,1563	0,0313
C		0,2219	0,3898	0,2739	0,0962	0,0169	0,0012
D		0,2887	0,4072	0,2297	0,0648	0,0091	0,0005
A	XI	0,0002	0,0043	0,0392	0,1786	0,4069	0,3707
B		0,0024	0,0284	0,1323	0,3087	0,3602	0,1681
C		0,0380	0,1755	0,3240	0,2990	0,1380	0,0255
D		0,0459	0,1956	0,3332	0,2838	0,1209	0,0206
A	XII	0,0000	0,0000	0,0000	0,0010	0,0480	0,9510
B		0,0000	0,0000	0,0006	0,0142	0,1699	0,8154
C		0,0000	0,0001	0,0019	0,0299	0,2342	0,7339
D		0,0000	0,0002	0,0043	0,0498	0,2866	0,6591

The DPMs are based on intensity scale so the assessment of seismic risk on a large scale is made possible in both an efficient and cost-effective manner because in the past seismic hazard maps were also defined in terms

of macroseismic intensity. The use of observed damage data to predict the future effects of earthquakes also has the advantage that when the damage probability matrices are applied to regions with similar characteristics, a realistic indication of the expected damage should result and many uncertainties are inherently accounted for.

However, there are various disadvantages associated with the use of DPM's:

- A macroseismic intensity scale is defined by considering the observed damage of the building so both the ground motion input and the vulnerability are based on the observed damage due to earthquakes.
- Large magnitude earthquakes occur relatively infrequently near densely populated areas and so the data available tends to be clustered around the low damage/ground motion end of the matrix and limiting the statistical validity of the high damage/ground motion end of the matrix.
- The use of observed vulnerability definitions in evaluating retrofit options or in accounting for construction changes cannot be explicitly modelled.
- Seismic hazard maps are now defined in terms of PGA (or spectral ordinates) and thus PGA needs to be related to intensity; however, the uncertainty in this equation is frequently ignored.
- When PGA is used in the derivation of observed vulnerability, the relationship between the frequency content of the ground motions and the period of vibration of the buildings is not taken into account.

In order to overcome some of the drawbacks of the Damage Probability Matrices derived using observed damage, recent proposals have been made using the data derived by a computational analyses.

#### **1.4.2 Vulnerability Index Method**

The Vulnerability Index Method (Benedetti and Petrini, 1984; GNDT, 1993) has been used extensively in Italy in the past few decades and is based on a large amount of damage survey data.

This approach is based on estimating the vulnerability of masonry buildings by calculating a “vulnerability index” (I<sub>v</sub>). This vulnerability index derives from the summation of weighted parameters associated with

the structural features of the building typology, which have been observed to affect their seismic response.

There are eleven parameters in total (quality of materials, state of conservation, plan and elevation configuration ecc...), which are each identified as having one of four qualification coefficients,  $K_i$ , in accordance with the quality conditions – from A (optimal) to D (unfavorable) – and are weighted to account for their relative importance ( $W_i$ ).

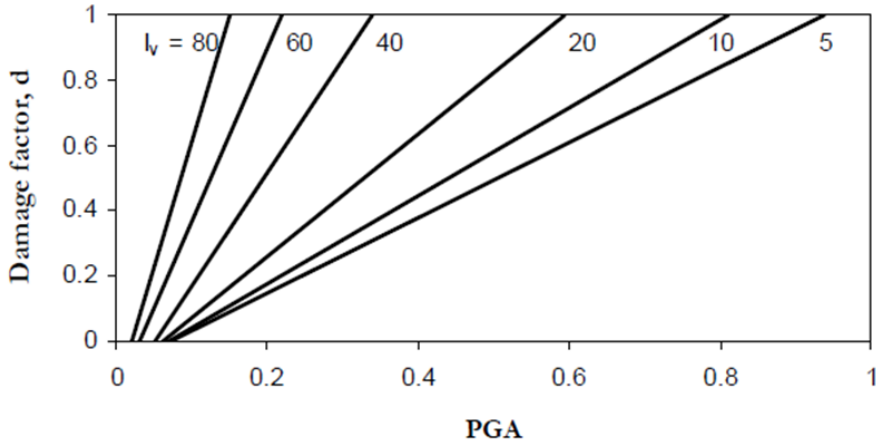
The global vulnerability index  $I_v$  of each building is then evaluated using the following formula (2):

$$I_v = \sum_{i=1}^{11} K_i W_i \quad (2)$$

The vulnerability index ranges from 0 to 382.5, but is generally normalised from 0 to 100, where 0 represents the least vulnerable buildings and 100 the most vulnerable.

The data from past earthquakes is used to calibrate vulnerability functions. By relating the vulnerability index ( $I_v$ ) to the observed global damage levels for a building typology with reference to macroseismic intensity levels, the  $I_v$  can be applied to regions characterized by the same building typologies and same level of macroseismic intensity or peak ground acceleration.

The damage factor ranges between 0 and 1 and defines the ratio of repair cost to replacement cost. The damage factor is assumed negligible for PGA values less than a given threshold and it increases linearly up until a collapse PGA, from where it takes a value of 1 (**Fig. 9**).



**Fig. 9 Vulnerability functions to relate damage factor (d) and peak ground acceleration (PGA) for different values of vulnerability index ( $I_v$ ) (adapted from Guagenti and Petrini(1989))**

The main advantage of the vulnerability index method is that it allow to determine the vulnerability characteristics of the building not only on the base of its typology.

Nevertheless, the methodology still requires expert judgment to be applied in assessing the buildings, and the coefficients and weights applied in the calculation of the index have a degree of uncertainty that is not generally accounted for.

Furthermore, in order to do the vulnerability assessment of buildings on a large (e.g., national) scale, in a country where data is not already available, the calculation of the vulnerability index for a large building stock would be very time consuming. However, in any risk or loss assessment model a detailed collection of input data is required for application at the national scale.

### 1.4.3 Vulnerability Curves

Vulnerability functions are a mathematical function representing the probability of exceeding a given damage state as a function of an engineering demand parameter that represents the ground motion (pick ground acceleration, spectral displacement at a given frequency, macroseismic intensity).

The damage state data, recording on the base of calculations or based on experience data (the later could be from real earthquakes or dynamic tests), are collected and grouped by one or more attributes (e.g., by model building type). For each group a regression analysis is performed in order to fit a fragility function. The results are continuous vulnerability curves that can be expressed in a table of mean and standard deviation of loss at each of many levels of excitation for the given class of building.

The most common forms of a seismic vulnerability function are:

- Normal cumulative distribution function (3)

$$\begin{aligned} F_d(x) &= P[D \geq d | X = x] \quad d \in \{0,1,2,3,4,5\} \\ &= \Phi((x/\theta)/\beta) \end{aligned} \quad (3)$$

- Lognormal cumulative distribution function (4) (Fig. 10):

$$\begin{aligned} F_d(x) &= P[D \geq d | X = x] \quad d \in \{0,1,2,3,4,5\} \\ &= \Phi\left(\frac{\ln(x/\theta)}{\beta_{\ln}}\right) \end{aligned} \quad (4)$$

Where

$P[A|B]$  is the probability that A is true given that B is true;

D is the uncertain damage state of a particular component. It can take on a value in  $\{0,1,.. \}$ , where  $D = 0$  denotes the undamaged state,  $D = 1$  denotes the first damage state, etc.;

d is a particular value of D, i.e., with no uncertainty;

X is the uncertain excitation (peak zero-period acceleration, macroseismic intensity);

x is a particular value of X, i.e., with no uncertainty;

$F_d(x)$  is a vulnerability function for damage state d evaluated at x;

$\Phi(s)$  is the standard normal cumulative distribution function (often called the Gaussian);

$\ln(s)$  is the natural logarithm of s;

$\theta$  is the median capacity of the asset to resist damage state d measured in the same units as X.

$\beta$  is the standard deviation of the capacity of the asset to resist damage state d.

$\beta \ln$  is the logarithmic standard deviation defined as the standard deviation of the natural logarithm of the capacity of the asset to resist damage state d.

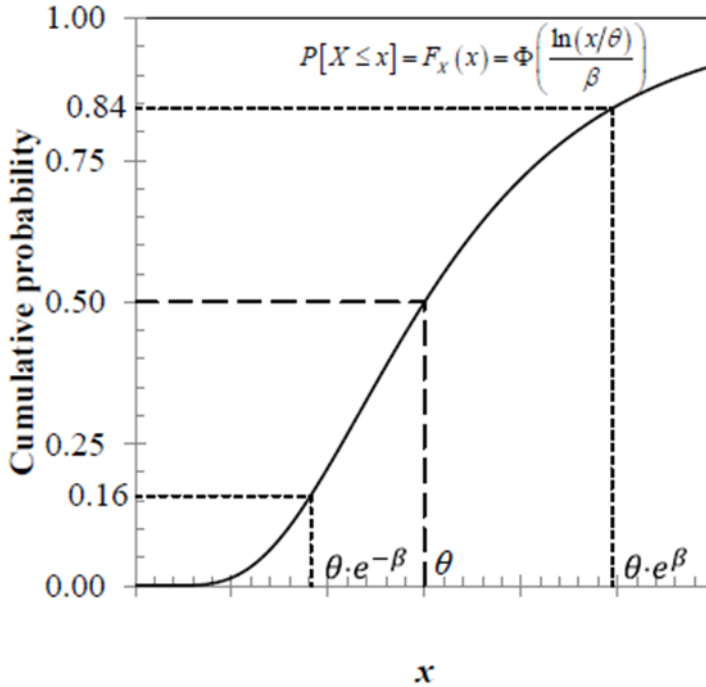


Fig. 10 Lognormal cumulative distribution function.

Three general classes of vulnerability functions can be distinguished by the method used to create them:

- Observed vulnerability function.

An observed vulnerability function is one that is created by fitting a function to approximate observational data after an earthquake. This kind of fragility functions were introduced slightly later than DPMs; one obstacle to their derivation being the fact that macroseismic intensity is not a continuous variable. This problem was overcome by Spence et al. (1992) through the use of the Parameterless Scale of Intensity (PSI) to derive vulnerability functions based on the observed damage of buildings



using the MSK damage scale (Fig. 11). Subsequently the PSI was converted to PGA using empirical correlation functions.

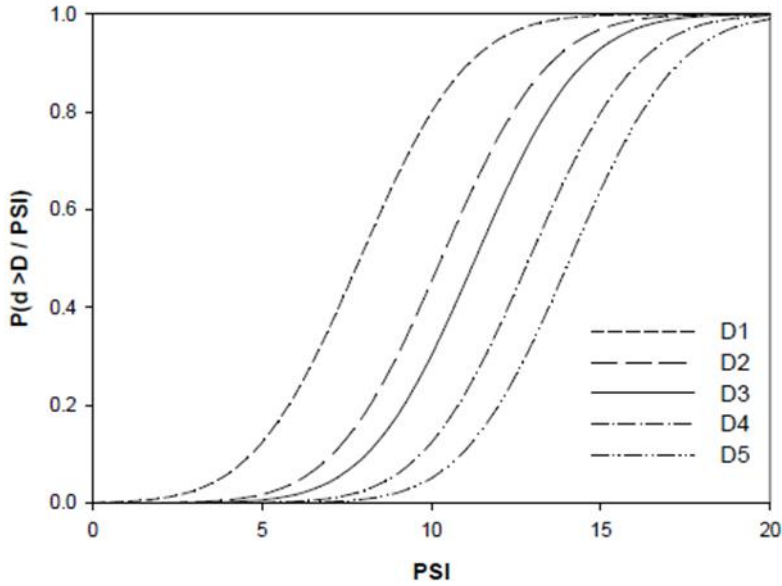


Fig. 11 Vulnerability curves produced by Spence et al. (1992). D1 to D5 relate to damage states in the MSK scale.

- Mechanical vulnerability functions.

A mechanical vulnerability function is one derived by structural analysis. Although vulnerability curves have traditionally been derived using observed damage data, recent proposals have made use of the computational analyses to overcome some of the drawbacks of the statistical method.

Singhal and Kiremidjian (1996) developed vulnerability curves for three categories of reinforced concrete frame structures using Monte Carlo simulation. The probabilities of structural damage were determined using nonlinear dynamic analysis with an ensemble of ground motions. The structural models employed in this study were representative of the buildings designed and constructed in Italy over the past 30 years. The seismic response of the structures, subjected to ground motions of various levels of intensity, was estimated through nonlinear dynamic analyses with artificial and natural accelerograms.

One of the principle disadvantages of the derivation of mechanical vulnerability curves is that the procedure is extremely computationally intensive and the curves cannot be easily developed for different areas or countries with diverse construction characteristics. However, mechanical vulnerability curves have frequently been used to support, rather than to replace, the empirical DPMs and vulnerability curves based on the observational damage data.

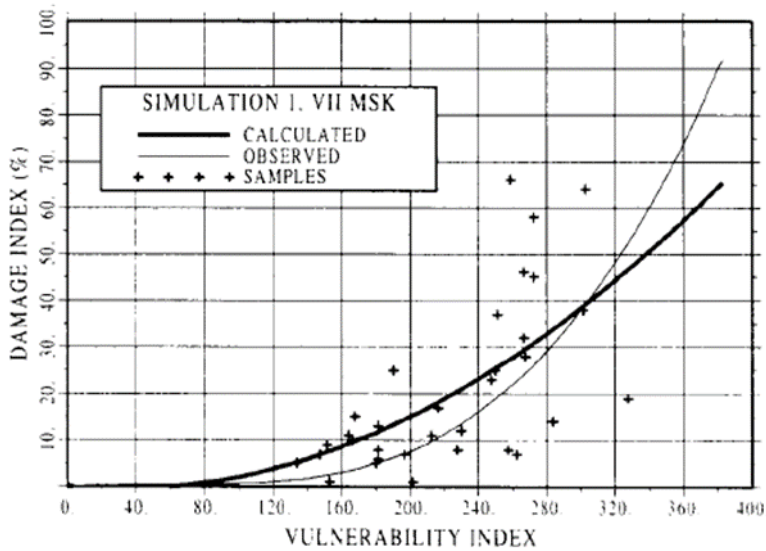
- Hybrid vulnerability function.

This vulnerability function is derived by a mechanical model calibrated using the observational data.

Barbat et al. (1996) used the Italian “Vulnerability Index Methodology” for a hybrid vulnerability assessment of Spanish urban areas. A post-earthquake study was initially performed for two earthquakes with a maximum intensity of VII on the MSK scale.

The structural and non-structural damage to masonry structures was analyzed and statistical analyses were then performed to obtain the vulnerability function for the MSK intensity level VII.

An analytical simulation process was subsequently used to obtain the vulnerability functions at other intensity levels. Sixty hypothetical buildings with characteristics obtained from the building stock in the area were generated using Monte Carlo simulation and the capacity of the structures is calculated. The vulnerability index was calculated for each building, this was plotted against the global damage index for the MSK intensity level VII, and a curve was obtained by regression analysis; this curve was then re-calibrated so as to match the field observations (**Fig. 12**).



**Fig. 12 Simulated (thick line) and observed (thin line) vulnerability functions for MSK intensity VII (Barbat et al., 1996).**

The difference between the calculated and observed curves was assumed to be due to the use of the proposed weighting factors for Italian buildings and so the weighting factors were modified such that the observed and calculated vulnerability functions matched. Once the calibration with the 60 random buildings had been carried out, the vulnerability functions for the other intensity levels were then produced using 2000 hypothetical buildings in conjunction with the calibrated weighting factors.

This research follows a hybrid vulnerability assessment method proposed by Zuccaro et al. (2012) who using the high reliability of the observational approach data in order to validate the results of the mechanical analysis. Combining the "observed" and the "mechanical" vulnerability, this method allows to analyze the correlations among the structural-typological characteristics which define Italian masonry buildings and the trigger acceleration (PGA) of the possible collapse mechanisms (in-plan and out-of-plan).

Starting from a statistical analysis of existing Italian masonry buildings, based on the data collected on the observed damages caused by previous earthquakes taken place in Italy since 1980, the mechanical buildings vulnerability is obtained using a Monte-Carlo simulation model and

evaluating the trigger accelerations (PGA) of the collapse mechanisms (in plan and out of plan).

For each typological vulnerability classes of the buildings, the results are fixed in order to generate the vulnerability curves, which are representatives of the occurrence probability of the building to trigger a failure mechanism at a specific PGA value.

## 2 THE MASONRY STRUCTURE

### 2.1 INTRODUCTION

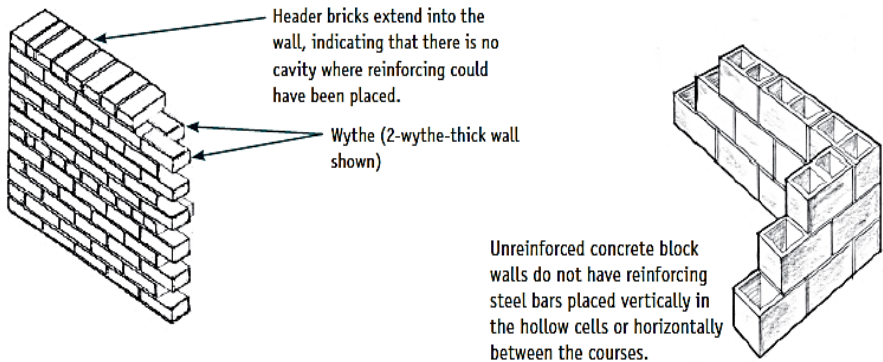
The masonry material is one of the oldest building material, as confirmed by the historical heritage. The development of a method that analyses the structural behaviour of masonry represents an important task to verify the stability of masonry constructions as old buildings, historical town and monumental structures.

The analysis of masonry structures is not simple because it can be considered as a composite material obtained by assembling bricks by means of mortar joints.

The masonry buildings can be classify in two main categories:

- a) Unreinforced masonry buildings (UBM) (**Fig. 13**).

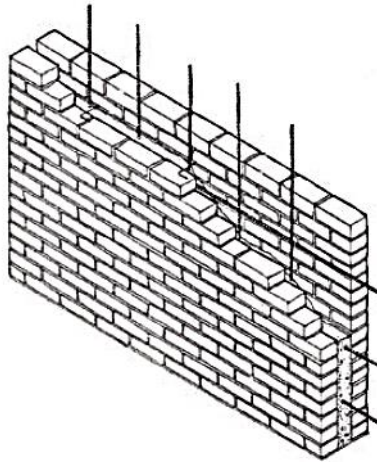
Unreinforced masonry can be defined generally as masonry that contains no reinforcing in it. It is made with natural or artificial stones and the proper filling of mortar between the spaces of stones. This type of structures are the most vulnerable during an earthquake.



**Fig. 13** Components of unreinforced brick (left) and unreinforced concrete block (right) walls. FEMA P-774 (2009).

- b) Reinforced masonry buildings (RBM) (**Fig. 14**).

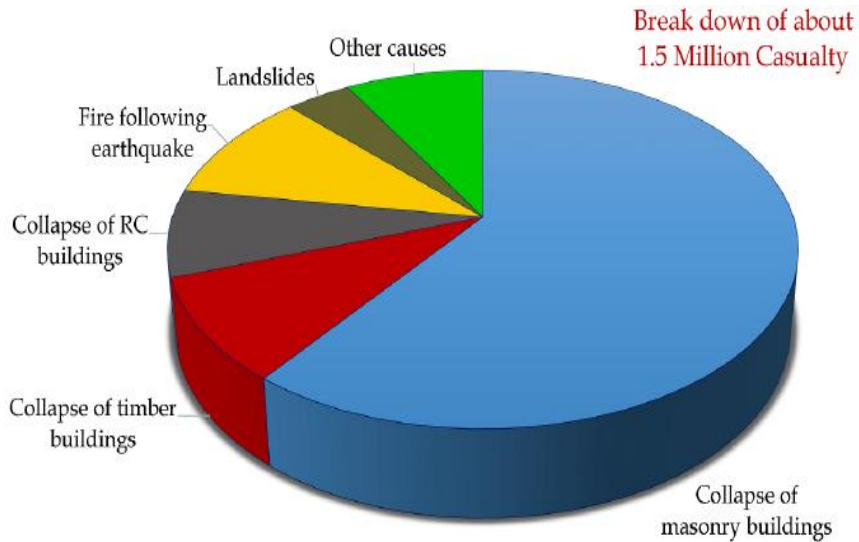
Reinforced masonry is any type of brick, concrete or other type of masonry that is strengthened with the use of mild steel flats, hoop iron, expanded mesh or bars. The use of reinforced brick masonry (RBM) it has been development by Marc Isambard Brunel in the nineteenth century. The reinforced brick masonry is capable of resisting both compressive as well as tensile and shear stress. On account of its ability to resist lateral forces, reinforced brick masonry is extensively used in seismic areas. It is essential to use good quality of bricks (having crushing strength of 140 kg/sq. cm or more) and rich and dense cement mortar in the reinforced brick work. The reinforcement should be effectively bedded and surrounded with mortar cover of 15 to 25 cm. This is necessary to protect the reinforcement against corrosion.



**Fig. 14 Reinforced brick wall (FEMA 1994).**

The collapse of masonry buildings is the primary cause for loss of life during an earthquake (Coburn & Spence, 2002).

**Fig. 15** shows the breakdown of the fatalities due to earthquakes in the period of 1900-1999 to different causes. About 75% of the fatalities attributed to earthquakes are caused by the collapse of buildings and the greatest proportion is from the collapse of masonry buildings (Navaratnarajah, Sathiparan, 2015).



**Fig. 15 Breakdown of fatalities attributed to earthquake by cause (Period 1900-1999) Navaratnarajah, Sathiparan (2015).**

This study includes a detailed analysis of the unreinforced masonry (UBM) used in buildings structures.

## 2.2 MASONRY STRUCTURE

Masonry structure is defined as a manufactured product made with natural or artificial stone elements joined with or without mortar (Baratta, 1991). The strength of masonry is conditioned by the characteristics of its elements and by the quality of the links between them (Table 8).

**Table 8 Typology of masonry components**

Masonry units	<ul style="list-style-type: none"> <li>• Adobe (Sun dried blocks);</li> <li>• Stone, Laterite blocks;</li> <li>• Clay bricks;</li> <li>• Concrete blocks (solid or hollow);</li> <li>• Stabilized mud blocks (SMB);</li> </ul>
---------------	--

	<ul style="list-style-type: none"> <li>• Calcium silicate bricks;</li> <li>• Gypsum blocks</li> </ul>
Mortar	<ul style="list-style-type: none"> <li>• Lime mortar;</li> <li>• Cement mortar;</li> <li>• Composite mortar;</li> <li>• Lime- pozzolana mortar;</li> <li>• Soil-cement mortar;</li> </ul>

Giuffré (1991) defined for the first time two categories of masonry structure depending on its layout: “folk tradition” and “civilized tradition”. These big categories are in general defined as:

### 1. Rubble masonry or “folk tradition”.

It is an irregularly masonry and is usually made with mortar and square or polygonal natural stones (rounded or spiky river pebble, lava stone etc.).

The strength of rubble masonry depend on the quality of mortar, the use of long through stones and the proper filling of mortar between the spaces of stones.

Further classifications of this kind of masonry are (**Fig. 16**):

a) Coursed rubble masonry.

In coursed random rubble masonry there are stone courses of equal height.

b) Un-coursed rubble masonry.

In un-coursed random rubble masonry, the courses are not maintained regularly. The larger stones are laid first and the spaces between them are then filled up by small stones.

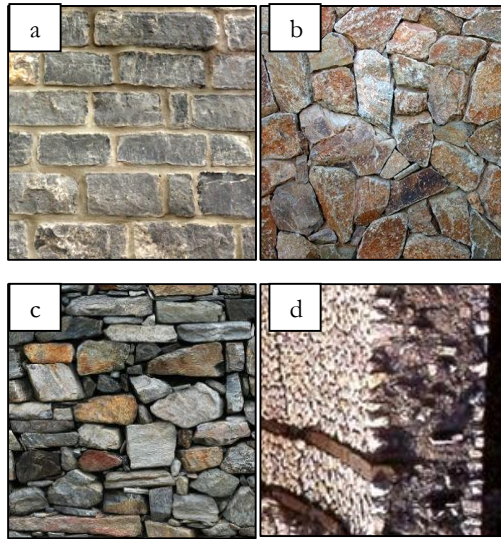
c) Dry rubble masonry.

In the dry masonry the strength of a wall is not dependent on the bond between the stones and the mortar; the friction between the interlocking blocks of masonry and the force of gravity are often strong enough to provide a great link between the elements.

d) “Composite” rubble masonry.



This kind of masonry has performed extremely well over the past millennium and it can be still found in many old town of Italy. It is made with two skins of stonework and a rubble core.



**Fig. 16** General classification of rubble masonry: (a) coursed masonry, (b) uncoursed masonry, (c) dry masonry, (d) “composite” masonry.

## 2. Ashlar masonry or “civilized tradition”.

This kind of masonry has in general a good quality structures. It is made with natural stones (tuff, adobe etc.) or artificial stones (bricks etc.). In this masonry all joints are regular, thin, and of uniform thickness.

Further classifications of this kind of masonry are (Fig. 17):

e) Ashlar fine masonry.

In this kind of masonry, each stone is cut to uniform size and shape with all sides rectangular, so that the stone gives perfectly horizontal and vertical joints with adjoining stone.

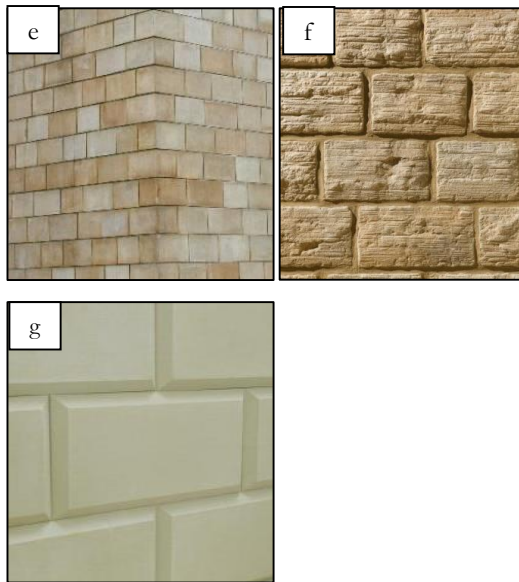
f) Ashlar rough masonry.

In this type of masonry the exposed faces of stone generally have a fine dressed chisel drafting all

round the edges. The portion the face stone enclosed by the chisel draft is rough tooled. The stones thickness should never exceed 6mm.

g) Ashlar chamfered masonry.

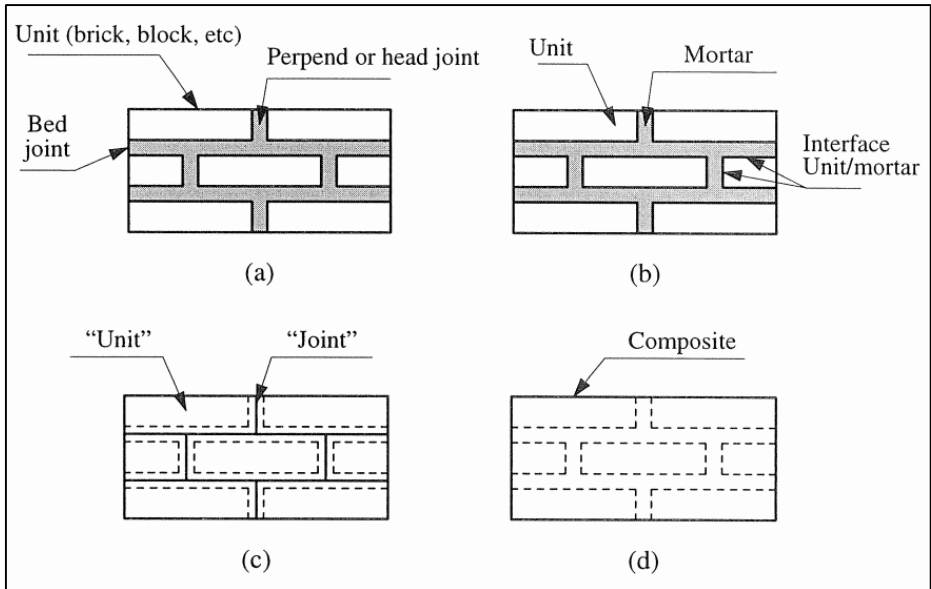
This type masonry is similar to the one described above with the only difference that the edges around the exposed faces of stone are bevelled off at an angle of  $45^\circ$  for depth of 25mm or more.



**Fig. 17 General classification of ashlar masonry: (e) Fine masonry, (f) Rought masonry, (g) Chamfered masonry.**

## 2.3 MECHANICAL MODELS OF MASONRY STRUCTURE

There are two different scale approaches to study the structural response of masonry elements: *micro-mechanical model* and *macro-mechanical model* (Laurenço et al., 1995; Addessi et al., 2014) (**Fig. 18**).



**Fig. 18 Modeling method for masonry structures: (a) masonry sample, (b) detail micro-mechanical model, (c) simplified micro-mechanical model, (d) macro-mechanical model (Laurenço et al., 1995).**

- In the *micro-mechanical model* the masonry is considered as a heterogeneous material, represented as an assemblage of mortar and rigid particles of stone or bricks joined held together by compressive forces. The cracks occurring in masonry are usually located at the mortar joint-brick interfaces, which represent planes of weakness due to the coupling of two different materials.
- The *macro-mechanical model* is based on the use of phenomenological constitutive laws for the masonry material, considered as a homogenized medium. The very small size of the stones compared to the dimension of the whole structure allows us to consider continuous body instead of a discrete system composed of a large number of particles. The masonry is considered as a continuous body instead of a discrete system composed of a large number of particles (Como, 1992).

## 2.4 THE CONSTITUTIVE MODEL

The masonry does not apparently respect any hypothesis assumed for other materials (isotropy, elastic behaviour, homogeneity) and the continued modifications happened in the building history produce several uncertainties in the model definition (geometry, materials, connection etc.).

In order to define a formulation of the constitutive model, according to the macro-mechanical model, the behaviour of the masonry is generally considered intermediate between the behaviour of the brick and mortar, (Fig. 19).

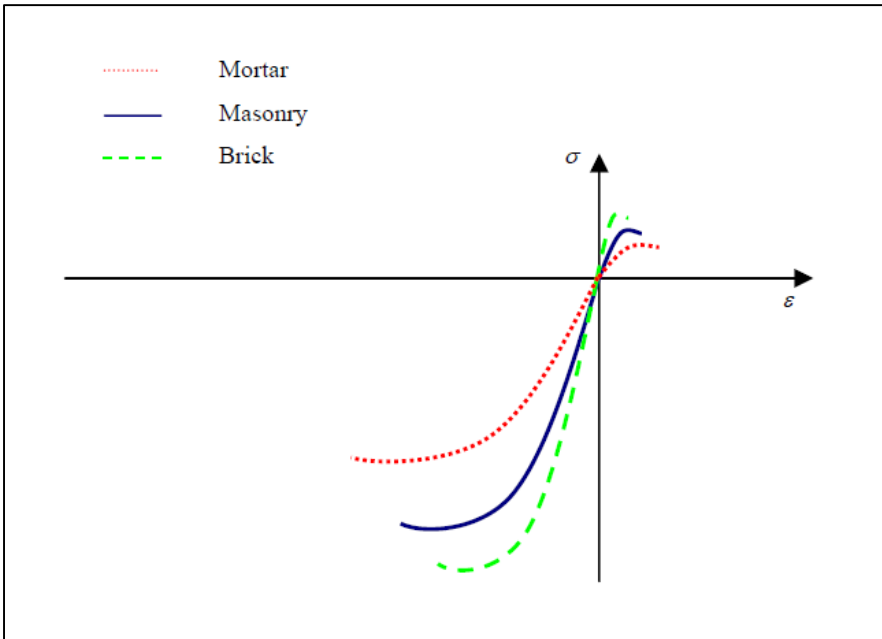
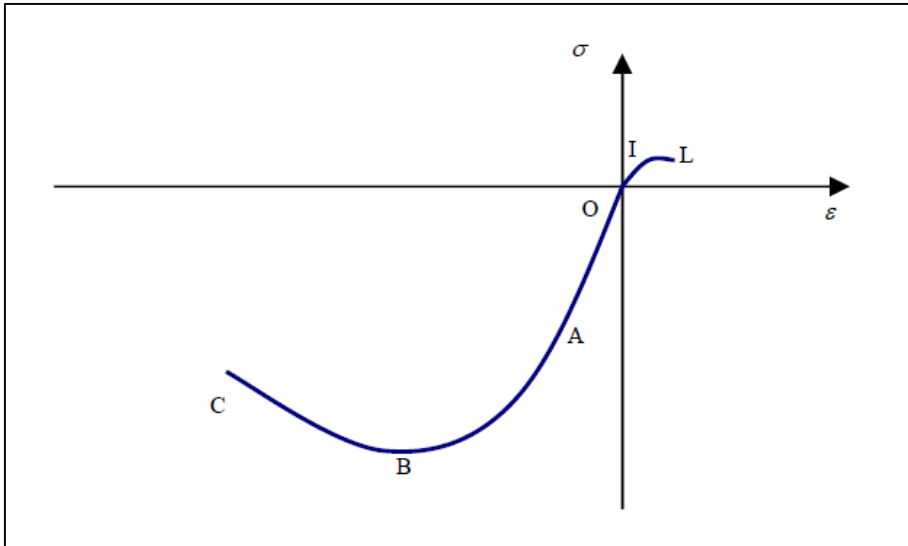


Fig. 19 Qualitative stress-strain diagram in uniaxial tension and compression (Ricamato et al, 2007).

Subjected to a uniaxial load, the masonry material has a stress-strain curve that presents a brittle failure, characterized by a compression stress failure value greater than the tensile one, as illustrated in (Fig. 20).



**Fig. 20 Stress - strain masonry curve (Ricamato et al, 2007).**

In particular, it can be individuated the following characteristic features:

- compression 0-A that is essentially linear; A-B characterized by a nonlinear behaviour, increasing until the maximum value of the compression stress; B-C, decreasing feature with nonlinear behaviour and softening; the point B represents the peak load and the point C represents the point in correspondence of which the masonry material collapses in compression.
- tension 0-I very short feature that has a linear behaviour and I-L decreasing feature.



### 3 NO-TENSION MATERIAL (NTM)

The theory of No Tension Material (NTM), originally formulated by Heyman (Heyman, 1966; Heyman, 1969), is a simple and complete macro-mechanical model in which the masonry continuum can be represented as an assemblage of rigid particles of stone held together by compressive force, incapable of sustaining any tensile stress. Isotropy and homogeneity are assumed.

In-depth studies into the behaviour of elastic no-tension bodies have been conducted by many authors ( e.g. Di Pasquale (1984), Del Piero (1989), Romano and Sacco (1984), Baratta (1991), Como (1992), Giuffrè (1993), Angelillo(1994), Zuccaro and Papa (1996), Addessi et al. (2014)).

This model is a drastic representation of the real behaviour of the masonry and it is considerable as a safety precaution for the structural calculation of the buildings.

The hypotheses of the theory of NTM are that masonry material constituting the structures of monumental and old constructions is often characterized by very low tension strength with respect to the compression strength. Moreover, the tension strength of the masonry can decrease related to the age of the material and for ground vibrations. This model it is almost exactly true if a structure has an irregular texture, made up of bricks laid either dry or with very weak mortar.

In this kind of structures, it isn't possible apply the classic theory of elasticity because the only one reliable resistance is to compression.

In order to define the model of NTM, it is useful to recall the key assumptions introduced by Heyman (Heyman, 1966; Heyman, 1969). He assumed that:

1. *Stone has no tension strength (NTM).*

It is excluded the capacity of the material to resist to tension strength with the possibility of inelastic deformation and the collapse mechanisms are often characterized by the opening of cracks in tension zones.

Concerning this first point Heyman explained that although the stone itself may have some tensile strength, the joints will not, and

no tensile forces can be transmitted from one portion of the structure to another.

2. *Stone has an infinite compressive strength.*

This is equivalent to the assumption that stresses are so low in masonry that there is no danger of crushing of the material. For compressive strength the material has a classic linear-elastic behaviour.

The assumption is obviously unsafe, but the errors introduced are very small: this assumption can be considered adequate only when the collapse mechanism is accompanied by low compressive stresses. On the contrary, when the compression strength plays a significant role in the structural collapse load, the no tension model does not appear to be suitable.

3. *Sliding failure cannot occur.*

It will be assumed that friction is high enough, or that the stone are effectively interlocked, so that they cannot slide one on another. This is assumption did to Coulomb (1773). It implies that wherever there is a weak plane, for example between the bricks, the line of thrust should not depart too far from normality in the plan.

The above no-tension conditions for the masonry continuum can be formulated in a more general form:

The condition (5):

$$\sigma_{max} \leq 0 \tag{5}$$

Holds in the sense that, at any point of the body, the maximum eigenvalue of the normal stress tensor  $\sigma_{max}$  cannot be positive because the stone has not tension strength and the 3x3 matrix  $[\sigma_{ij}]$  ( $i, j = x, y, z$ ) results in being negative and semi-definite.

In the stress components the no-tension condition can be restated as follows (6):



$$\varphi = \sigma_{max} = \frac{\sigma_x + \sigma_y}{2} + \sqrt{\frac{(\sigma_x - \sigma_y)^2}{4} + \tau_{xy}^2} \leq 0 \quad (6)$$

The above equation, that in plane stress conditions takes the shape of a convex cone (Fig. 21), gives the analytical expression of the yield surface  $\varphi$ . The cone has its axis defined by (7):

$$\sigma_x = \sigma_y, \tau_{xy} = 0 \quad (7)$$

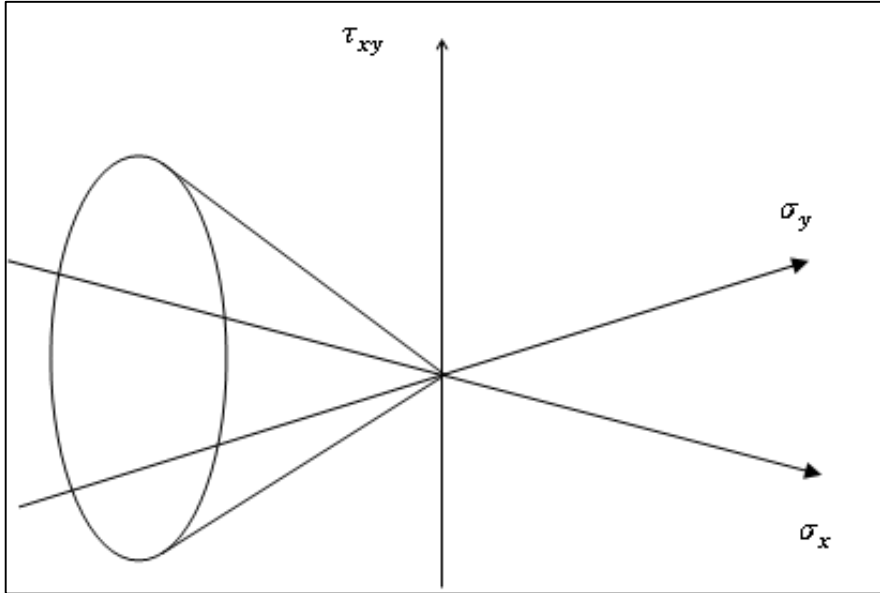


Fig. 21 NTM model: yield surface in  $\sigma_x, \sigma_y, \tau_{xy}$  stress space (Zuccaro and Papa, 1996).

The decomposition of total strain tensor  $\varepsilon_{ij}$  ( $i, j = x, y, z$ ) is assumed also to hold (8):

$$\varepsilon_{ij} = \varepsilon_{ij}^e + \varepsilon_{ij}^c \quad (8)$$

Where:

$\varepsilon_{ij}^e$  is the elastic strains;

$\varepsilon_{ij}^c$  is the inelastic strains or crack strains;

The crack strains  $\varepsilon_{ij}^c$  are produced by the internal fracture of the material and take place if  $\sigma_{max} = 0$ .

### 3.1 THE CONSTITUTIVE MODEL OF NO-TENSION MATERIAL.

#### 3.1.1 Simplified uniaxial models

In paragraph 6.4 a constitutive model for masonry material is presented (Fig. 20). According to the assumptions introduced by Heyman (Heyman, 1966; Heyman, 1969) for the NT material, it is possible analysed simplified models for idealizing the uniaxial masonry-like behaviour.

Fig. 22 shows three simplified models analysed by Angelillo (2014):

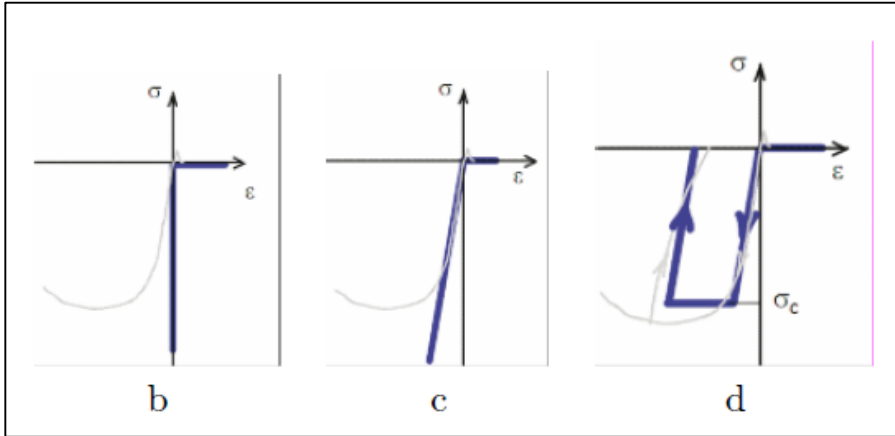


Fig. 22: (a) model *zero*, (b) model *one*, (c) model *two*, (Angelillo, 2014).

The first model proposed the Rigid No-Tension material (Model zero RNT) (Fig. 22 a). This model describes the masonry material as indefinitely strong and stiff in compression but incapable of sustaining tensile stresses. This material is rigid in compression and can elongate freely, a positive deformation of the bar being interpreted as a measure of fracture into the

material (either smeared or concentrated). This statement, that may appear “paradoxical”, derives from the primitive definition of elasticity: stress determined by strain, and the stress has actually a definite value (zero) if the bar elongates.

The second model (Model one ENT) (**Fig. 22 b**) proposed the Elastic No-Tension material (Romano and Romano (1979), Baratta and Toscano (1982), Como and Grimaldi (1985), Romano and Sacco (1985), Castellano (1988), Del Piero (1989), Angelillo (1993)). In this case the uniaxial stress state can be represented with a linear-elastic behaviour for compressive strength and no tension strength. The strain can be positive or negative, positive strain being the fracture part of deformation and negative strain the elastic part.

The last model (Model two ML) (**Fig. 22 c**) adding to model ENT (**Fig. 22 b**), the assumption of a limited strength  $\sigma_c$  in compression. It is assumed that the material behaves as perfectly plastic in compression, therefore the constitutive response becomes incremental and the actual stress state is path dependent, being determined by the whole strain history.

The anelastic part of deformation is further decomposed into a reversible fracture part and in an irreversible crushing part. This is a peculiar perfectly plastic material, since, due to the different behaviour in tension (elastic fracture) and compression (incremental plasticity), the plastic deformations cannot be cancelled by reversing the strain. This model requires the setting of two material parameters: the elastic modulus  $E$  and the strength in compression  $\sigma_c$ , strength and stiffness being still completely neglected in tension.

Any attempt to enrich this model for real applications is usually frustrated by the lack of sufficient confidence on the material properties of the real materials and of their assemblages.

Below will be proposed some formulations of the constitutive problem, all based on the use of mathematical algorithmic.

In order to define the relationship between stress and strain, the NTM model can be divided in two categories, according as it is valid or not the Drucker's stability postulate<sup>3</sup>:

---

<sup>3</sup>Drucker (1952,1958) introduced the idea of a stable plastic material. This postulate, when applied to an element of elastic-plastic materials in equilibrium under the action of surface loads and body forces, may be stated as follows:

- Standard NTM
- No-Standard NTM

### 3.1.2 Approach formulated by G. Del Piero (1989)

This approach stems from three constitutive assumptions:

- infinitesimal elasticity;
- a unilateral constraint on the stress;
- a Drucker postulate of normality;

A material which does not support tension is a material in which the Cauchy stress  $T$  is constrained to be negative- semidefinite (9):

$$T \in \text{Sym}^- \quad (9)$$

---

*“Consider an element initially in some state of stress, to which by an external agency ad additional set of stresses is slowly applied and slowly removed. Then, during the application of the added stresses and in a cycle of application-and-removal of the added stresses, the work done by the external agency is non-negative”.*

Drucker’s stability postulate can be shown to lead to the following two important inequalities:

$$W = \int_{C_0} \Delta\sigma : \partial\varepsilon^p \geq 0 \quad W = \int_{C_0} (\sigma - \sigma^0) : \partial\varepsilon^p \geq 0$$

where

$C_0$  is the closed stress cycle, a loading-unloading path in the stress space.

$W$  is the work done by the external agency.

$\varepsilon^p$  is the plastic deformation

$\sigma$  is the stress tensor

The integrals represent the work done by the external agency over  $C_0$ . It was shown by Drucker (1956) that any material that does not obey this inequality is unstable. It follows, from inequality that:

1. During the application of the additional stress  $\Delta\sigma$ , the work  $W$  done by the external agency must be positive.
2. Over the cycle of the application and removal of the additional stress  $\Delta\sigma$ , the work done by the external agency must be nonnegative. It is zero if only elastic deformation  $\varepsilon^e$  occurs over the cycle; it is positive if there is plastic deformation  $\varepsilon^p$  over the cycle. (A.Khan S.Huang, v,wiley-Interscience Publication, 1995) (Hai-Sui Yu, Plasticity and geothermics, Springer, 2006)

Assume that the infinitesimal strain tensor  $E$  be decomposed into the sum of an “elastic” part  $E^e$  and an “anelastic” part  $E^c$  (10):

$$E = E^e + E^c \quad (10)$$

Assume that there is a linear relationship between  $T$  and elastic strain  $E^e$  (11):

$$T = CE^e \quad (11)$$

$C$  is the elasticity tensor.

Then the anelastic part is defined as (12)

$$E^c = E - E^e = [E - (C^{-1}T)] \quad (12)$$

Assume that  $E^c$  obeys the following hypothesis Drucker’s stability postulate (13):

$$(T - T') \cdot E^c \geq 0 \quad \forall T' \in \text{Sym}^- \quad (13)$$

Eqs. (9) and (13) define a linear elastic masonry-like material.

In the case of a unilateral constraint on the stress (14)

$$\delta(T) \leq 0 \quad (14)$$

And

$$(T' - T) \cdot E^c \leq 0 \quad E^c \in \text{Sym}^+ \quad (15)$$

Then the normality assumption reduces to the linear variation inequality that defined the constitutive equation of no-tension material (16)

$$(T' - T) \cdot E^c = (T' - T) \cdot (E - C^{-1}T) \leq 0 \quad \forall T' \in \chi \quad (16)$$

Where

$$\chi^{def} \{T \in Sym^- : \delta(T) \leq 0\} \quad (17)$$

It is known that this problem admits a unique solution for any  $E \in Sym$  whenever  $\chi$  is convex and  $C$  is positive-definite.

The constitutive equation of the linear elastic masonry-like material can be defined, alternatively, by the system:

- $E = E^e + E^c = C^{-1}T + E^c$ ;
- $T \in Sym^-$  that is the internal constraint;
- $E^c \in Sym^+$
- $T \cdot E^c = 0$  that implies that  $T$  and  $E^c$  are coaxial.

These conditions together are equivalent to variation inequality (16).

### 3.1.3 Approach formulated by A. Baratta et al. (1991, 2005)

This approach starts from the assumptions of the Drucker's stability postulate. The Drucker's postulate assumption implies an analogy of the NRT model with elastic- perfectly- plastic associated flow law.

Assuming that  $\sigma$  is the stress tensor at a generic point P of the wall and denoting by  $\sigma_1$  and  $\sigma_2$  ( $\sigma_2 \leq \sigma_1$ ) the respective principal stress components.

Since the material is not able to resist tensile stresses, it allows for the development of the anelastic strain  $\varepsilon^f$ , defined as "fracture strain tensor".

The fracture strain  $\varepsilon^f$  has the role of transferring the forces deriving from inadmissible tensile stresses to the neighbouring material, in cases where the body has the capacity to achieve equilibrium with the same forces in pure compression.

Assuming that the displacement satisfies the conditions for the strain to be treated as infinitesimal, and denoting by  $\varepsilon$  the total strain tensor at the point, it is possible to write (18, 19):

$$\varepsilon = \varepsilon^e + \varepsilon^f \quad (18)$$

$$\varepsilon^e = C\sigma \quad (19)$$

Where  $C$  denotes the usual tensor of elastic constants and  $\sigma$  is the admissible stress.

The following hypothesis can be assumed:

- i. From Durcker's stability postulate the fracture strain is positive semi-definite (fracture corresponds to a strain state which does not produce contraction of any material element) (20):

$$\varepsilon^f_a \geq 0 \quad \forall a \in r_p \quad (20)$$

$r_p$  denotes the set of lines passing through the generic point  $P$ .

- ii. The stress state is negative semi-definite (the stress state cannot suffer tractions) (21).

$$\sigma_a \leq 0 \quad \forall a \in r_p \quad (21)$$

- iii. On any principal direction where the material is actually compressed, the corresponding coefficient of linear dilatation of the fracture strain must be zero. That is, in symbols (22):

$$\sigma_i < 0 \leftrightarrow \varepsilon^f_i = 0 \quad (22)$$

Then the fracture work is zero. In symbols (23):

$$\sigma \cdot \varepsilon^f = 0 \quad (23)$$

From the hypothesis it follows that:

- If  $\sigma = 0 \rightarrow \sigma_2 = \sigma_1 = 0$

In this case the material hasn't a compression stress and it can be fractured in any directions.

When the tensor stress is equal to zero, any directions are principal directions so the fracture strain tensor and the stress tensor are coaxial.

- If  $\sigma < 0 \rightarrow \sigma_2 < 0 ; \sigma_1 < 0$   
In this case the material is compressed in any directions. From hypothesis (iii):

$$\sigma_a < 0 \leftrightarrow \varepsilon_{fa} = 0 \quad \forall a \in r_p$$

The fracture strain tensor is equal to zero so also in this case the fracture strain tensor and the stress tensor are coaxial.

- If  $\sigma \leq 0 \rightarrow \sigma_2 < 0 ; \sigma_1 = 0$   
From hypothesis (iii):

$$\sigma_2 < 0 \leftrightarrow \varepsilon_a^f = 0 \quad \forall a \in r_p$$

From hypothesis (ii) fracture strain tensor is always not negative than  $\varepsilon_n^f$  is a minimum value and it is a principal direction. Also in this case the fracture strain tensor and the stress tensor are coaxial.

From the Drucker's stability postulate (24):

$$(\sigma' - \sigma) \cdot \varepsilon^f \leq 0 \quad \forall \sigma' \in \Sigma \quad (24)$$

Where  $\sigma'$  is any admissible stress state other than the effective  $\sigma$ .

Summarizing, the fracture strain is characterized by nonnegative principal components and it is coaxial with the strain tensor because they have the same principal directions.

In order to formulate explicitly the relationships that express the fracture strain as a function of the stress, let us consider that the space of symmetrical bidimensional second-order coaxial tensors is a two-dimension vector space.

Consider the two-dimension vector space constituted by the stress tensor  $\sigma$  and the unit tensor  $\mathbf{I}$ , it is possible to express the fracture strain through the superposition of two tensor, both coaxial to the stress tensor (25):



$$\varepsilon^f = \theta_f \left[ \sigma - \frac{|\sigma|^2}{|\sigma_1 + \sigma_2|} \mathbf{I} \right] + \delta_f \varepsilon^{f*} \quad (25)$$

where  $\varepsilon^{f*}$  is the free fracture that can develop at the point when the stress state is zero.

The coefficients  $\theta_f$  and  $c$  are parameters that control the activation of the different types of fracture strain, and are subject to the following conditions (26-31):

$$\theta_f \cdot \delta_f = 0 \quad (26)$$

Then if  $\theta_f = 0 \leftrightarrow \delta_f c \neq 0$  and viceversa.

$$|\sigma|^2 \cdot \delta_f = 0 \quad (27)$$

Then if  $\sigma = 0 \leftrightarrow \delta_f \neq 0$  and viceversa.

$$\delta_f \cdot \varepsilon^{f*} \geq 0 \quad (28)$$

Then

$$\varepsilon_n^f \geq 0 \quad \forall n \in r_p \quad (29)$$

$$\theta_f \cdot \sigma_1 = 0 \quad (30)$$

$$\theta_f \geq 0 \quad (31)$$

### 3.1.4 Approach formulated by D. Addessi et al. (2014)

This approach assumed that the total strain  $\varepsilon$  is partitioned into the sum of an elastic part  $\varepsilon^e$  and two inelastic contributions  $\varepsilon^f$  and  $\varepsilon^c$ , which account for fracture (in tension) and crushing (in compression), respectively (32):

$$\boldsymbol{\varepsilon} = \boldsymbol{\varepsilon}^e + \boldsymbol{\varepsilon}^f + \boldsymbol{\varepsilon}^c \quad (32)$$

A linear elastic relationship between the admissible stress  $\sigma$  and the elastic strain  $\boldsymbol{\varepsilon}^e$  is assumed:

$$\sigma = \boldsymbol{\varepsilon}^e C \quad (33)$$

$$C = \frac{E}{1-\nu^2} \begin{vmatrix} 1 & \nu & 0 \\ \nu & 1 & 0 \\ 0 & 0 & (1-\nu)/2 \end{vmatrix} \quad (34)$$

Where:

$C$  is the isotropic elasticity matrix;

$E$  is the masonry Young's modulus;

$\nu$  is Poisson ratio;

The inelastic fracture strain  $\boldsymbol{\varepsilon}^f$  occurs in the masonry material when the maximum normal stress reaches the zero strength value.

Defined a two-dimensional plane stress elastoplastic and denoting with  $\sigma_1$  and  $\sigma_2$  the principal values of the stress.

The admissible stress domain  $K$  is defined as:

$$K = \{\sigma: \sigma_1 \leq 0, \sigma_2 \leq 0\} \quad (35)$$

The fracture strain tensor  $\boldsymbol{\varepsilon}^f$  is assumed to fulfil a normality rule with respect to  $K$ .

The Drucker's postulate hypothesis implies the conditions:

$$(\sigma' - \sigma) \boldsymbol{\varepsilon}^f \leq 0, \quad \sigma \in K \quad \forall \sigma' \in K \quad (36)$$

Where  $\sigma'$  is any admissible stress state other than the effective one  $\sigma$ .

Accordingly, the fracture strain  $\varepsilon^f$  can be characterized as the solution of the following nonlinear problem:

$$\varepsilon^f = \arg \min_{H \in K^o} \left\{ \frac{1}{2} (\varepsilon^{ec} - H)^T C (\varepsilon^{ec} - H) \right\} \quad (37)$$

Where:

$$\varepsilon^{ec} = \varepsilon^e + \varepsilon^c$$

$K^o$  is the polar cone of  $K$ .

It can be proved that, for the isotropic case, the fracture strain  $\varepsilon^f$ , the strain  $\varepsilon^{ec}$  and the stress  $\sigma$  are coaxial and they present common principal directions.

Setting  $\varepsilon^{ec}_1 \leq \varepsilon^{ec}_2$ , the fracture strain principal components are determined as:

- $\varepsilon^{ec}_1 \leq 0$   $\varepsilon^{ec}_2 + \nu \varepsilon^{ec}_1 \leq 0$  no fracture is possible, so that the fracture principal strains result:

$$\varepsilon^f_1 = 0 \quad \varepsilon^f_2 = 0$$

- $\varepsilon^{ec}_1 > 0$  the material is completely fractured and the  $\varepsilon^{ec}_1$  fracture principal strains result:

$$\varepsilon^f_1 = \varepsilon^{ec}_1 \quad \varepsilon^f_2 = \varepsilon^{ec}_2$$

- $\varepsilon^{ec}_1 \leq 0$   $\varepsilon^{ec}_2 + \nu \varepsilon^{ec}_1 > 0$  no fracture is possible, so that the fracture principal strains result:

$$\varepsilon^f_1 = 0 \quad \varepsilon^f_2 = \varepsilon^{ec}_2 + \nu \varepsilon^{ec}_1$$

The plastic yield function, based on the Drucker-Prager written in terms of the principal stresses  $\sigma_1$  and  $\sigma_2$  as:

1

$$F = \sigma_1 + \sigma_2 - \beta \sigma_1 \sigma_2 - \sigma_y^2 \leq 0 \quad (38)$$

Where:

$\beta$  is a material parameter;  
 $\sigma_y$  is the initial yield limit value;

The evolution law of the plastic strain is ruled by the equation:

$$\dot{\epsilon}^c = \dot{\lambda} \frac{\delta F}{\delta \sigma} \quad (39)$$

Where:

$\lambda$  is Lagrange multiplier satisfying the loading-unloading and the consistency conditions:

$$\dot{\lambda} \geq 0, F \leq 0, \dot{\lambda} \cdot F = 0 \quad (40)$$

In Fig. (Fig. 23), the set of admissible stresses and the inelastic strain are schematically illustrated.

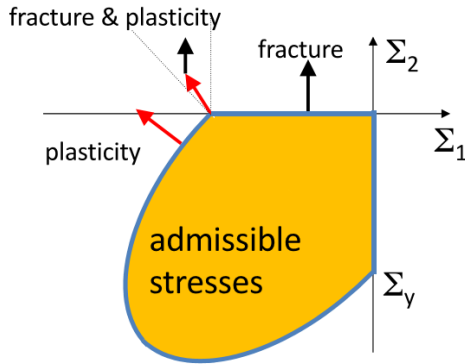


Fig. 23 No-tension plastic admissible stresses: normality rule of the fracture and crushing tensors. (D. Addessi, S. Marfia, E. Sacco and J. Toti , 2014)

## 4 COLLAPSE MECHANISMS OF MASONRY STRUCTURES

### 4.1 INTRODUCTION

The seismic assessment of historical masonry buildings is a complex task because the global behaviour of this kind of structures depends on various factors, as the behaviour of the single walls, the connections between them, the typology and stiffness of the floor (flexible or rigid diaphragms), and the strong nonlinearities of the material.

This work, based on Heyman's general principles of limit analysis (Heyman 1966, 1995, 1998), examines the collapse mechanisms of masonry structures in response to horizontal ground accelerations. The masonry structure is analyzed using rigid block or “macro-elements” analysis based on equilibrium and making work calculations in order to verify the stability of the structure and determine the critical collapse mechanism.

The collapse of a masonry structure may be caused by one of three general actions:

- i. applied loading (as in the overloading of a masonry bridge);
- ii. applied displacements (as in the differential settlement of foundations);
- iii. applied ground accelerations (as in the case of an earthquake) (**Fig. 24**);

Engineers have already explored the first action in some detail, particularly for masonry bridges.

The second action is a very real problem, particularly due to the long-term movements of the deformable foundations of a masonry building. Likewise, ground accelerations as a result of seismic activity are also a significant threat to masonry structures.

This study focusses on the third actions and seeks to determine the influence of applied accelerations on the stability of masonry structures.

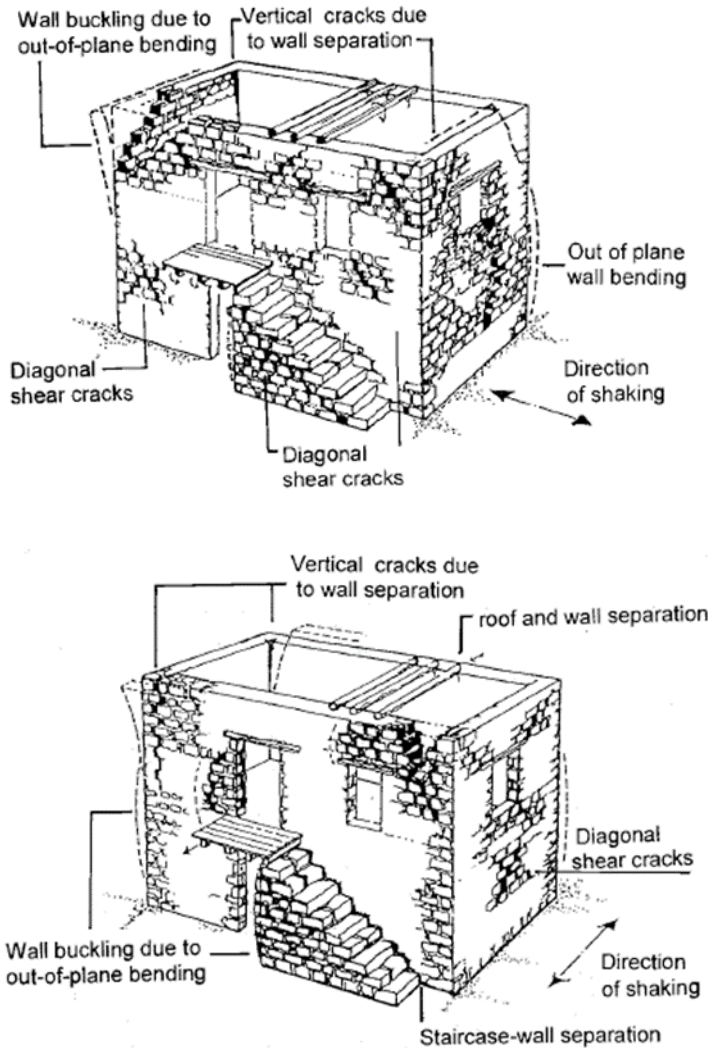


Fig. 24 Typical earthquake damage of masonry structures due to different direction of shaking (Pitta, 2000).

In particular, the research investigates the conditions necessary for collapse to occur on the structure. The influence of seismic action can be approximated to first order by equivalent static analysis to determine the initial collapse mechanism.

## 4.2 THEORY OF MASONRY STRUCTURES

There are two dominant theories for the structural analysis of masonry (Ochsendorf, 2002): elastic analysis and limit analysis. Both theories require the analyst to make assumptions about the material properties.

### 4.2.1 Elastic analysis

The classic elastic analysis requires numerous assumptions, many of which are not justifiable for masonry structures. This structural analysis was introduced by Navier (1826) to determine the stress state in statically indeterminate structures. The engineers have applied this theory to the design and assessment of structures.

Elastic analysis assumes that the material is a continuum, which behaves as a linear-elastic solid. The method is inappropriate for assessing masonry structures for the following reasons:

- The deformations in masonry structures are not due to elastic deformations of the masonry material, and cannot be predicted satisfactorily by an elastic analysis.
- The exact stress state is unknowable in a masonry structure, due to the unknown loading history, boundary conditions, and material properties.
- The material is heterogeneous, and is separated by joints and fractures throughout, making it unreasonable to model as an elastic continuum.

### 4.2.2 Limit analysis

In the 20th century there were many studies (Kooharian (1952), Como (1985), Heyman 1998; Giuffrè, 1999; D'Ayala et al, 2002, Zuccaro et al, 2009 ) based on the limit analysis for masonry structures by using equilibrium, combined with kinematic analysis of mechanisms, to examine the safety of masonry structures.

The problem is to define the stability conditions for rigid-block structures using conventional structural mechanics.

The three well-known assumptions required to apply limit analysis to masonry are (Heyman 1966, 1995, 1998):

- i. masonry has no tensile strength;
- ii. masonry has an infinite compressive strength;
- iii. sliding failure does not occur;

The first assumption is slightly conservative, but is accurate. Stone is very weak in tension, and mortar joints do not provide significant tensile resistance between stones. The final assumption is generally true, since the very high friction between stones is sufficient to prevent sliding in most cases.

These three assumptions, analysed in details in the previous chapter of this thesis, lead to simple computations which provide accurate predictions of the behaviour of masonry structures.

The aim of the limit analysis is to evaluate the load capacity and the collapse mechanism of structures. Considering the limit behaviour of the material, through a definition of a yield function  $\phi$  in terms of stresses, it is assumed that if  $\phi < 0$  the material remains in the elastic phase, if  $\phi = 0$  the material becomes plastic and if  $\phi > 0$  the stress state is inadmissible. The conditions  $\phi \leq 0$  represent the admissible stresses.

According to the definition of  $\phi$ , all points that are inside or on the yield surface are admissible, while all points located outside the yield surface are inadmissible.

For a structure, it is possible to define a statically admissible state (safe state) for which the internal stresses are in equilibrium with the external forces and the yield conditions are fulfilled in all the points.

This research follows a simplified limit state analysis proposed by the MEDEA methodology (Zuccaro et al, 2002). MEDEA (Manual for Earthquake Damage Evaluation and safety Assessment) is a manual used for the evaluation of the damage due to a seismic event on masonry or reinforced concrete building. According to this methodology, the limit state analysis consists in modelling the analyzed building structure by means of macro-elements and in assuming a set of the collapse mechanisms which have been observed as the most significant in the structures.



### 4.3 COLLAPSE MECHANISMS CLASSIFICATION

According to MEDEA (Zuccaro et al, 2002) the Collapse Mechanisms are classified as:

- Global mechanisms (Fig. 25).

Global mechanisms are those mechanisms involving the structures as a whole and then related to the evolution of the cracks in a sufficient number of elements such that a total compromising of the static and dynamic equilibrium of the structural system is achieved.

For masonry structures, the global mechanisms have been subdivided as follows:

- i. in plane: these mechanisms occurs when the walls of the masonry box, excited by in plan actions in both versus, respond by showing the classical diagonal X cracks, consequent to the formation of diagonal compressive beams. This mechanisms are due to poor tensile strength of the masonry material;
- ii. out of plane: damage mechanisms that appear through an out of plane kinematism of one or more walls of the masonry box that, under seismic actions, loses his own original tothing connection between the walls of the facade and the orthogonal ones, possibly aided by the action of thrusting floors and roofs;
- iii. other mechanisms: in this category are classified those mechanisms that couldn't directly be recognized as in plane or out of plane, nevertheless are able to involve the building as a whole, generating the total collapse of the structure.











GLOBAL MECHANISMS					
1	Storey shear mechanism		2	Storey shear mechanism (upper storeys)	
3	Whole wall overturning		4	Partial wall overturning	
5	Vertical instability of the wall		6	Wall bending rupture	
7	Horizontal sliding failure		8	Foundation subsidence	
9	Irregularity between adjacent structures		10	Floor and roof beam unthreading	

Fig. 25 MEDEA: Global Collapse Mechanisms (masonry). (Zuccaro et al. 2010).

- Local mechanisms (Fig. 26).

This kind of mechanisms are concerned to marginal parts of the structure; their evolution, even if determines the collapse of a single element, generally does not involve the whole structural equilibrium.

The local mechanisms have been classified as:

- for localized dislocation: these mechanisms are those, for example, that arise for arch or architrave failure, or in part of the structure characterized by different irregularities, often connected to significant stiffness variations.
- for thrusting elements: these mechanisms are determined by the action of single elements at produce horizontal thrust on the supporting structures.







LOCAL MECHANISMS					
11	Lintel or masonry arch failure		12	Material irregularity, local weakness	
13	Roof gable wall overturning		14	Corner overturning in the upper part	
15	Overturning of the wall supporting the roof		16	Vault and arch overturning	

Fig. 26 MEDEA: Local Collapse Mechanisms (masonry) (Zuccaro et al. 2010).

#### 4.4 GLOBAL COLLAPSE MECHANISMS

This research analysed a set of global collapse mechanisms, which have been observed as the most significant in masonry structures.

According to the MEDEA classification (Zuccaro et al, 2002), considering a single wall, it is possible to distinguish two different types of failure that lead to two different collapse mechanisms: out-of-plane and in-plane failures, which correspond to collapses that are called first mode and second mode collapse mechanisms respectively.

The first mode mechanism regards only parts of the wall and occurs when a wall is subjected to an out-of-plane action and there is poor anchorage of the orthogonal walls or a poor connection between floor and walls. The second mechanism regards entire panels and occurs when a load is applied in the same plane of the masonry wall (Fig. 27).

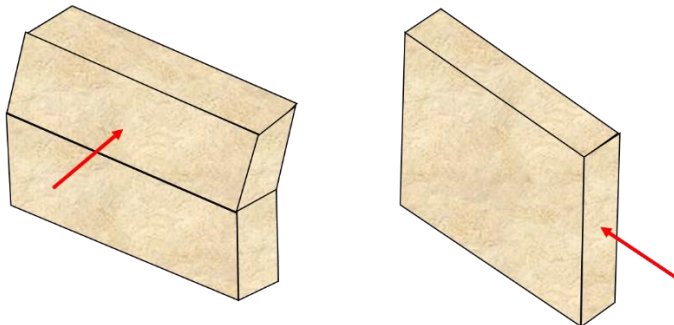


Fig. 27 Out-of-plane (left) and in-plane (right) behaviour of a single wall.

The analysis method is based on the Equilibrium Limit Analysis. It takes in consideration Kinematic theorem, applied to the masonry considered as an assemblage of rigid blocks or “macro-element”, held together by compressive force and liable to crack as soon as tension stress begin to be development.

More in detail, a macro-element is the building portions structurally recognisable with an autonomous behaviour respect to the whole building. Macro-elements are defined by single or combined structural components, (walls, floors and roof), considering their mutual bond, (potential damage pattern, cracks, borders of poor connections, etc...), and restraints, (e.g. the presence of ties or ring beams), the constructive deficiencies and the characteristics of the constitutive materials. They behave independently as a whole without any support by other portions of the building, but they follow kinematic mechanisms, both out- and in-plane.

This approach is based on the observation of the real behaviour of masonry structures. They are generally characterized by a negligible elastic deformation of the single parts, although displacement and rotations are possible.

Once defined a set of possible mechanisms the equilibrium is possible only under load particular conditions. The value of the load multiplier  $\alpha$  for which the structure is in equilibrium is defined collapse load multiplier. The effective collapse mechanism is the one for which the load multiplier (or collapse multiplier) determines an admissible stress state (no tension) in the whole structure.

For each of the adopted limit states, the analysis computes the collapse multiplier  $\alpha$ , significant of the horizontal loads, for which the macro-element model attains the ultimate limit state relevant to each considered mechanism. The corresponding value  $a_g$  of the trigger seismic base acceleration is computed by the typical relationship (41) [CM, 2009-C8A.4.9]:

$$a_g = \frac{\alpha q}{S} g \quad (41)$$

where:

- $a$  is the horizontal mass multiplier;
- $q$  is the ductility factor;
- $S$  is the subsoil factor, fixed equal to 1.25;

$g$  is the gravity acceleration ( $9,81 \text{ m/s}^2$ );

It is worth to emphasize that value of the collapse acceleration depends on the typological and structural properties assumed for the analysed virtual model. Such structural features can be considered as *typological vulnerability factors* since their combination has a great influence on the building capacity.

## 4.5 IN-PLANE COLLAPSE MECHANISMS

In-plane collapse mechanisms, according Giuffrè definition (Giuffrè, 1993), can be considered as “second mode mechanisms”. The associated damage (shear cracks) generally does not lead the structure to collapse, but it can facilitate contemporary out-of-plane mechanisms.

In general, several in-plane collapses present a classical X-shaped crack pattern due to diagonal orientations of the tensile-compressive principal stresses. Such a behaviour is typical of shear or slip failure which are assumed as the first two collapse mechanisms of the presented procedure. Moreover, it is considered a further collapse behaviour, although not as frequent as the previous ones, consisting in the vertical buckling of the rectangular panel (Fig. 28).

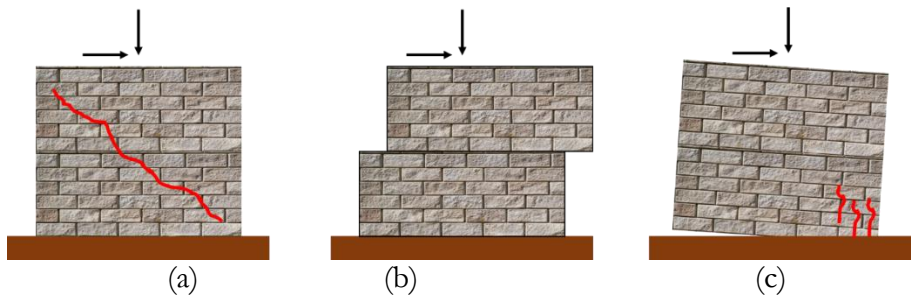


Fig. 28 In-plane collapse mechanisms: failure modes in unreinforced masonry walls (a ) Shear crack, (b) Failure by slip, (c) Buckling failure.

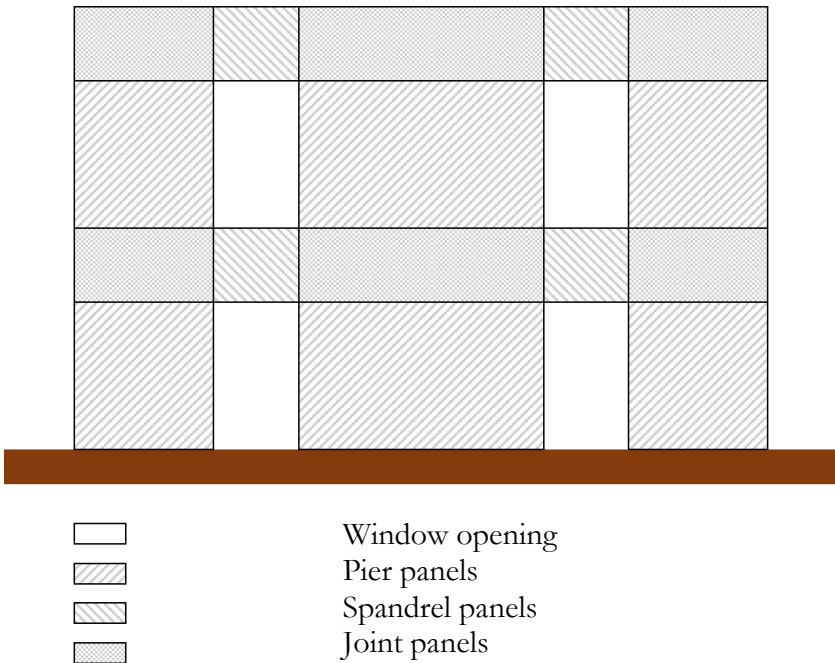
Different models for the assessment of masonry structures exist in the literature. A simple approach includes models that schematize a masonry wall in one-dimensional model with macro-elements. Various authors

proposed these kinds of models (D'Ayala et al, 1995, Gambarotta and Lagomarsino, 1997).

In this approach the wall is described by a set of macroscopic no tensile elements, which represent (Fig. 29):

- the pier panels, which are the vertical macro-elements between two or more consecutive openings. They are the principal vertical resistant elements for seismic loads.
- the spandrel panels, which are the horizontal macro-elements between two or more consecutive openings- They are the second resistant elements.
- the joint panels, which link pier and spandrel panels;

The advantage of the macro-elements approach is represented by a reduction of the degrees of freedom that reduces the computational effort.



**Fig. 29 Macro-Element model of the masonry structure.**

In this approach, the value of trigger acceleration of the mechanism is calculated to a single masonry panel considering the distribution of the seismic forces on the different panels.

It is worth being emphasized that, whenever the original wall is composed by more than a single panel, each sub-element presents a peculiar value of the collapse mass multiplier  $\alpha$  and, subsequently, of the trigger acceleration  $a_g$ . In such a case, the original wall is assumed to behave as a series system so that its collapse multiplier corresponds to the minimum  $\alpha$  computed in all its sub-elements.

All the considered in-plane collapse mechanisms are analysed by considering a rectangular panel with thickness  $s$ , height  $h$  and width  $l_p$  subject to vertical compression  $N$  and to a shear action  $T$  at the lower and upper base. In conclusion, the in-plane collapse mechanisms considered in this study are:

- Shear crack,
- Failure by slip,
- Buckling failure.

Their limit conditions are reported below.

#### **4.5.1 Shear crack**

Shear strength of masonry structure significantly affects the seismic behaviour of existing masonry buildings. Usually, masonry panels subjected to seismic loads in their plane collapse for shear with diagonal cracking and a specific failure criterion has been formulated to predict the ultimate shear strength. Originally, this criterion was proposed by Turnsek and Cacovic (Turnsek V. et al, 1971), and it has been included in the current Italian seismic Code for buildings (NTC, 2008).

The assumed limit state condition consists in the opening of a diagonal crack, as shown in **Fig. 30**, **Fig. 31**, **Fig. 32**, depending on the attainment of the tensile limit value by the stress components orthogonal to the crack direction.



Fig. 30 Diagonal shear cracks due to earthquake Central Italy- Amatrice 2016.



Fig. 31 Diagonal shear cracks due to earthquake Central Italy- Arquata del Tronto 2016.





**Fig. 32 Diagonal shear cracks due to earthquake Central Italy- Illica (Accumuoli) 2016.**

Denoted by  $\tau_k$  the characteristic value of the limit shear stress component and setting  $N$  equal to the normal compression strength, the shear strength  $T_u$ , i.e. the value of the horizontal shear corresponding to the attainment of the ultimate limit state, is computed as the equation (42):

$$T_u = (l_p s \tau_k) \sqrt{1 + \frac{N}{p(l_p s \tau_k)}} \quad (42)$$

Where  $p$  is a coefficient accounting the distribution of the shear stress components over the panel. Usual values of  $p$  span between 1, in the case of thick walls, and 1.5, for thin panels.  $l_p$  is the length of the panel and  $s$  is the wall thickness;

Turnsek and Cacovic obtained equation (42) considering a masonry panel loaded in its plane by a vertical compressive action and a horizontal shear force, with double bending boundary conditions (**Fig. 33**).

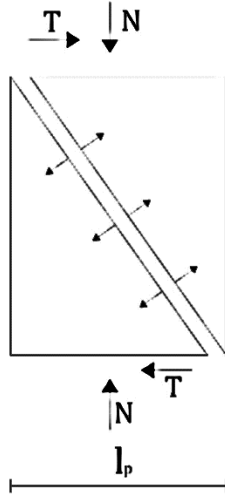


Fig. 33 Shear crack mechanism

They supposed that the first crack appears at the centre of the panel when the principal tensile stress reached the tensile strength of the masonry.

Defined:

- a)  $\sigma_n = \frac{N}{l_p s}$  the normal compressive stress;
- b)  $\tau_n$  the medium shear stress;
- c)  $\tau_r = \frac{T_u}{l_p s}$  the shear stress at failure;
- d)  $\tau_m = p\tau_r$  the maximum limit shear stress;
- e)  $\sigma_k = p\tau_k$  the characteristic value of the limit compressive stress;
- f)  $\tau_k = \frac{\sigma_k}{p}$  the characteristic value of the limit shear stress;

The state of stress which is located at the intersecting point of the diagonals cracks can be analysed by the Mohr's circle (Fig. 34).

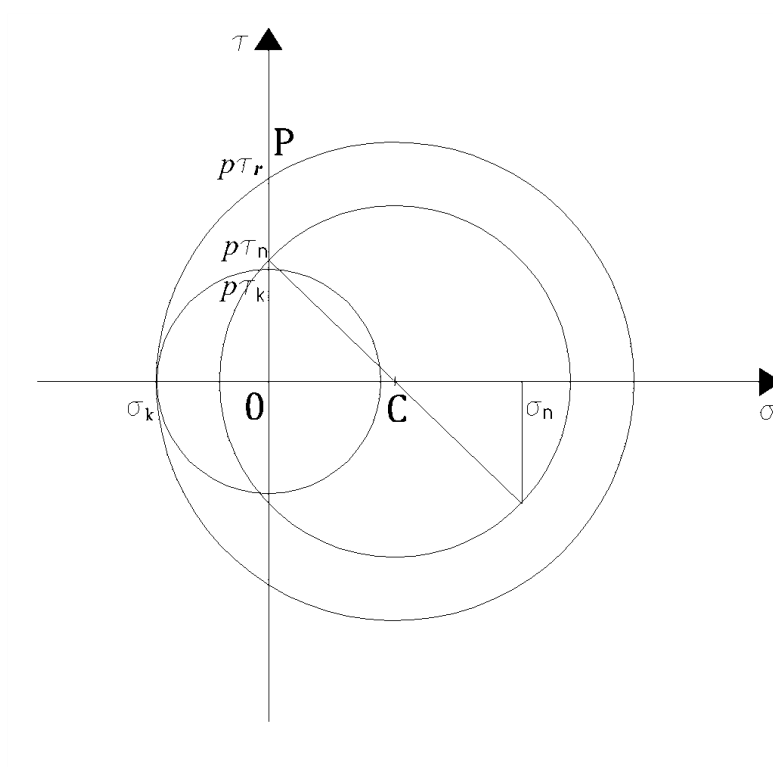


Fig. 34 Mohr's circle for shear crack stress.

Considering the triangle CPQ, using Pitagoras's theorem it is possible to write the analytic relation (43) between  $\sigma_n$ ,  $\sigma_k$ ,  $\tau_r$  :

$$\left(\sigma_k + \frac{\sigma_n}{2}\right)^2 = (p\tau_r)^2 + \left(\frac{\sigma_n}{2}\right)^2 \quad (43)$$

From the definition of the characteristic value of the limit compressive stress (e) it is possible to defined  $\tau_r$  (44):

$$\tau_r = \tau_k \cdot \sqrt{1 + \frac{\sigma_n}{p\tau_k}} \quad (44)$$

From the definition of shear stress at failure (c) it is possible to write the final equation (42) of the limit shear strength  $T_u$ .

From the limit shear strength  $T_u$  and the value of the mass of the panel  $M$  it is possible to write the horizontal mass multiplier (45):

$$\alpha = \frac{T_u}{M} \quad (45)$$

#### 4.5.2 Failure by slip

A similar limit state condition concerns the slip collapse mechanism shown in **Fig. 35**, **Fig. 36**, where the crisis of the panel is assumed to be activated by the attainment of the tensile limit of the stress component parallel to the crack.

In such a case, the shear strength  $T_u$  is computed by the relationship (46) provided by the Italian structural code (NTC08) (**Fig. 37**):

$$T_u = l_p s f_{vk} \quad (46)$$

where  $f_{vk}$  is the characteristic value of the limit shear stress of the panel. According with the Mohr–Coulomb failure criterion (Coulomb, 1775; Mohr, 1882)  $f_{vk}$  is defined by (47):

$$f_{vk} = f_{vk0} + \mu \sigma_n \quad (47)$$

With  $f_{vk0}$  is denoting the characteristic shear stress of the material and  $\sigma_n$  the normal compressive stress component acting among the panel.  $\mu$ , whose value is between  $0,30 \div 0,80$ , is the coefficient of friction. The

Italian structural code (NTC08) suggests to use a coefficient of friction of 0,4.

From the limit shear strength  $T_u$  and the value of the mass of the panel  $M$  it is possible to write the horizontal mass multiplier (45).



Fig. 35 Failure by slip due to earthquake Central Italy- Pescara del Tronto 2016.



Fig. 36 Failure by slip due to earthquake Central Italy- Illica (Accumuli) 2016.

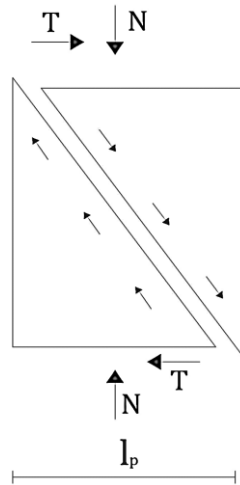


Fig. 37 Failure by slip

### 4.5.3 Buckling failure

The last in-plane collapse condition, considered in this research, models the crisis due to the combination of vertical compression and uniaxial bending of a rigid rectangular panel.

Assuming a compressive-only behaviour of the material, the maximum values of the compressive stress, for which collapse is induced, are clustered at the extreme base region of the panel, as sketched in **Fig. 38**, **Fig. 39**, **Fig. 40**. In fact, because of the rigid behaviour of the panel, bending induces a rigid rotation about the axis orthogonal to the middle plane.

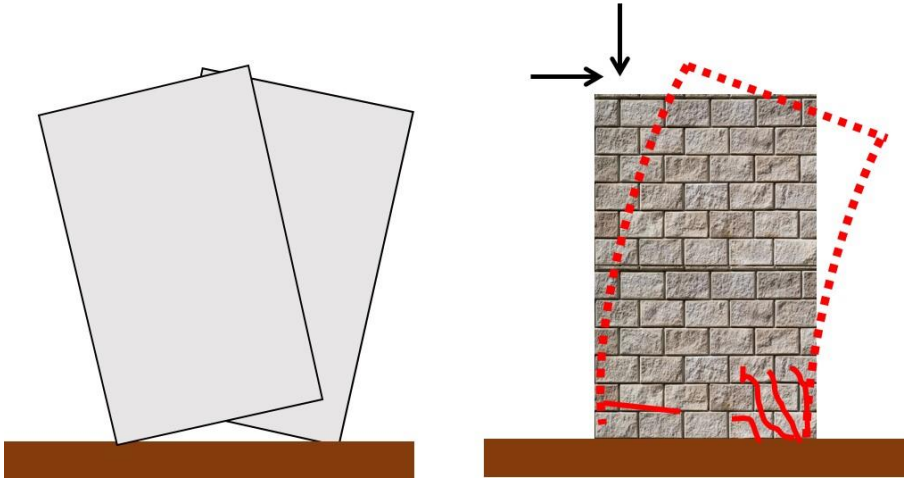


Fig. 38 Buckling failure of a masonry wall



Fig. 39 Buckling failure due to earthquake Central Italy- Accumuli, 2016

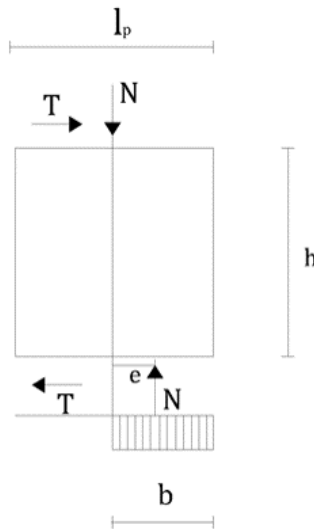


Fig. 40 Buckling ultimate limit state



Defined:

The normal compressive strength  $N$ :

$$N = \sigma_n l_p s \quad (48)$$

The length of stress diagram  $b$ :

$$b = \frac{N}{0,85 f_d s} \quad (49)$$

The eccentricity of the normal compressive strength  $e$ :

$$e = \frac{l_p - b}{2} \quad (50)$$

The panel limit state is defined by the ultimate value of the bending moment  $M_u$  which is computed:

$$M_u = N e \quad (51)$$

From Eqn. (49-50-51) it is possible to write the simplified equation for the ultimate value of the bending moment  $M_u$  (52), provided by the Italian code [NTC, 2008]:

$$M_u = \left( l_p^2 s \frac{\sigma_n}{2} \right) \left( 1 - \frac{\sigma_n}{0,85 f_d} \right) \quad (52)$$

where  $\sigma_n$  is the vertical compressive stress component of the panel and  $f_d$  is the characteristic value of the compressive limit stress of the masonry. Assuming the static constraint of the wall be fixed at the base and linked support at the top, by equilibrium considerations (53), the ultimate shear strength  $T_u$  of the panel is (54):

$$T_u h = 2M_u \quad (53)$$

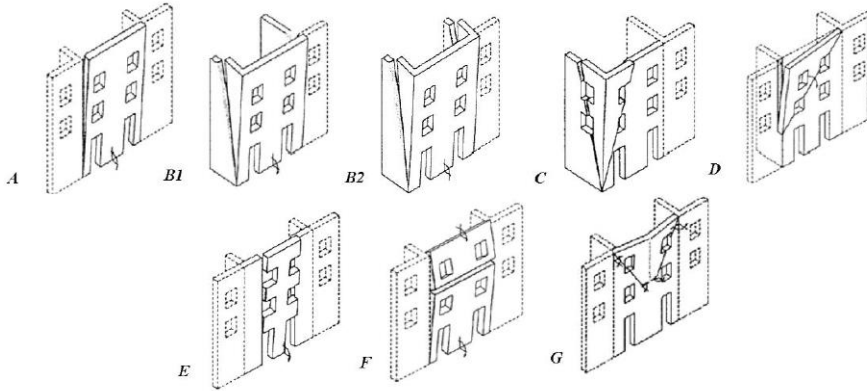
$$T_u = \frac{2M_u}{h} \quad (54)$$

with  $h$  denoting the height of the panel.

From the limit shear strength  $T_u$  and the value of the mass of the panel  $M$  it is possible to write the horizontal mass multiplier (45).

#### 4.6 OUT-OF-PLANE COLLAPSE MECHANISM

Out of plane collapse mechanisms consist in cinematically indeterminate displacements of one or more structural elements compromising the structural capacity of the model (Fig. 41). Such behaviours can be induced by different phenomena, such as ineffective connections between contiguous walls, insufficient anchoring of the floors or out-of-plane horizontal loadings due to vaults, floors and roofs. In some cases, diagonal cracks due to in-plane mechanisms behave as cylindrical hinges although this last case usually occurs for high levels of overall damage.



**Fig. 41 Out-of-plane failure mechanisms of the FaMIVE method (D'Ayala and Speranza 2003)**

Regardless of the nature of kinematic collapse, such mechanisms are particularly dangerous in absence of temporary retaining structures even if the incipient kinematic indeterminacy has not completely developed. In this respect, after the attainment of in-plane limit states, structural elements usually present a residual capacity due to their ductility so that the structural model is capable of achieve a sufficiently stable equilibrium condition. On the contrary, several cases of incipient out-of-plane collapse correspond to values of the potential energy which, although stationary, are not local minima; thus, even limited perturbations can trigger disastrous failure. For this reason, the analysis of such a class of collapse mechanisms is of outmost importance in estimating the structural vulnerability.

Because of the kinematic indeterminacy of the schemes modelling out-of-plane mechanisms, the estimation of the collapse multiplier  $\alpha$  related to a structural panel must be performed by applying the virtual work theorem according to the Lagrange's procedure.

To this end, following the macro-element philosophy adopted in this analysis, the limit state conditions are computed by means of rectangular panels subject to a standardised set of loads. In particular, the generic panel is subject to  $m$  vertical loads  $P_{Si}$  due to the floorings; the horizontal load  $P_H$  due to the roof; the horizontal load  $T_i$  due to any tie-beams at top; and  $r$  static actions related to arches and vaults, characterized by means of their vertical  $F_{Vi}$  and horizontal  $F_{Hi}$  components where subscripts  $i$  are progressive indexes.

Each collapse mechanism is characterized by the presence of a cylindrical hinge; therefore, the panel is partitioned in  $n$  regions, whose self-weight is defined as  $W_i$ , which can rotate independently about the hinge's axis. The kinematic scheme determines the distances of the static actions with respect to the location of the hinge. Specifically, assumed the hinge as origin of a horizontal-vertical reference system, the centre of mass of the  $i$ -th sub-panel is located at  $[X_{Gi}, Y_{Gi}]$ ; the actions  $P_H$  and  $P_{Si}$  are applied at  $[d_i, h_i]$ , while the coordinates of actions  $F_{Hi}$  and  $F_{Vi}$  are  $[d_{vi}, h_{vi}]$ . Analogously to the in-plane mechanisms, the simplified analysis aims to determine the collapse multiplier  $\alpha$  of the horizontal loads which is computed by defining a rotational equilibrium relationship with respect to the hinge location:

$$\begin{aligned} \alpha \left( \sum_n W_i Y_{Gi} + \sum_m P_{Si} d_i \right) + \sum_r F_{Hi} h_{vi} \\ = \sum_n W_i X_{Gi} + \sum_m P_{Si} h_{si} + \sum_s F_{Vi} d_{vi} \end{aligned} \quad (55)$$

It is worth being emphasized that the left side of Equation (55) represents the momentum of the horizontal actions about the hinge axis. The presence of  $W_i$ ,  $P_{Si}$  and  $F_{Vi}$ , formally vertical actions, is due to the fact that multiplier  $\alpha$  is significant of the horizontal acceleration; therefore, the terms inside the brackets physically represent horizontal inertia forces. In this sense, the overturning moment at the left side of Equation (55), is in equilibrium with the resisting moment computed in the right side.

The trigger horizontal acceleration  $a_g$  is then computed by a relationship conceptually analogous to the one reported in Equation (56) which yields [CM, 2009- C8A.4.9]:

$$a_g = \frac{\alpha(\sum_{i=1}^n W_i + \sum_{i=1}^m P_i)}{M^*} \cdot \frac{q}{S} \quad (56)$$

where  $q$  is the ductility factor,  $S$  is the subsoil factor assumed to be equal to 1.25,  $g$  is the gravity acceleration and  $M^*$  is the participating mass. This last quantity is due to the presence of the non-uniform displacements

distribution presented by the system of rigid sub-elements excited by the base acceleration and is computed by:

$$M^* = \frac{(\sum_{i=1}^n W_i d_{x,i} + \sum_{j=1}^m P_j d_{x,j})^2}{g \cdot (\sum_{i=1}^n W_i d_{x,i}^2 + \sum_{j=1}^m P_j d_{x,j}^2)} \quad (57)$$

where  $d_{x,i}$   $d_{x,j}$  are the values of the virtual displacement computed at the application points of actions  $W_i$  and  $P_j$ , respectively.

The values of the weights and external actions and their locations are computed by the simplified structural analysis for each macro-element while the location of the kinematic hinge depends on the peculiar collapse mechanism considered in the analysis. In particular, each macro-element has been analyzed with respect to three out-of-plane failure schemes, namely:

- simple overturning;
- vertical bending;
- horizontal bending.

whose analyses are reported in the following subsections.

#### 4.6.1 Simple overturning

The simple overturning of external walls could be considered as one of the most frequent collapse mechanism. The mechanism consists in a rigid rotation about one of the edges of the base section, as shown in **Fig. 42** where the wall is represented by its transverse vertical section and a counter-clockwise rotation is assumed. In such a case, the panel does not present any internal discontinuity. The boundary conditions are, in general, the lack of effective connections and constraints.

The mechanism is easy recognisable by vertical crack patterns between the wall and the orthogonal lateral walls (**Fig. 43**) and the presence of horizontal cracks. In some cases, the floor beams collapse (**Fig. 44**). The mechanism could be limited to one or more building floors, related to the floor connection, masonry typologies, restrain geometry etc.



Fig. 42 Simple overturning due to earthquake Central Italy, Accumuli, 2016



Fig. 43 Vertical crack patterns between the wall and the orthogonal lateral walls, Illica, 2016



Fig. 44 Simple overturning due to earthquake Central Italy, Amatrice, 2016

Fig. 45 reports all the forces acting on the generic panel and contributing to the kinematic equilibrium; The collapse multiplier  $\alpha$  is calculated after evaluating the forces which determine the overturning of the body (the overturning moment) (58) and the forces that oppose the rotation (the stabilizing moment) (59).

$$M_r = \alpha[WY_G + F_v h_v + Psh] + F_H h_v + P_H h \quad (58)$$

$$M_s = WX_G + F_v d_v + Psd + Th \quad (59)$$

Where:

$W$  is the weight of the wall;

$Y_G$  is the vertical distance of the center of gravity  $G$  respect to the hinge  $A$ ;

$F_v$  is the vertical component of the push of arches on the wall;

$h_v$  is the vertical distance from the hinge  $A$  of the point of application of  $F_v$  and  $F_H$ ;

- $P_s$  is the weight loaded by the horizontal structure acting on the wall;  
 $h$  is the height of the wall respect to the hinge A;  
 $F_H$  is the horizontal component of the push of arches or vaults on the wall;  
 $P_H$  is the thrust of the horizontal structure acting on the wall;  
 $X_G$  is the horizontal distance of the center of gravity G respect to the hinge A;  
 $d_v$  is the horizontal distance from the hinge A of the point of application of  $F_v$ ;  
 $d$  is the horizontal distance from the hinge A of the point of application of  $P_s$ ;  
 $T$  is the maximum resistance due to architectural constrains (tensile tie if present, friction by the slab etc...);  
 $s$  is the wall thickness;

The equilibrium equation (55) can be specialized as:

$$\alpha[WY_G + F_v h_v + P_s h] + F_H h_v + P_H h = WX_G + F_v d_v + P_s d + Th \quad (60)$$

and the collapse multiplier  $\alpha$  turns out to be:

$$\alpha = \frac{WX_G + F_v d_v + P_s d + Th - F_H h_v - P_H h}{WY_G + F_v h_v + P_s h} \quad (61)$$

representing the relationship proposed by Milano et al.(2008).



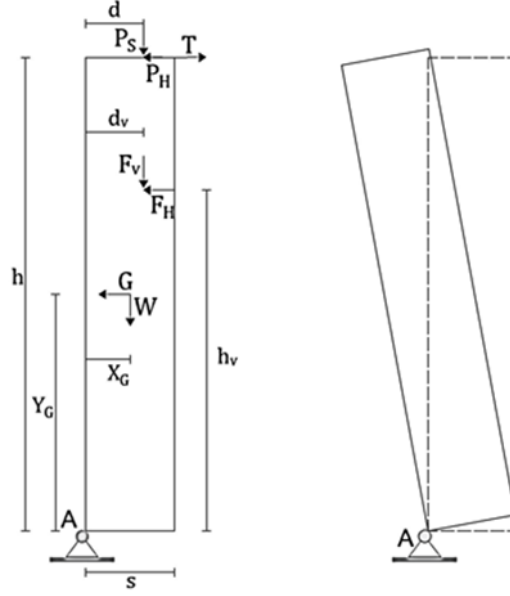


Fig. 45 Simple overturning failure, vertical section of the wall

#### 4.6.2 Vertical bending

The vertical bending mechanism (**Fig. 46**) involves a vertical instability of the wall induced by the seismic inertial forces and the action of an intermediate floor. For this reason, the hinge is located in correspondence of an intermediate floor (point C) while the neighboring floors act as horizontal restraints (points A and B). Subsequently, the panel is partitioned in two sub-elements which can rotate about point C (**Fig. 47**).

**Fig. 48** shows a vertical transverse section of the considered model and reports all the assumed actions and their locations.

The collapse multiplier  $\alpha$  derived from the kinematic analysis of the two sub-elements which can rotate about point C. Imposing a unitary rotation  $\psi = 1$ , the boundary conditions of A and B are:

$$\begin{cases} u_A = 0 \\ v_A = 0 \\ \psi = 1 \end{cases} \quad \begin{cases} u_B = 0 \\ v_B = s_2 \\ \varphi = -\psi \cdot \frac{h_1}{h_2} = -\frac{h_1}{h_2} \end{cases} \quad (62)$$



Fig. 46 Vertical bending of masonry wall due to earthquake Central Italy, Fonte del Campo, 2016.

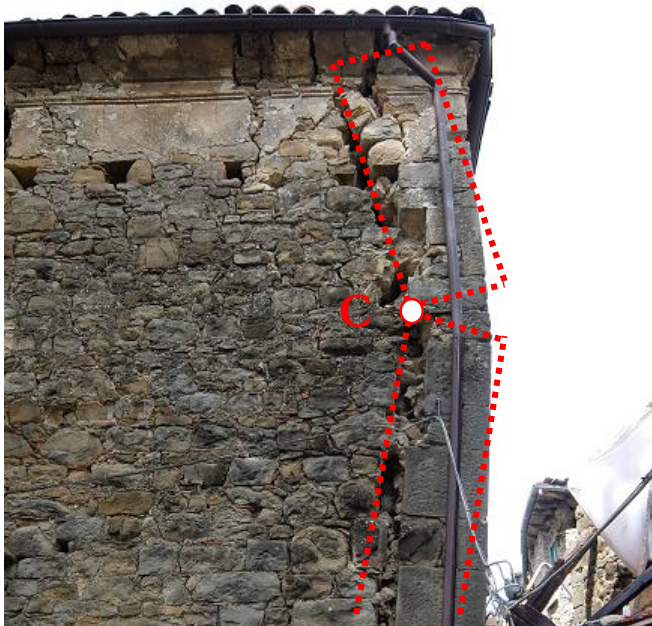


Fig. 47 Vertical bending of masonry wall due to earthquake Central Italy, Illica, 2016

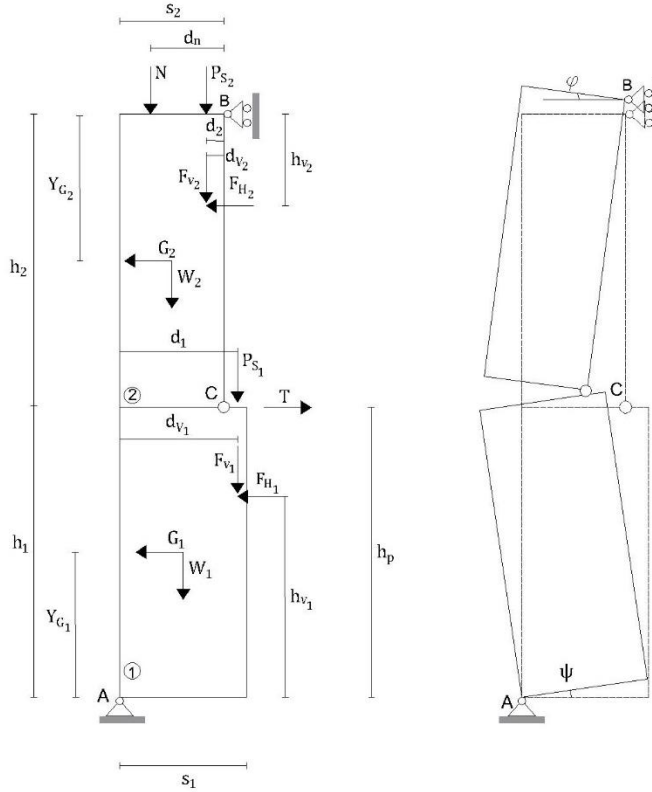


Fig. 48 Vertical bending failure, vertical section of the wall

Calculated the virtual displacements of the point of application of the force acting on the two sub-elements, it is possible to evaluate the forces which determine the overturning of the body (the overturning moment) (63) and the forces that oppose the rotation (the stabilizing moment) (64).

$$M_r = \alpha \left[ W_1 Y_{G_1} + W_2 Y_{G_2} \frac{h_1}{h_2} + F_{v_1} h_{v_1} + F_{v_2} h_{v_2} \frac{h_1}{h_2} + P_{s_1} h_p \right] + F_{H_1} h_{v_1} + F_{H_2} h_{v_2} \frac{h_1}{h_2} \quad (63)$$

$$\begin{aligned}
 M_s = W_1 \frac{s_1}{2} + W_2 s_2 \left( 1 + \frac{1}{2} \frac{h_1}{h_2} \right) + F_{v_1} d_{v_1} \\
 + F_{v_2} \left( s_2 + d_{v_2} \frac{h_1}{h_2} \right) + N \left( s_2 + d_n \frac{h_1}{h_2} \right) \\
 + P_{S1} d_1 + P_{S2} \left( s_2 + d_2 \frac{h_1}{h_2} \right) + Th_p
 \end{aligned} \quad (64)$$

Where:

$W_1$  is the weight of the wall panel 1;

$Y_{G_1}$  is the vertical distance of the center of gravity  $G_1$  respect to the hinge A;

$W_2$  is the weight of the wall panel 2;

$Y_{G_2}$  is the vertical distance of the center of gravity  $G_2$  respect to the hinge B;

$h_1$  is the height of the wall panel 1 respect to the hinge A

$h_2$  is the height of the wall panel 2 respect to the hinge B

$F_{v_1}$  is the vertical component of the push of arches or vaults on the panel 1;

$h_{v_1}$  is the vertical distance from the hinge A of the point of application of  $F_{v_1}$  and of  $F_{H_1}$ ;

$F_{v_2}$  is the vertical component of the push of arches on the panel 2;

$h_{v_2}$  is the vertical distance from the hinge B of the point of application of  $F_{v_2}$  and of  $F_{H_2}$ ;

$P_{S1}$  is the weight loaded by the horizontal structure acting on the panel 1;

$h_p$  is the vertical distance from the hinge A of the point of application of  $P_{S1}$  and  $T$ ;

$F_{H_1}$  is the horizontal component of the push of arches or vaults on the panel 1;

$h_{v_1}$  is the vertical distance from the hinge B of the point of application of  $F_{v_2}$  and of  $F_{H_2}$ ;

$F_{H_2}$  is the horizontal component of the push of arches or vaults on the panel 2;

- $h_{v_2}$  is the vertical distance from the hinge B of the point of application of  $F_{v_2}$  and of  $F_{H_2}$ ;  
 $s_1$  is the thickness of the panel 1;  
 $s_2$  is the thickness of the panel 2;  
 $d_{v1}$  is the horizontal distance from the hinge A of the point of application of  $F_{v_1}$ ;  
 $d_{v2}$  is the horizontal distance from the hinge B of the point of application of  $F_{v_2}$ ;  
 $N$  is normal compression strength;  
 $d_n$  is the horizontal distance from  $N$  to the hinge C;  
 $Ps_1$  is the weight loaded by the horizontal structure acting on the panel 1;  
 $d_1$  is the horizontal distance from the  $Ps_1$  to the hinge A;  
 $Ps_2$  is the weight loaded by the horizontal structure acting on the panel 2;  
 $d_2$  is the horizontal distance from the  $Ps_2$  to the hinge B;  
 $T$  is the maximum resistance due to architectural constraints (tensile tie if present, friction by the slab etc.);  
 $h_p$  is the vertical distance from the hinge A of the point of application of  $Ps_1$  and  $T$ ;

The virtual work relationship is derived assuming a counter-clockwise rotation of the bottom sub-element. As shown in Milano et al. [2008], the equilibrium equation (55) can be specialized for this kinematic scheme as:

$$\begin{aligned}
 \alpha & \left[ W_1 Y_{G_1} + W_2 Y_{G_2} \frac{h_1}{h_2} + F_{v_1} h_{v_1} + F_{v_2} h_{v_2} \frac{h_1}{h_2} \right. \\
 & \quad \left. + P_{S_1} h_p \right] + F_{H_1} h_{v_1} + F_{H_2} h_{v_2} \frac{h_1}{h_2} \\
 & = W_1 \frac{s_1}{2} + W_2 s_2 \left( 1 + \frac{1}{2} \frac{h_1}{h_2} \right) + F_{v_1} d_{v_1} \\
 & \quad + F_{v_2} \left( s_2 + d_{v_2} \frac{h_1}{h_2} \right) + N \left( s_2 + d_n \frac{h_1}{h_2} \right) \\
 & \quad + P_{S_1} d_1 + P_{S_2} \left( s_2 + d_2 \frac{h_1}{h_2} \right) + Th_p
 \end{aligned} \tag{65}$$

Defined:

$$\begin{aligned}
 E & = \frac{W_1}{2} s_1 + F_{v_1} d_{v_1} + (W_2 + P_{S_2} + N + F_{v_2}) s_2 + \\
 & + \frac{h_1}{h_2} \left( \frac{W_2}{2} s_2 + P_{S_2} d_2 + N d_n + F_{v_2} d_{v_2} - F_{H_2} h_{v_2} \right) + P_{S_1} d_1 \\
 & \quad - F_{H_1} h_{v_1} + Th_p
 \end{aligned} \tag{66}$$

the collapse multiplier  $\alpha$  is:

$$\alpha = \frac{E}{W_1 Y_{G_1} + F_{v_1} h_{v_1} + P_{S_1} h_p + (W_2 Y_{G_2} + F_{v_2} h_{v_2}) \frac{h_1}{h_2}} \tag{67}$$

#### 4.6.3 Horizontal bending

The last out-of-plane mechanism considered in this study concerns horizontal bending of two adjacent panels. Restrained panels to orthogonal walls but not in the upper side could be damaged by bending in the horizontal plane.

The general behaviour involves an arch mechanism within the wall section caused by the out of plane actions (Fig. 49 a-c) (Fig. 50). In case of good quality of the lateral masonry and effectiveness of the connections, the collapse does not happen but the inner side of the wall could be compressed (Fig. 49 b).

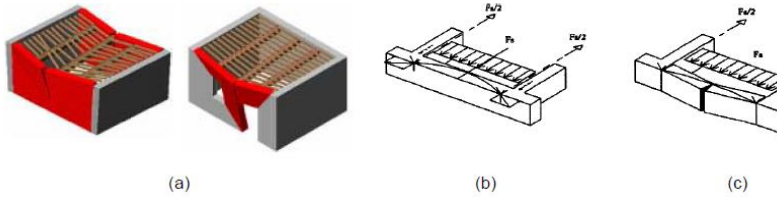


Fig. 49 Horizontal bending of a masonry wall (Borri, 2004)

In multiple leaf masonry, the mechanism could involve only the external leaf that could collapse.

Chimney flues, internal masonry discontinuities like holes for rainwater pipes or ducts for other technical plants reduce the load bearing section, localising the hinges for the kinematic mechanism.

In such a case, three hinges, reported in Fig. 51, are considered. Moreover, apart from the standard actions introduced before, a further contribution must be considered. It consists in a horizontal force accounting for architectural constraints, such as the action of steel ties, if present, and the friction between the panel and the floor slab.



**Fig. 50 Horizontal bending due to earthquake Central Italy, Pescara del Tronto, 2016**

The collapse multiplier  $\alpha$  is derived from the kinematic analysis of the two sub-elements which can rotate about point C. Imposing a unitary rotation  $\psi = -1$ , the boundary conditions of A and B are:

$$\begin{cases} u_A = 0 \\ v_A = 0 \\ \psi = -1 \end{cases} \quad \begin{cases} u_B = s \left( 1 + \frac{L_1}{L_2} \right) \\ v_B = 0 \\ \varphi = -\psi \frac{L_1}{L_2} = \frac{L_1}{L_2} \end{cases} \quad (68)$$



Calculated the virtual displacements of the point of application of the force acting on the two sub-elements, it is possible to evaluate the forces which determine the overturning of the body (the overturning moment) (69) and the forces that oppose the rotation (the stabilizing moment) (70).

$$M_r = \alpha \left[ W_1 X_{G_1} + W_2 \frac{l_{p_1}}{l_{p_2}} X_{G_2} + \sum_i P_{S_{i1}} d_{H_{i1}} + \sum_i P_{S_{i2}} \frac{l_{p_1}}{l_{p_2}} d_{H_{i2}} \right] \quad (69) \quad ($$

$$M_s = Ts \left( 1 + \frac{l_{p_1}}{l_{p_2}} \right) + \sum_i P_{H_{i1}} d_{H_{i1}} + \sum_i P_{H_{i2}} \frac{l_{p_1}}{l_{p_2}} d_{H_{i2}} \quad (70) \quad (($$

Where:

$W_1$  is the weight of the wall panel 1;

$X_{G_1}$  is the horizontal distance of the center of gravity  $G_1$  respect to the hinge A;

$W_2$  is the weight of the wall panel 2;

$X_{G_2}$  is the horizontal distance of the center of gravity  $G_2$  respect to the hinge B;

$l_{p_1}$  is the is the length of the panel 1;

$l_{p_2}$  is the is the length of the panel 2;

$P_{S_{i1}}$  is the weight loaded by the horizontal structure acting on the panel 1;

$d_{H_{i1}}$  is the horizontal distance of the hinge A and the point of application of  $P_{H_{i1}}$ ;

$P_{S_{i2}}$  is the weight loaded by the horizontal structure acting on the panel 2;

$d_{H_{i2}}$  is the horizontal distance of the hinge B and the point of application of  $P_{H_{i2}}$ ;

$T$  is the maximum resistance due to architectural constraints (tensile tie if present, friction by the slab etc.);

$s$  is the wall thickness;

$P_{H_{i1}}$  is the thrust of the horizontal structure acting on the panel 1;

$P_{H_{i2}}$  is the thrust of the horizontal structure acting on the panel 2;

$\alpha P_{S_{i1}}$  is the horizontal component of the weight loaded by the horizontal structure acting on the panel 1;

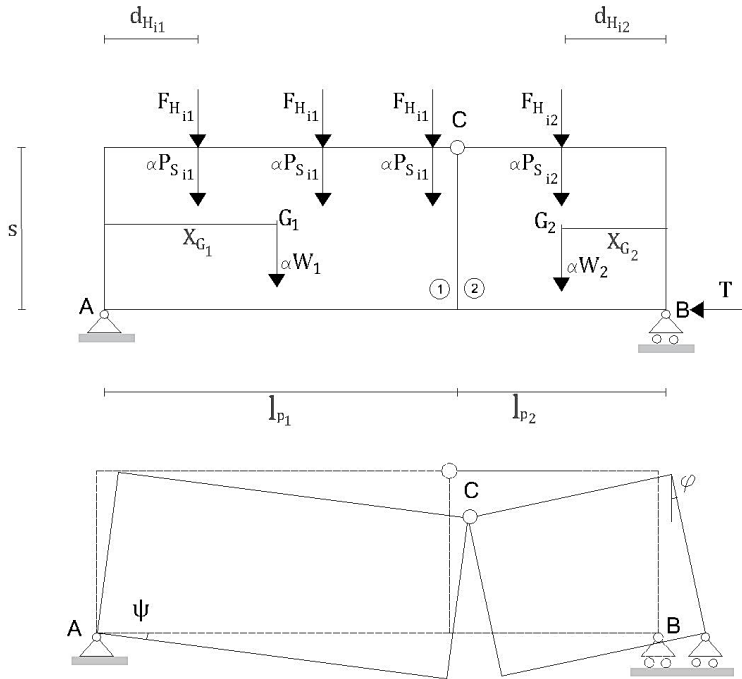
$\alpha P_{S_{i2}}$  is the horizontal component of the weight loaded by the horizontal structure acting on the panel 2;

As shown in Milano et al. [2008], the equilibrium equation (55) can be specialized for this kinematic scheme as:

$$\begin{aligned}
 \alpha \left[ W_1 X_{G_1} + W_2 \frac{l_{p1}}{l_{p2}} X_{G_2} + \sum_i P_{S_{i1}} d_{H_{i1}} \right. \\
 \left. + \sum_i P_{S_{i2}} \frac{l_{p1}}{l_{p2}} d_{H_{i2}} \right] \\
 = Ts \left( 1 + \frac{l_{p1}}{l_{p2}} \right) + \sum_i P_{H_{i1}} d_{H_{i1}} \\
 + \sum_i P_{H_{i2}} \frac{l_{p1}}{l_{p2}} d_{H_{i2}}
 \end{aligned} \tag{71}$$

The equilibrium condition of Equation (55), computed by the application of the rigid displacement and considering the distances reported in **Fig. 51**, permits to determine the collapse multiplier which turns out to be (Milano et.al 2008):

$$\alpha = \frac{T_s \left( 1 + \frac{l_{p1}}{l_{p2}} \right) + \sum_i P_{H_{i1}} d_{H_{i1}} + \sum_i P_{H_{i2}} \frac{l_{p1}}{l_{p2}} d_{H_{i2}}}{W_1 X_{G_1} + W_2 \frac{l_{p1}}{l_{p2}} X_{G_2} + \sum_i P_{S_{i1}} d_{H_{i1}} + \sum_i P_{S_{i2}} \frac{l_{p1}}{l_{p2}} d_{H_{i2}}} \quad (72)$$



**Fig. 51** Horizontal bending, horizontal section of the wall.

## 4.7 ANALYSIS OF THE MECHANISMS OF COLLAPSE: THE CASE STUDY OF FONTE DEL CAMPO

In this paragraph, the study of the mechanisms of collapse is used to analyze the seismic damage caused by the earthquake that hit the central Apennines on 24th August, 2016. Several information related different towns were collected during the surveys activities performed in October 2016. In particular, among all towns, it is investigated the case study of Fonte del Campo. This is because the dimensions of Fonte del Campo town make it possible a more thorough and quicker analysis then the other towns analysed.

### 4.7.1 Earthquake central Italy

On August 24th, 2016, at 03:36 (CEST) a MW 6.0 earthquake hit the central Apennines in Italy (Fig. 52). A number of aftershocks continued after the main event (Fig. 53), the largest one of Mw 5.5 On October 26th,

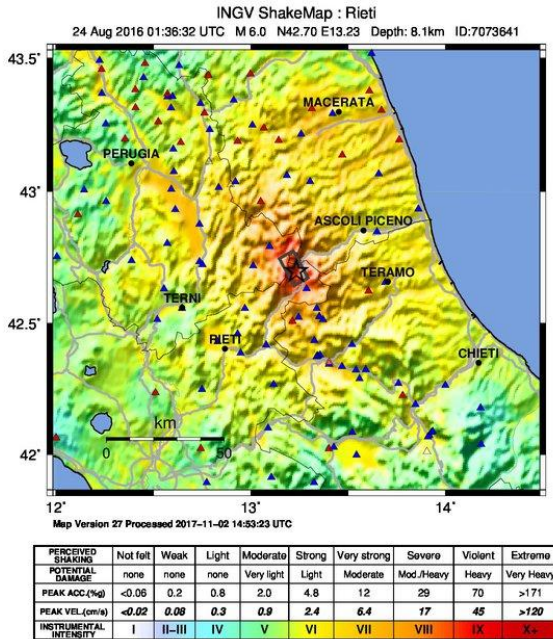
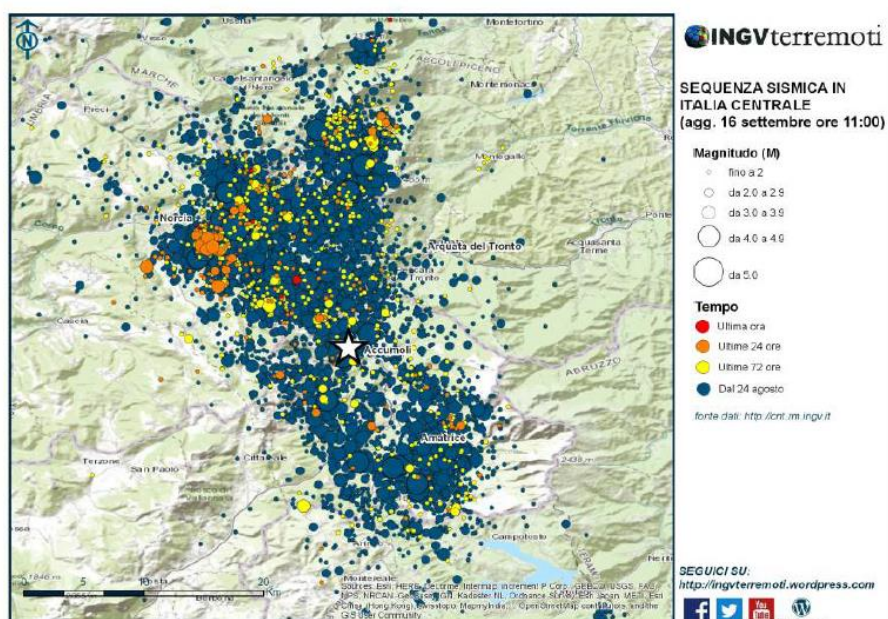


Fig. 52 Shake Map on 24 August in the Rieti, Ascoli and Perugia provinces. Source: INGV

two aftershocks of magnitude 5.5 and 6.1 hit Visso, north of Amatrice. On October 30th, a magnitude 6.6 earthquake struck Norcia, situated between Amatrice and Visso. Overall 299 lives were lost. The depth of the 24th August earthquake was 4 km and the epicenter area was between Norcia and Amatrice, at the boundaries among Lazio, Marche, Abruzzo and Umbria regions. The epicenter is just tens of kilometers NW of L'Aquila (Abruzzo), hit by a slightly larger seismic event (MW 6.3) on April 6, 2009.



**Fig. 53** The seismic sequence started on 24th August in the Rieti, Ascoli and Perugia provinces (updated 16 September 2016). Source: INGV

The distribution of the dislocation is concentrated in two areas: one, quite shallow near Accumoli and Amatrice, and a deeper one near Norcia. This suggests a bilateral rupture, along the NW - SE direction, with coherent directivity effects.

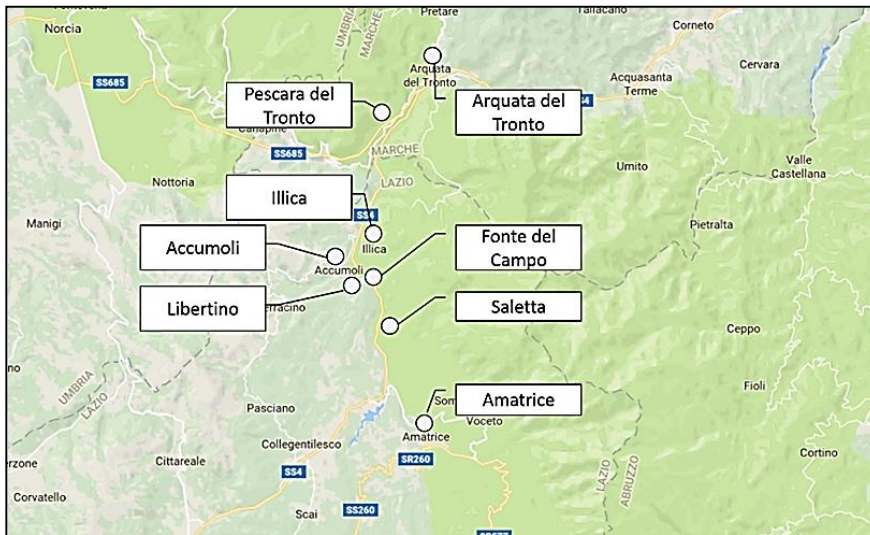
Despite the relatively low moment release, the event occurred on August 24 has been particularly devastating. Field reports indicate severe damage in the epicentral area and, in particular, in the town of Amatrice.

The number of victims is almost equal to that calculated after the 2009 L'Aquila event, which had greater 5 magnitude (Mw 6.3). Major causes for such loss of lives in 2016 are both the occurrence of the main shock in night-time (3:36 am local time) and the presence of many tourists in holiday houses, including those from other countries.

#### 4.7.2 Impact on the buildings

On October 2016 visual surveys were made in the places affected by the earthquake Central Italy.

The towns analysed are: Amatrice, Libertaino, Fonte del Campo, Saletta, Accumoli, Illica, Pescara del Tronto and Arquata del Tronto (**Fig. 54**). The observed data showed that in these places most of the buildings are unreinforced masonry ones. The main construction technique used for



**Fig. 54** Towns analysed by visual surveys on October 2016.

URM buildings is coursed or un-coursed rubble masonry (**Fig. 55**, **Fig. 56**). This kind of masonry, usually made with mortar and irregular natural stones, it can be still found in many old town of Italy.

The buildings seismic damage depends on their “vulnerability factors” (the quality of the masonry, the plan layout and structural irregularities etc.). The observed buildings are characterized by poor wall-to-wall and wall-



to-floor connections. The seismic vulnerability of this type of buildings is therefore very high because of their poor resistance to lateral loads.



**Fig. 55** Coursed rubble masonry, Illica October 2016.



**Fig. 56** Un-coursed rubble masonry, Fonte del Campo October 2016

The main observed failures on the URM buildings are:

- Out-of-plane collapse mechanisms of the wall due to ineffective connection to walls (Fig. 57).
- In-plane collapse mechanisms activated in buildings with a better degree of connection of the walls exhibited (Fig. 58).



Fig. 57 Out-of-plane collapse mechanisms, Accumoli October 2016.



Fig. 58 In-plane collapse mechanisms, Illica October 2016.



Several buildings in which the original timber floors and roofs were replaced with reinforced concrete elements have collapsed partially or totally. The addition of R.C. roofs does not seem to have been supported by the existing masonry walls. The insertion of concrete elements has, in fact, only increased the mass of the buildings making them even more vulnerable (**Fig. 59**).

A good seismic behavior and low level of damage have been recorded in buildings in which the quality of the masonry walls was improved (mortar injections etc..) and the out-of-plane mechanism was minimized inserting steel ties and properly connected ring beams (**Fig. 60, Fig. 61**).



**Fig. 59** Masonry building with RC roof, Accumoli October 2017.



**Fig. 60** Masonry building renovated with mortar injection (on the left) and old collapsed masonry building (on the right), Saletta, October 2017.



**Fig. 61** Old masonry building with steel ties, Accumoli October 2017.

#### 4.7.3 Analysis of Fonte del Campo

Fonte del Campo is a district of the village of Accumoli (**Fig. 62**). On October 2016 visual surveys showed that in the town there are 100 buildings, most of them (90) are residential buildings (**Fig. 63**). Only 27 people live in Fonte del Campo and most of the residential buildings are uninhabited during the most part of the year. This involves that most of the buildings are abandoned and in bad conditions.



**Fig. 62** Planimetry of Fonte del Campo.

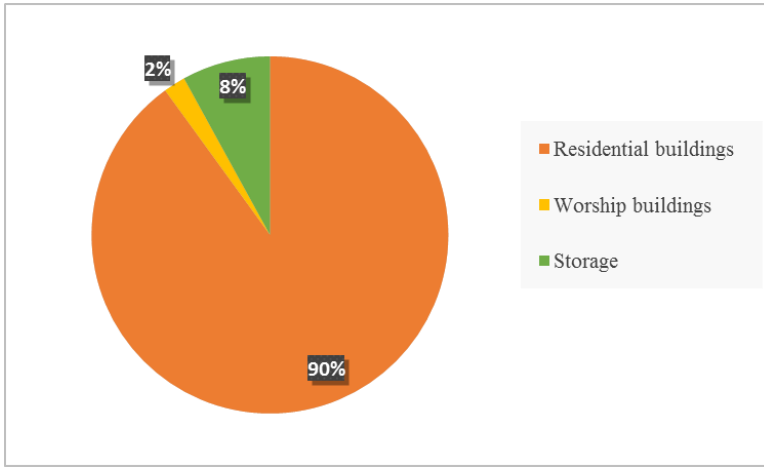


Fig. 63 Classification of Fonte del Campo buildings.

#### 4.7.3.1 Data collection

During the survey activities the collection of the buildings information were performed using two different forms:

- **AeDES form.**

AeDES (Agibilità e Danno nell'Emergenza Sismica) is a first level form for post-earthquake damage assessment, created by National Seismic Survey (SSN) and GNDT (Italian national seismic protection group). The form is the outcome of the field experience, matured after several past earthquakes, when forms with different levels of detail were used (Irpinia '80, Abruzzo '84, Basilicata '90, Reggio Emilia '96).

AeDES form allows a quick survey and a first identification of the building stock, with the collection of metrical and typological data of the buildings. The form has 9 sections concern information about position of the building, classification, material, structural typology, damage of the current event and previous damages (Fig. 64).

**SEZIONE 3 Tipologia** (multiscelta; per gli edifici in muratura indicare al massimo 2 tipi di combinazioni strutture verticali-solai)

Strutture orizzontali \ Strutture verticali		Strutture in muratura								Altre strutture			
		Non identificate		A tessitura irregolare e di cattiva qualità (Pietrame non squadrato, ciottoli,...)		A tessitura regolare e di buona qualità (Blocchi; mattoni; pietra squadrata,...)		Pilastrini isolati	Mista	Rinforzata	Telai in c.a.		
				Senza catene o cordoli		Con catene o cordoli					Pareti in c. a.		
				A	B	C	D				E	Telai in acciaio	
		A	B	C	D	E	F	G	H	REGOLARITA'			
											Non regolare		
											Regolare		
											A B		
1	Non identificate	<input type="radio"/>	<input type="checkbox"/>	<input type="checkbox"/>	<input type="checkbox"/>	<input type="checkbox"/>	<input type="checkbox"/>	SI	<input type="checkbox"/>	<input type="checkbox"/>	1 Forma pianta ed elevazione <input type="radio"/> <input type="radio"/>		
2	Volte senza catene	<input type="checkbox"/>	<input type="checkbox"/>	<input type="checkbox"/>	<input type="checkbox"/>	<input type="checkbox"/>	<input type="checkbox"/>	<input type="radio"/>	G1	H1	2 Disposizione tamponature <input type="radio"/> <input type="radio"/>		
3	Volte con catene	<input type="checkbox"/>	<input type="checkbox"/>	<input type="checkbox"/>	<input type="checkbox"/>	<input type="checkbox"/>	<input type="checkbox"/>	<input type="checkbox"/>	<input type="checkbox"/>	<input type="checkbox"/>			
4	Travi con soletta <b>deformabile</b> (travi in legno con semplice tavolato, travi e volte,...)	<input type="checkbox"/>	<input type="checkbox"/>	<input type="checkbox"/>	<input type="checkbox"/>	<input type="checkbox"/>	<input type="checkbox"/>	NO	G2	H2			
5	Travi con soletta <b>semirigida</b> (travi in legno con doppio tavolato, travi e tavelloni,...)	<input type="checkbox"/>	<input type="checkbox"/>	<input type="checkbox"/>	<input type="checkbox"/>	<input type="checkbox"/>	<input type="checkbox"/>	<input type="radio"/>	<input type="checkbox"/>	<input type="checkbox"/>			
6	Travi con soletta <b>rigida</b> (solai di c.a., travi ben collegate a solette di c.a.,...)	<input type="checkbox"/>	<input type="checkbox"/>	<input type="checkbox"/>	<input type="checkbox"/>	<input type="checkbox"/>	<input type="checkbox"/>	<input type="checkbox"/>	G3	H3			

Copertura	
1	<input type="radio"/> Spingente pesante
2	<input type="radio"/> Non spingente pesante
3	<input type="radio"/> Spingente leggera
4	<input type="radio"/> Non spingente leggera

**SEZIONE 4 Danni ad ELEMENTI STRUTTURALI e provvedimenti di pronto intervento (P.I.) eseguiti**

Livello - estensione Componente strutturale - Danno preesistente		DANNO <sup>(1)</sup>									PROVEDIMENTI DI P.I. ESEGUITI							
		D4-D5 Gravissimo			D2-D3 Medio grave			D1 Leggero			Nullo	Nessuno	Demolizioni	Carchiature edo tranti	Riparazione	Puntelli	Trasferimento e protezione passaggi	
		> 2/3	1/3 - 2/3	< 1/3	> 2/3	1/3 - 2/3	< 1/3	> 2/3	1/3 - 2/3	< 1/3								
																		A
1	Strutture verticali	<input type="checkbox"/>	<input type="checkbox"/>	<input type="checkbox"/>	<input type="checkbox"/>	<input type="checkbox"/>	<input type="checkbox"/>	<input type="checkbox"/>	<input type="checkbox"/>	<input type="checkbox"/>	<input type="checkbox"/>	<input type="radio"/>	<input type="radio"/>	<input type="checkbox"/>	<input type="checkbox"/>	<input type="checkbox"/>	<input type="checkbox"/>	<input type="checkbox"/>
2	Solai	<input type="checkbox"/>	<input type="checkbox"/>	<input type="checkbox"/>	<input type="checkbox"/>	<input type="checkbox"/>	<input type="checkbox"/>	<input type="checkbox"/>	<input type="checkbox"/>	<input type="checkbox"/>	<input type="checkbox"/>	<input type="radio"/>	<input type="radio"/>	<input type="checkbox"/>	<input type="checkbox"/>	<input type="checkbox"/>	<input type="checkbox"/>	
3	Scale	<input type="checkbox"/>	<input type="checkbox"/>	<input type="checkbox"/>	<input type="checkbox"/>	<input type="checkbox"/>	<input type="checkbox"/>	<input type="checkbox"/>	<input type="checkbox"/>	<input type="checkbox"/>	<input type="checkbox"/>	<input type="radio"/>	<input type="radio"/>	<input type="checkbox"/>	<input type="checkbox"/>	<input type="checkbox"/>	<input type="checkbox"/>	
4	Copertura	<input type="checkbox"/>	<input type="checkbox"/>	<input type="checkbox"/>	<input type="checkbox"/>	<input type="checkbox"/>	<input type="checkbox"/>	<input type="checkbox"/>	<input type="checkbox"/>	<input type="checkbox"/>	<input type="checkbox"/>	<input type="radio"/>	<input type="radio"/>	<input type="checkbox"/>	<input type="checkbox"/>	<input type="checkbox"/>	<input type="checkbox"/>	
5	Tamponature-tramezzi	<input type="checkbox"/>	<input type="checkbox"/>	<input type="checkbox"/>	<input type="checkbox"/>	<input type="checkbox"/>	<input type="checkbox"/>	<input type="checkbox"/>	<input type="checkbox"/>	<input type="checkbox"/>	<input type="checkbox"/>	<input type="radio"/>	<input type="radio"/>	<input type="checkbox"/>	<input type="checkbox"/>	<input type="checkbox"/>	<input type="checkbox"/>	
6	Danno preesistente	<input type="checkbox"/>	<input type="checkbox"/>	<input type="checkbox"/>	<input type="checkbox"/>	<input type="checkbox"/>	<input type="checkbox"/>	<input type="checkbox"/>	<input type="checkbox"/>	<input type="checkbox"/>	<input type="checkbox"/>	<input type="radio"/>	<input type="radio"/>	<input type="checkbox"/>	<input type="checkbox"/>	<input type="checkbox"/>	<input type="checkbox"/>	

(1) - Di ogni livello di danno indicare l'estensione solo se esso è presente. Se l'oggetto indicato nella riga non è danneggiato campare **Nullo**.

**Fig. 64 AeDes form: sections 3 and 4**

- **MEDEA form.**

MEDEA (Manual for Earthquake Damage Evaluation and safety Assessment) (Zuccaro et al, 2002), is a manual used for the evaluation of the damage due to a seismic event on masonry or reinforced concrete building. The first sections of MEDEA form concern the description of vulnerability characteristics of the building. The other sections concern the damages classification of the structures of the buildings (**Fig. 65**). The damage assessment survey is supported by forms where every damage type is described with notes, iconographic representations showing different damage levels, and possible links to their associated collapse mechanisms. This helps to reduce the level of uncertainty in the assessment of safety during the survey.

\* Damages different from the mechanisms V1-V23 and H1-H13

**Fig. 65 MEDEA survey form.**

For each building the great number of information collected with AeDES and MEDEA forms are synthesized. During the survey each building is identified with an ID number, so it is possible to join the information from both different forms.

**Table 9** summarizes some building dataset analysed in this research. In particular, the first column represent a building identification number. Moreover, columns 2-10 report the main structural characteristics reported by AeDES and MEDEA forms.

Table 9 A sample of the information collected by AeDES and MEDEA forms.

ID	Typology	Vertical structure	Horizontal structure	Number of floors	Pushing roof	Tie rod/ Ring beams	Regularity	Level of Damage	Mechanism of collapse
782	R	A	3	2	1	0	1	3	TC
525	R	A	3	2	1	0	1	1	0
532	R	A	3	3	1	0	0	4	TC
528	R	A	3	2	1	0	1	4	TC
385	R	A	1	2	1	0	1	4	FO
390	R	A	1	2	1	0	1	4	RIB
393	R	A	1	2	1	0	1	4	RIB
386	R	A	3	3	1	0	1	4	RIB
397	R	A	3	3	1	0	0	3	TC
394	R	A	3	1	1	0	1	4	RIB
401	R	A	3	3	1	0	1	3	FV
408	R	A	3	3	0	1	0	2	TC
412	R	A	1	2	1	0	0	4	FV
404	R	A	1	2	1	0	1	4	RIB
424	R	A	1	2	1	0	1	4	RIB
415	R	A	1	2	1	0	1	4	RIB
....	....	....	....	....	....	....	....	....	....
....	....	....	....	....	....	....	....	....	....

#### 4.7.3.2 *Seismic Vulnerability classification of the buildings by “SAVE” method*

A Seismic Vulnerability classification of the buildings (A,B,C,D) is made using the “SAVE” method [Zuccaro et al. 2015]. According to this assignment procedure the vulnerability level of each building is evaluated considering the typological characteristic as vulnerability modifiers (**Table 10**) and giving to each of these a numerical weight calibrated using a wide database of seismic damage observed after the most important earthquakes occurred in Italy in the last forty years. The vulnerability classes (A, B, C, D) have different structural characteristics and other vulnerability factors (age of construction, number of floor, height of the building etc...).

Identified the vulnerability classes (A, B, C, D) of the buildings (**Table 11**) it is possible to analyze their distribution on the village of Fonte del Campo (**Fig. 66**).

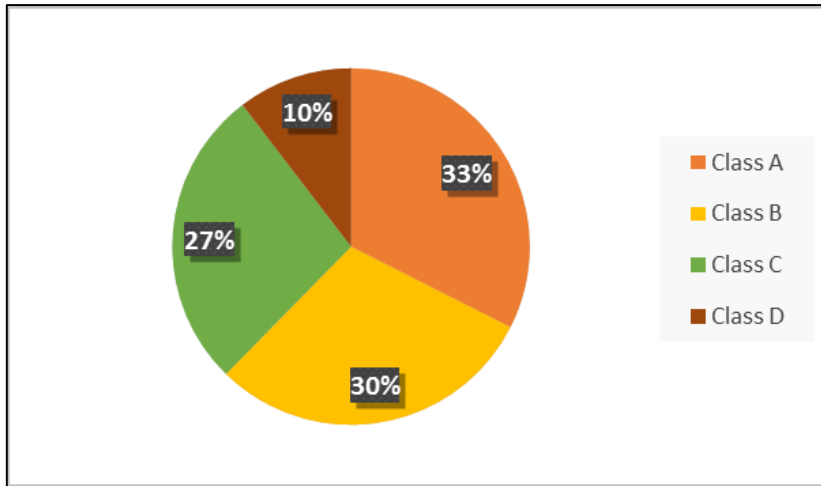
**Table 10** Typological characteristics identified on buildings of Fonte del Campo.

Typological parameter	Characteristics	Identification parameter
Typology of vertical structure	Irregular stonework	A
	Hollow bricks	B
	Tuff	B
	Regular stonework	C
	Solid bricks	C
	RC buildings	D
Typology of horizontal structure (Intermediate slabs and roof)	Wooden beams	1
	Iron beams	2
	R.C. with hollow brick	3
	Vaults	4
Number of floors	1 to 5	1 to 5
Pushing roof	On/off	(1/0) variable
Tie rod / ring beams	On/off	(1/0) variable
Regularity	On/off	(1/0) variable



**Table 11 A sample of the Seismic Vulnerability classification of the buildings of Fonte del Campo.**

ID	Typology	Vertical structure	Horizontal structure	Number of floors	Pushing roof	The roof/ Ring beams	Regularity	Level of Damage	Mechanism of collapse	Vulnerability class of Buildings "SAVE"
782	R	A	3	2	1	0	1	3	TC	A
525	R	A	3	2	1	0	1	1	0	A
532	R	A	3	3	1	0	0	4	TC	A
528	R	A	3	2	1	0	1	4	TS	A
385	R	A	1	2	1	0	1	4	FO	A
386	R	A	3	3	1	0	1	4	RIB	A
397	R	A	3	3	1	0	0	3	TC	A
394	R	A	3	1	1	0	1	4	RIB	A
401	R	A	3	3	1	0	1	3	FV	A
408	R	A	3	3	0	1	0	2	TC	A
412	R	A	1	2	1	0	0	4	FV	A
404	R	A	1	2	1	0	1	4	RIB	A
424	R	A	1	2	1	0	1	3	RIB	A
415	R	A	1	2	1	0	1	4	RIB	A
383	R	A	1	3	1	0	0	4	RIB	A
..	..	..	..	..	..	..	..	..	..	..



**Fig. 66 Analysis of the Vulnerability class of the buildings of Fonte del Campo.**

The visual surveys showed that most of the 100 buildings are Class A and Class B buildings. Moreover in Fonte del Campo there are many buildings with vulnerability Class C. This is because many buildings were renovated using steel ties or RC ring beams, so most of the buildings that have a class B typology of vertical structure, according with SAVE method, are classified as vulnerability class C.

Using a GIS software it is possible to visualize this data on the map of Fonte del Campo (**Fig. 67** Distribution of the Vulnerability classes of the buildings of Fonte del Campo.).

In this study only the residential buildings are take in account so the other buildings are indicated with “NA” symbol.

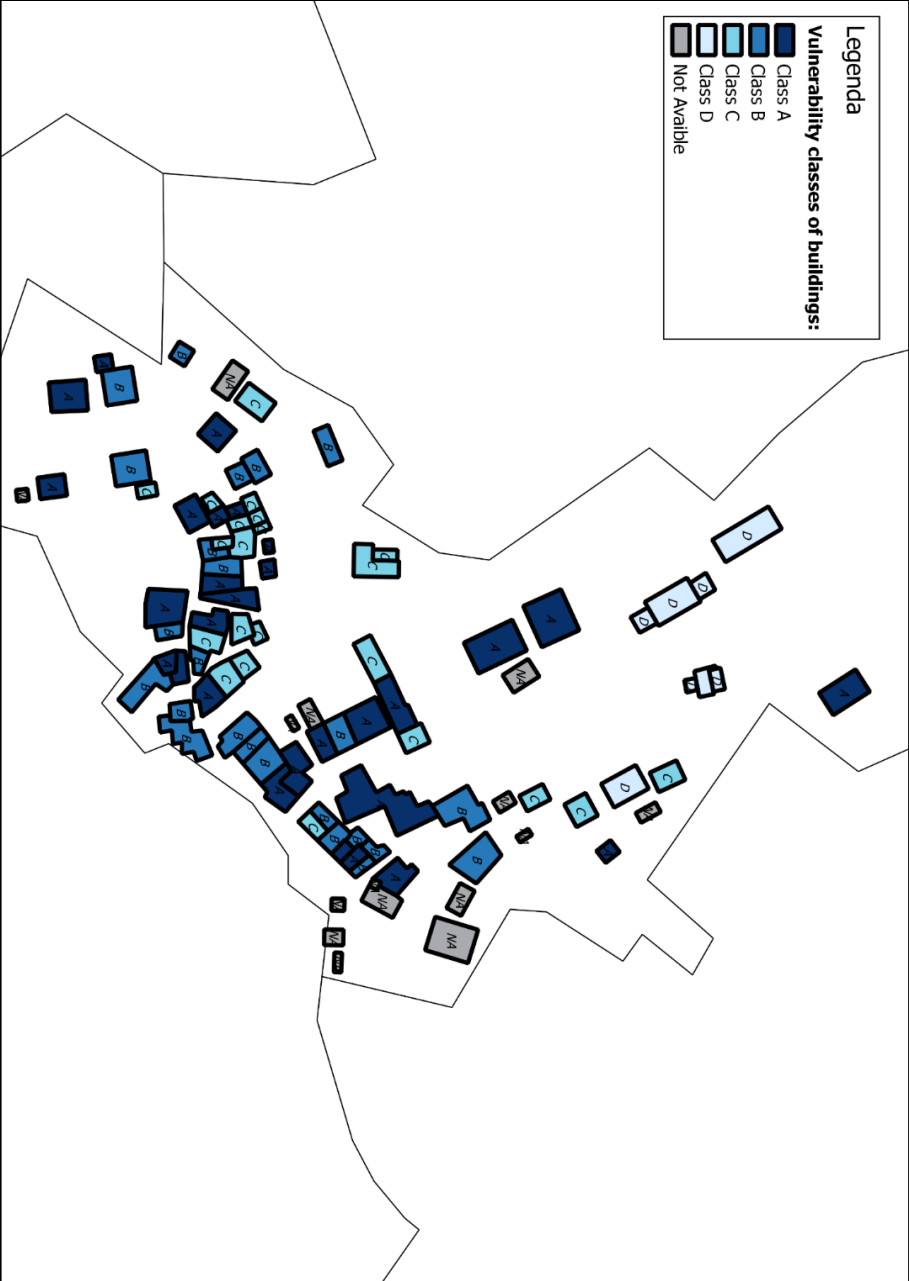


Fig. 67 Distribution of the Vulnerability classes of the buildings of Fonte del Campo.

#### 4.7.3.3 Damage distribution

The visual survey showed for each building class the level of damage due to earthquake on the 24th August 2016. Using a GIS software it is possible to visualize the observed data on the map of Fonte del Campo (Fig. 68).

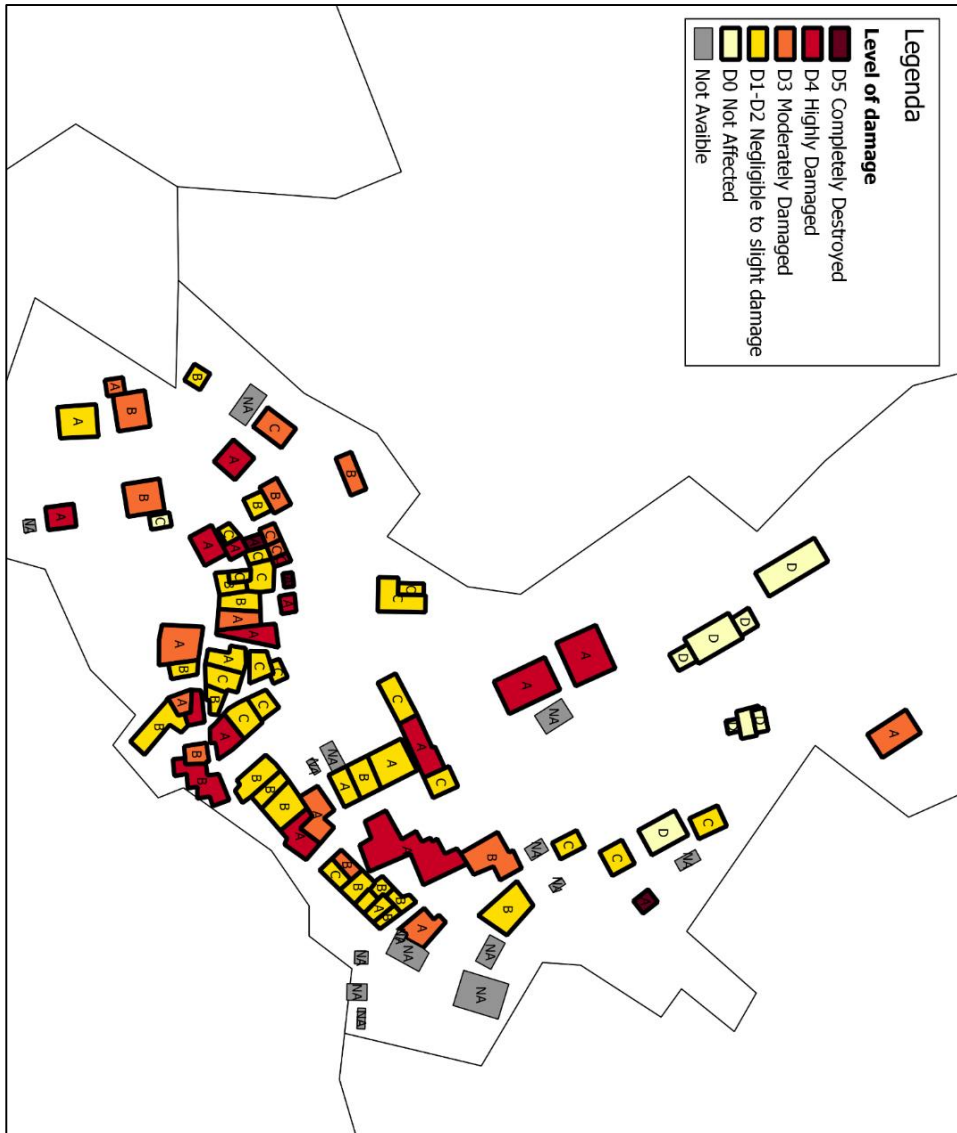
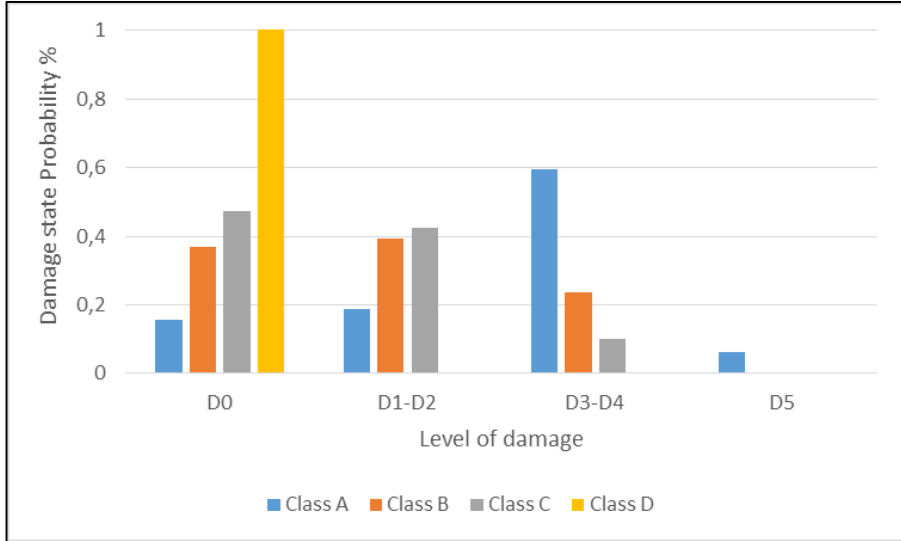


Fig. 68 Levels of damage distribution on Fonte del Campo map.

In **Fig. 69** the observed data were used to calculate, for the vulnerability class of buildings, the damage state probability (D0, D1-D2, D3-D4, D5).



**Fig. 69** Damage state probability (D0, D1, D2, D3, D4, D5) observed on the vulnerability class of buildings of Fonte del Campo.

In particular, **Fig. 70** and **Fig. 71** show the damage state probability observed for each mechanisms of collapse on the vulnerability classes of buildings of Fonte del Campo. The mechanisms of collapse taken in to account are:

- Out of plane collapse mechanisms: Horizontal Bending (HB), Vertical Bending (VB), Simple Overturning (SO),
- In plane collapse mechanisms: Bucking failure (BF), Shear Damage (SD) and Failure by slip (FS).

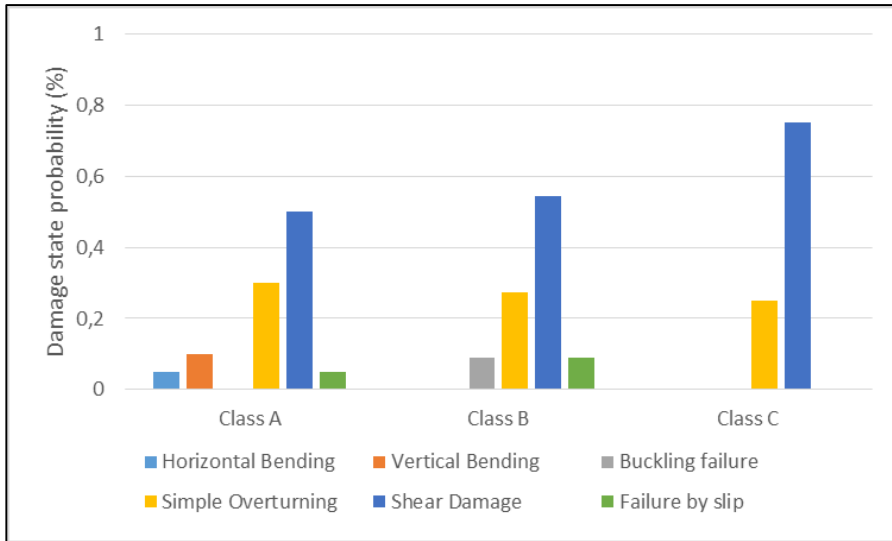


Fig. 70 Damage state probability observed for each mechanisms of collapse on the vulnerability classes of buildings of Fonte del Campo.

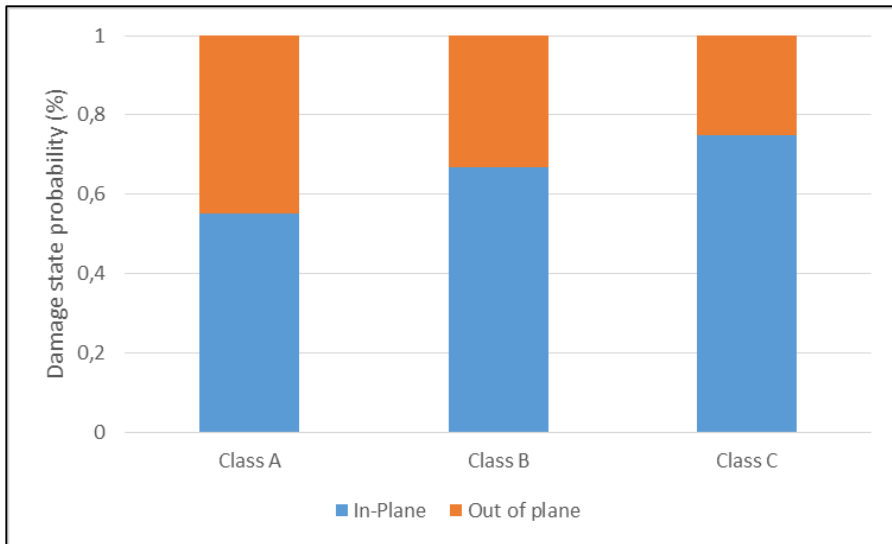


Fig. 71 Damage state probability observed for in-plane and out of plane mechanisms of collapse on the vulnerability classes of buildings of Fonte del Campo.

In conclusion, the visual survey showed that most of the vulnerability class A buildings got a level of damage 3-4 after the earthquake of 24 August (Fig. 69). In particular, in this vulnerability class, the out of plane collapse mechanisms, especially the “simple overturning” mechanism, are triggered more frequently than the in-plane collapse mechanisms (Fig. 70, Fig. 71). This is because this class identified old buildings with irregular stone masonry and bad conditions of structure (Fig. 72).

Low levels of damages are showed in class B and in class C (Fig. 69).

In these vulnerability classes the in-plane collapse mechanisms, especially the “shear damage” mechanism, are triggered more frequently than the out of plane collapse mechanisms (Fig. 70, Fig. 71).

This is because the class B and class C identified buildings with a good quality of masonry or old buildings renovated with steel tie or RC ring beams (Fig. 73).

Finally the visual surveys showed that in Fonte del Campo the RC buildings (vulnerability class D) did not experience any damage caused by the earthquake on the 24th August 2016 (Fig. 69).



Fig. 72 Before and after the 24th August 2016 earthquake. Damage level 4 on vulnerability class A building in Fonte del Campo.



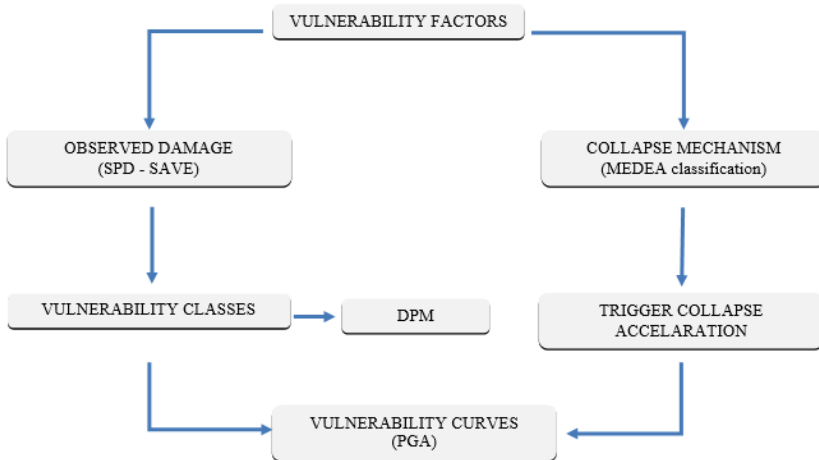
**Fig. 73 Before and after the 24th August 2016 earthquake. Damage level 3 on vulnerability class B building in Fonte del Campo.**



## 5 RESEARCH STEPS: THE ITERATIVE MODEL

The aim of the research is to evaluate the correlations between the vulnerability factors of masonry buildings, based on their structural typologies, and the collapse mechanisms potentially triggered by the seismic action. This approach will allow to determine, for each vulnerability classes of buildings (A, B, C, D), the vulnerability curves depending on the ground accelerations.

The procedure (Fig. 74), aiming to determine the vulnerability curves as functions of the structural typology and of the seismic acceleration, involves different steps of both statistical and mechanical nature



**Fig. 74 Research methodology, Zuccaro et al. (2012).**

The result has been obtained by a Monte Carlo simulation analysis, and can be described in five steps analyzed in more detail in the following paragraphs:

- i. Statistical analysis of existing masonry buildings
- ii. Iterative model generation.
- iii. Seismic vulnerability classification by “save” method.
- iv. Collapse mechanisms calculation.

- v. Vulnerability curves assessment.

## 5.1 STATISTICAL ANALYSIS OF EXISTING MASONRY BUILDINGS

The research is based on a statistical analysis, made by Zuccaro et al. (2012), of the observed damages due to previous earthquakes on the existing masonry buildings. The analysis, pursued thanks to the PLINIVS Study Centre Database, is based on the survey performed all along the Italian peninsula post the main Italian earthquakes from 1980 to 2012 (**Fig. 75**). About 250,000 of the residential masonry buildings have been surveyed distributed on about 600 municipalities.

This analysis has allowed to investigate the geometrical and structural characteristics of Italian masonry building and identify the recurring combinations of these characteristics. The probability of combination between a particular characteristic (e.g. type of vertical structure) and other features (e.g. type of horizontal structure, presence of ties, etc.) have been then evaluated (**Table 12**).

The most probable combinations of these characteristics allow the development of an iterative model that can generate a great number of virtual buildings, varying the sensitive parameters (vertical structure, connections, floor stiffness, pushing roofs, etc.).

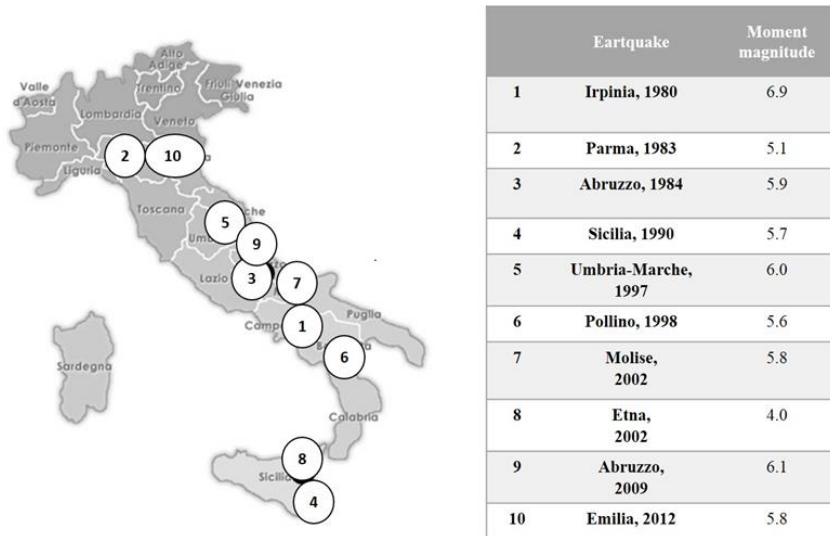


Fig. 75 Earthquakes investigated in the Plinius Study Centre Database.

Table 12 Probability of combination between the typology of vertical structure of the buildings and other features (typology of horizontal structure, number of floors and percentage of openings).

Typological parameter	Characteristics	Typology of vertical structure				
		Solid bricks	Regular stonework	Tuff	Hollow bricks	Irregular stonework
Typology of horizontal structure	Wooden beams	22	21	21	20	33
	Iron beams	50	52	52	20	13
	R.C. with hollow brick	18	18	18	60	42
	Vaults	10	9	9	0	12
Number of floors	1	47	47	47	47	35
	2	41	41	41	41	42
	3	10	10	10	10	17
	4	2	2	2	2	4
	5	0	0	0	0	2
Percentage of openings of the wall	10%	28	33	33	28	29
	20%	34	42	42	34	41
	30%	34	22	22	34	24
	40%	4	3	3	4	6

## 5.2 ITERATIVE MODEL GENERATION.

An iterative procedure has been implemented by ad-hoc MATLAB script developed in order to generate virtual model of buildings (about 100,000). The program adopts a random assignment procedure of the structural characteristics (Table 13) whose probability distributions are known from previous step.

Table 14 summarizes some occurrences of the virtual building dataset analysed in this research. In particular, the first column represent a progressive building identification number. Moreover, columns 2-11 report the structural characteristics assigned to the virtual buildings by the random assignment procedure.

**Table 13 Main typological characteristics identified on existing masonry buildings and assigned to the virtual buildings by a random procedure.**

Typological parameter	Characteristics	Identification parameter
Typology of vertical structure	Irregular stonework	5
	Hollow bricks	4
	Tuff	3
	Regular stonework	2
	Solid bricks	1
Typology of horizontal structure (Intermediate slabs and roof)	Wooden beams	1
	Iron beams	2
	R.C. with hollow brick	3
	Vaults	4

Number of floors	1 to 5	1 to 5
Inter-storey height	3- 3,5- 4- 4,5- 5 m	3- 3,5- 4- 4,5- 5
Wall thickness	0,27 to 0,8 m	0,27 to 0,8
Wall length	4- 5- 6- 7 m	4- 5- 6- 7
Percentage of openings of the wall	10- 20- 30- 40%	10- 20- 30- 40
Pushing roof	On/off	(1/0) variable
Tie rod/ Ring beams	On/off	(1/0) variable
Effectiveness of links	On/off	(1/0) variable

Table 14 Dataset of virtual buildings generated by a random procedure. (Sample of the first 13 occurrences of the computed dataset).

ID	Vertical structure	Horizontal structure	Number of floors	Pushing roof	The rod/ Ring beams	Effectiveness of links	Wall length	Inter-storey height	Wall thickness	Percentage of openings
1	5	4	2	1	0	0	5	4	0,5	10
2	5	1	2	1	1	0	4	4,5	0,6	20
3	4	3	1	0	1	0	6	3	0,36	30
4	4	3	2	0	0	0	6	4	0,45	10
5	3	3	2	0	0	0	5	3	0,5	30
6	2	4	1	0	1	1	5	4,5	0,5	20
7	4	2	1	0	1	1	7	3	0,36	30
8	4	3	1	0	0	0	6	3	0,45	30
9	3	1	4	0	1	1	6	5	0,3	30
10	1	1	2	0	0	1	6	3	0,36	30
11	2	2	4	1	0	1	5	5	0,5	20
12	1	4	1	0	0	1	6	3	0,46	20
13	4	3	1	0	1	0	5	3,5	0,45	10
...	...	...	...	...	...	...	...	...	...	...
100,000	4	2	1	0	1	1	5	3	0,45	10

### 5.3 SEISMIC VULNERABILITY CLASSIFICATION BY “SAVE” METHOD.

The generated virtual buildings have been classified in vulnerability classes: A, B, C, D (EMS'98) on the basis of their typological characteristics. According to the assignment procedure based on the criteria defined in the "SAVE" project (Zuccaro et al. 2015), the vulnerability level of each building is evaluated considering the typological characteristic as vulnerability modifiers, and giving to each of these a numerical weight calibrated using a wide database of seismic damage observed after the most important earthquakes occurred in Italy in the last forty years.

**Table 15** summarizes some occurrences of the virtual building dataset analyzed in this research. In particular, the first column represent a progressive building identification number. Columns 2-11 report the structural characteristics assigned to the virtual buildings by the random assignment procedure. Moreover, column 12 report the vulnerability class assigned to the model according to the SAVE methodology.

It is possible to analyse the distribution of the structural characteristics on the virtual buildings.

From **Table 16** it is possible to identify the main typological characteristics of the generated virtual buildings. **Table 17** shows that in most of the vulnerability class A buildings there are irregular stonework, wooden beams slabs and pushing roof. In most of the vulnerability class B and C buildings there are R.C. slabs, tie rod or ring beams. Moreover, in Class D buildings there are good quality of vertical and horizontal structure.

**Table 15 Seismic vulnerability classification of the virtual buildings (Sample of the first 13 occurrences of the computed dataset).**

ID	Vertical structure	Horizontal structure	Number of floors	Pushing roof	Tie rod/ Ring beams	Effectiveness of links	Wall length	Inter-storey height	Wall thickness	Percentage of openings	Vulnerability class "SAVE"
1	5	4	2	1	0	0	5	4	0,5	10	A
2	5	1	2	1	1	0	4	4,5	0,6	20	A
3	4	3	1	0	1	0	6	3	0,36	30	B
4	4	3	2	0	0	0	6	4	0,45	10	B
5	3	3	2	0	0	0	5	3	0,5	30	B
6	2	4	1	0	1	1	5	4,5	0,5	20	C
7	4	2	1	0	1	1	7	3	0,36	30	B
8	4	3	1	0	0	0	6	3	0,45	30	B
9	3	1	4	0	1	1	6	5	0,3	30	C
10	1	1	2	0	0	1	6	3	0,36	30	D
11	2	2	4	1	0	1	5	5	0,5	20	C
12	1	4	1	0	0	1	6	3	0,46	20	D
13	4	3	1	0	1	0	5	3,5	0,45	10	B
...	...	...	...	...	...	...	...	...	...	...	---
100,000	4	2	1	0	1	1	5	3	0,45	10	B

**Table 16 Percentage of the virtual buildings, classified in vulnerability class buildings, calculated for each structural characteristics.**

Typological parameter	Characteristics	Percentage of buildings ( %)			
		Class A	Class B	Class C	Class D
Typology of vertical structure	Solid bricks	0	15	33	34
	Regular stonework	0	16	33	21
	Tuff	11	20	13	22
	Perforated bricks	18	22	16	23
	Irregular stonework	71	27	5	0
Typology of horizontal structure (Intermediate slabs)	Wooden beams slabs	54	14	13	15
	Iron beams slabs	2	36	20	37
	R.C. with air brick slabs	28	46	60	41
	Vaults	16	4	7	7
Typology of horizontal structure (Roof)	Wooden beams slabs	78	36	36	40
	Iron beams slabs	16	16	9	13
	R.C. with air brick slabs	5	48	55	46
	Vaults	1	0	0	1
Number of floors	1-2	78	62	82	85
	3-4	21	34	17	14
	5	1	4	1	1
Interstorey height	3-3,5 m	64	63	64	64
	4-4,5m	32	27	23	22
	5 m	4	10	13	14
Wall thickness	0,27 to < 0,4 m	9	18	22	21
	0,4 to < 0,6m	61	64	70	72
	0,6 to <0,7m	25	17	7	6
	0,7 to 0,8 m	5	1	1	1
Wall length	4m	20	20	20	20
	5m	40	40	40	40
	6m	30	30	30	30
	7 m	10	10	10	10



Percentage of openings of the wall	10%	29	30	30	31
	20%	40	39	38	38
	30%	26	27	28	28
	40%	5	4	4	3
Pushing roof	No	26	81	90	94
	Yes	74	19	10	6
Tie rod/ Ring beams	No	60	38	20	20
	Yes	40	62	80	80
Effectiveness of links	No	75	60	50	50
	Yes	25	40	50	50

**Table 17 Main typological characteristics identified on the virtual buildings classified in vulnerability classes.**

Typological parameter	Structural characteristic			
	Class A	Class B	Class C	Class D
Typology of vertical structure	Irregular stonework	Irregular stonework/	Regular stonework/ Tuff	Solid bricks
Typology of horizontal structure (Intermediate slabs)	Wooden beams slabs	R.C. with air brick slabs	R.C. with air brick slabs	R.C. with air brick slabs
Typology of horizontal structure (Roof)	Wooden beams slabs	R.C. with air brick slabs	R.C. with air brick slabs	R.C. with air brick slabs
Number of floors	1-2	1-2	1-2	1-2
Interstorey height	3-3,5 m	3-3,5 m	3-3,5 m	3-3,5 m
Wall thickness	0,4 to < 0,6m	0,4 to < 0,6m	0,4 to < 0,6m	0,4 to < 0,6m
Wall length	5m	5m	5m	5m
Percentage of openings	20%	20%	20%	20%
Pushing roof	Yes	No	No	No
Tie rod/ Ring beams	No	Yes	Yes	Yes
Effectiveness of links	No	No	Yes	Yes

## 5.4 COLLAPSE MECHANISMS CALCULATION.

For each virtual building the trigger acceleration ( $a_g$ ) responsible of the relevant Collapse Mechanisms have been computed. The mechanisms

considered are assumed with reference to the classification adopted in the MEDEA methodology (Zuccaro et al., 2002).

The analysis procedure performed for each virtual building consists in computing the minimum value  $a_g$  of the horizontal acceleration for which any of its macro elements attains one of the limit state conditions corresponding to the kinematic schemes reported in Chapter 4 of this thesis.

To fix ideas, **Table 18** summarizes some occurrences of the virtual building dataset analysed in this research. In particular, the first two columns represent, respectively, a progressive building identification number and the vulnerability class assigned to the model. Moreover, columns 3-8 report the values of the trigger acceleration for which the weakest panel of the model attains at the corresponding ultimate limit state. Finally, assuming a series system behaviour, column 9 reports the minimum value of the trigger acceleration for which the global collapse of the model is assumed.

Table 18 Value of the trigger acceleration ( $a_g$ ) corresponding to the considered collapse mechanisms (sample of the first 8 occurrences of the computed dataset).

ID	Buildings Classes	In-plane mechanisms			Out of plane mechanisms			MIN
		Shear Crack	Buckling failure	Failure by slip	Vertical Bending	Horizontal Bending	Simple Overturning	
1	A	0,17	0,50	0,42	0,44	1,27	0,37	0,17
2	A	0,32	0,24	0,34	0,38	0,16	0,30	0,16
3	C	0,10	0,28	0,25	0,46	0,70	0,37	0,10
4	B	0,83	0,55	0,60	0,59	0,79	0,66	0,55
5	D	0,51	0,43	0,35	0,22	0,69	0,68	0,22
6	A	1,50	0,56	0,38	0,40	0,86	0,72	0,38
7	D	0,12	0,25	0,40	0,65	0,42	0,54	0,12
8	C	0,29	0,37	0,34	0,25	0,26	0,21	0,21
...	...	...	...	....	...	..	...	...
100,000	A	0,36	0,43	0,52	1,03	1,13	1,18	0,36

## 5.5 VULNERABILITY CURVES ASSESSMENT

Collecting the obtained results, for each typological class (A, B, C, D), vulnerability curves are built, expressing the collapse probability as a function of the ground acceleration ( $a_g$ ). The following chapter 6 includes more details about the vulnerability curves assessment.

## 6 RESEARCH RESULTS: THE VULNERABILITY CURVES

In order to assess the vulnerability curves as functions of the structural typology and of the seismic acceleration, the results of the iterative model described in chapter 5 are analyzed from a statistical point of view.

Grouping the generated vulnerability buildings by vulnerability class (Table 15), the arithmetic mean value and the standard deviation of the  $a_g$  values are calculated for each class and for all the mechanisms. These values consist in the first two moments of the Damage State Probability distributions characterizing the attainment of each limit state.

In general, the values of the first two moments are not exhaustive of the limit state statistics. Nevertheless, a widely accepted assumption consists in modelling damage state probability curves by means of lognormal distributions which can be exhaustively characterized by the computed mean and standard deviation (Table 19).

**Table 19 Data computed in order to plot the normal distribution curves (arithmetic mean and standard deviation) and the lognormal distribution curves (logarithmic arithmetic mean and logarithmic standard deviation).**

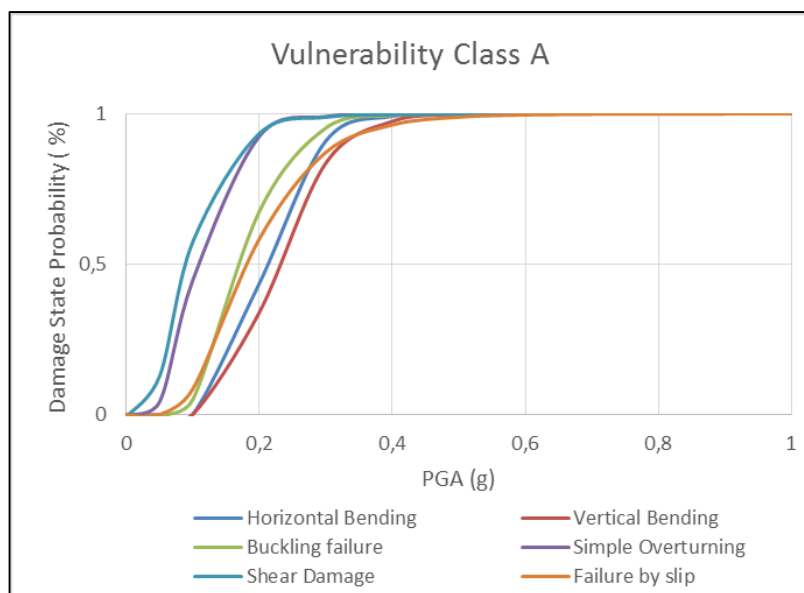
Vulnerability Class	Mechanism of collapse	Arithmetic Mean $a_g$	Standard Deviation	Logarithmic Arithmetic Mean $a_g$	Logarithmic Standard Deviation
Class A	Horizontal Bending	0,2165872	0,062478231	-1,567209683	0,27050748
Class A	Vertical Bending	0,2351457	0,070394931	-1,490216977	0,2917237
Class A	Buckling failure	0,1813519	0,060501745	-1,762112911	0,33286213
Class A	Simple Overturning	0,1173587	0,060027656	-2,246244711	0,44049067
Class A	Shear Damage	0,1027951	0,052650027	-2,403599619	0,52476719
Class A	Failure by slip	0,1996549	0,087279847	-1,704547508	0,44011794

Class B	Horizontal Bending	0,271212	0,095117419	-1,360719673	0,33029329
Class B	Vertical Bending	0,2627598	0,072399799	-1,373224726	0,27099213
Class B	Buckling failure	0,2332471	0,088962668	-1,528032736	0,38614182
Class B	Simple Overturning	0,1715077	0,109242739	-1,954948345	0,61874478
Class B	Shear Damage	0,13619	0,072361063	-2,137783025	0,56084326
Class B	Failure by slip	0,2069249	0,102414574	-1,688185858	0,47756231
Class C	Horizontal Bending	0,3364239	0,129308499	-1,16970677	0,41361358
Class C	Vertical Bending	0,2953593	0,088807544	-1,264617072	0,30274465
Class C	Buckling failure	0,2334368	0,098810356	-1,540120943	0,41553417
Class C	Simple Overturning	0,194785	0,124482239	-1,851441136	0,6739119
Class C	Shear Damage	0,1732577	0,084829372	-1,886447544	0,55000204
Class C	Failure by slip	0,244349	0,120432344	-1,531762906	0,50542271
Class D	Horizontal Bending	0,3266324	0,135750444	-1,200386379	0,40351075
Class D	Vertical Bending	0,316696	0,103509408	-1,20098466	0,32040324
Class D	Buckling failure	0,2679867	0,130790946	-1,426075072	0,46655155
Class D	Simple Overturning	0,3829595	0,133882023	-1,041016085	0,44710104
Class D	Shear Damage	0,1956977	0,095803596	-1,762913778	0,546965
Class D	Failure by slip	0,252516	0,128837951	-1,506494804	0,52313974

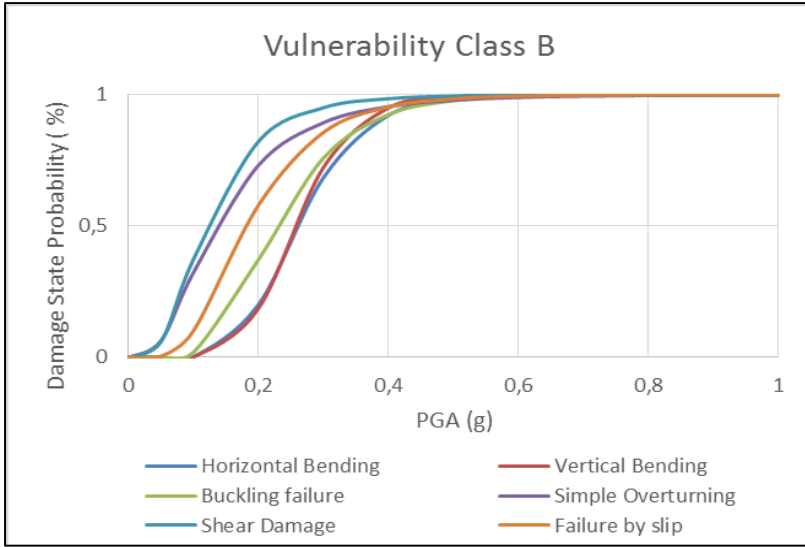
Probability curves related to each collapse mechanism and vulnerability class are reported **Fig. 76 - Fig. 79** where the collapse probability is plotted as function of the ground acceleration  $a_g$ . Building typology determining the vulnerability class turns out to have a great influence on the probability distribution trend. In particular, class A buildings, whose curves are reported in **Fig. 76**, present high vulnerability with respect to the shear crack and overturning collapse since these curves are shifted to the left of

the graph with respect to the remaining distributions. This result is consistent with expectations since shear vulnerability is related to the poor mechanical strength of the masonry belonging to class A. Moreover, such a building typology presents masonry walls without strong mutual connection; for this reason, overturning mechanisms are likely to be activated even for low values of the base acceleration.

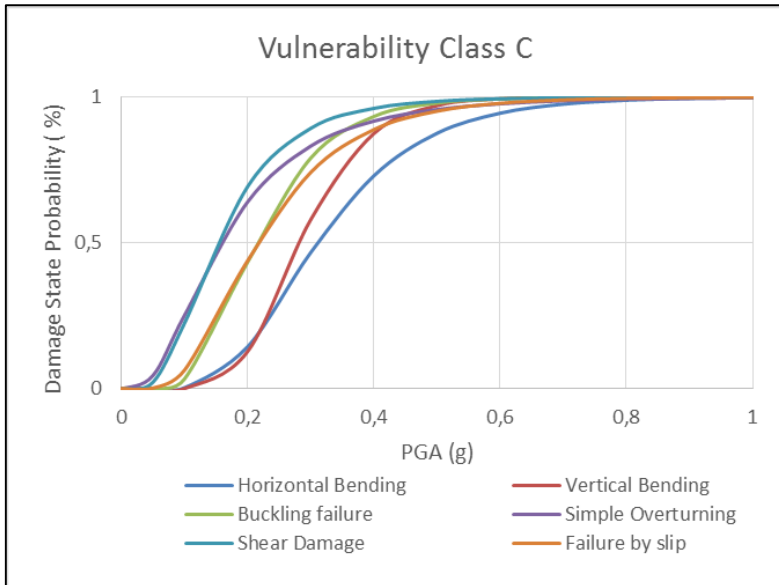
Structures belonging to vulnerability class B, shown in Fig. 77, present wall connections and a higher mechanical strength in fact probability distributions turn out to be shifted to the right of the graph with respect to the class A curves. Nevertheless, shear and overturning collapse mechanisms remain the governing limit states of such a structural typology.



**Fig. 76 Lognormal distribution curves for buildings vulnerability class A as functions of trigger acceleration of each Collapse Mechanism (PGA) vs the Damage State probability**

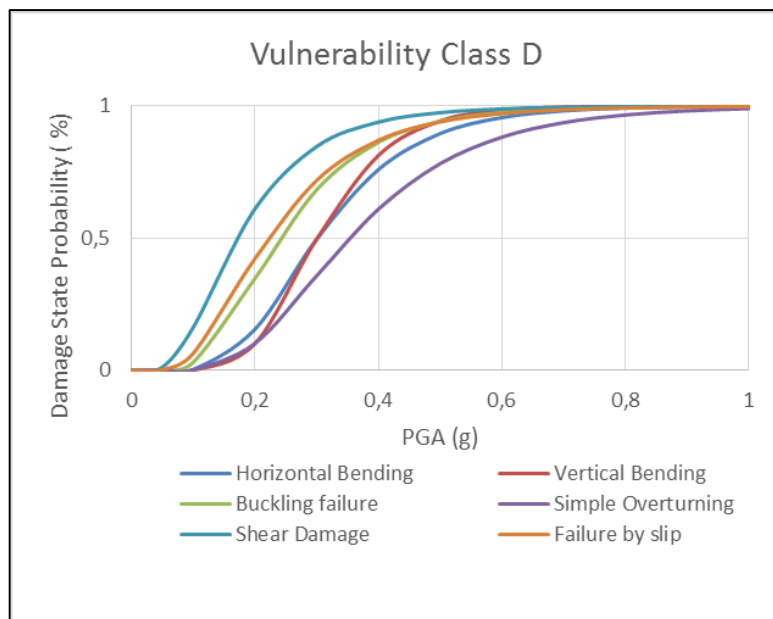


**Fig. 77 Lognormal distribution curves for buildings vulnerability class B as functions of trigger acceleration of each Collapse Mechanism (PGA) vs the Damage State probability**



**Fig. 78 Lognormal distribution curves for buildings vulnerability class C as functions of trigger acceleration of each Collapse Mechanism (PGA) vs the Damage State probability**





**Fig. 79 Lognormal distribution curves for buildings vulnerability class D as functions of trigger acceleration of each Collapse Mechanism (PGA) vs the Damage State probability**

Probability distributions corresponding to classes C and D, shown in Fig. 78 and Fig. 79, respectively, present a further shifting to the high accelerations meaning that the collapse probability is decreasing as long as the structural strength is improved. Moreover, since in classes C and D are present wall connections and a higher mechanical strength of the wall, the trigger acceleration of the overturning mechanisms is higher than in other buildings classes.

Further considerations can be made by analysing the predominant collapse typology. Fig. 80 presents, for each vulnerability class, the percentage of the structural models belonging to the virtual dataset collapsed either for in-plane or out-of-plane mechanisms. From a frequentistic point of view, and assuming that the dataset is significant of the Italian building asset, the graph reports the probability that the failure of a structure belonging to a specific class, if occurs, is expected to be determined by either in-plane or out-of-plane collapses.

In general, the probability of out-of-plane phenomena decreases proportionally to the vulnerability and, in the case of classes B, C and D does not present significant differences since the probability of out-of-

plane phenomena is about 40%. On the contrary, collapse of class A buildings has the 60% probability to be induced by out-of-plane collapses. This is an important aspect from a resilience point of view; in fact, out-of-plane failures turn out to be more disastrous than in-plane ones. In this sense, retrofit of out-of-plane collapses are far more difficult than the repair of in-plane damages and are expected to arouse significant casualties because of their rapid progression.

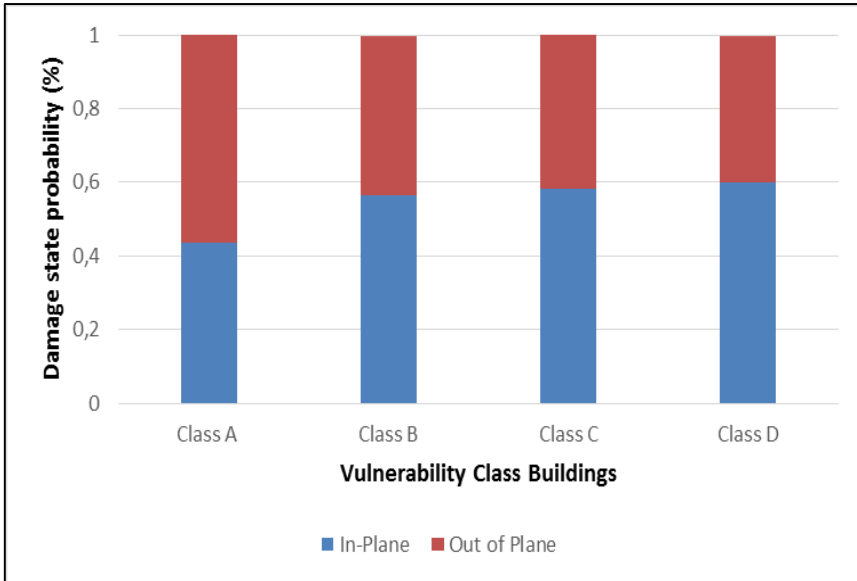
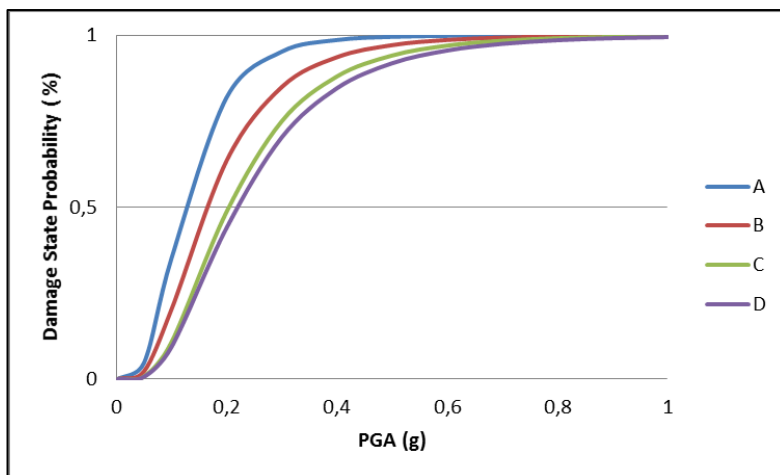


Fig. 80 Mechanism type activating probability for each vulnerability class (A, B, C, D)

## 6.1 DAMAGE VULNERABILITY CURVES

Global vulnerability curves, reported in Fig. 81, are obtained by assuming the global failure of each single structural model at the attainment of the first limit state condition. Thus, global distributions are computed by assuming lognormal trend and computing, for each vulnerability class, mean and standard deviation of the ground acceleration minimum values reported in the last column of Table 18.

The global curves are not merely an envelope of the single-mechanism distributions reported in **Fig. 76 - Fig. 79**. On the contrary, the computation of the first two probabilistic moments of  $a_g$  is capable of accounting for the mechanisms' correlation. In this sense, global failure curves represent the joint probability that any of the collapse mechanisms is triggered by the ground acceleration.



**Fig. 81 Damage Vulnerability Curves for each vulnerability Class (A, B, C, D).**

For convenience, a further representation of structural vulnerability is shown in **Fig. 82** where global failure probability is represented as function of a macro-seismic intensity index computed by the equation proposed by Faccioli and Cauzzi [2006].

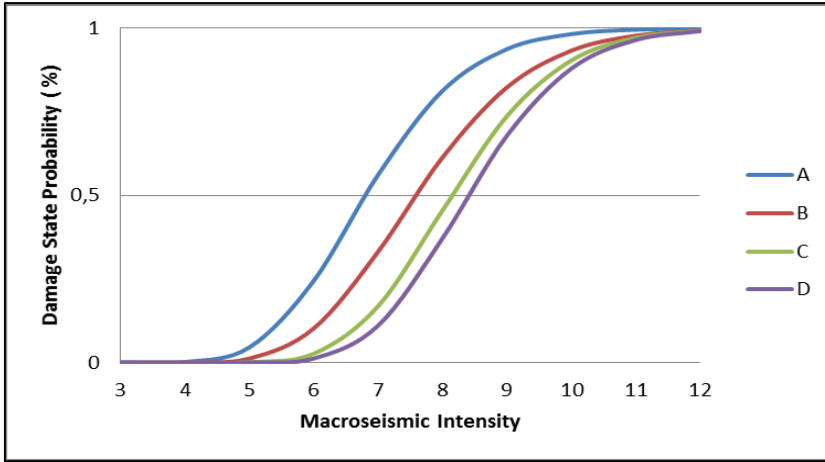


Fig. 82 Damage Vulnerability Curves for each vulnerability Class (A, B, C, D).

Although conceptually probabilities reported in Fig. 81 and Fig. 82 have the same physical sense, the plotted curves apparently have different trends. This issue is due to the fact that relationship between collapse ground acceleration and seismic intensity is, in general, non-linear. Nevertheless, both these representations are useful in order to compare the results of the proposed strategy with vulnerabilities computed by alternative procedures.

## 6.2 COMPARISON WITH ALTERNATIVE STRATEGIES

In order to investigate the accuracy of the proposed methodology, the probability curves reported in the previous paragraph are compared with the distributions obtained by the application of alternative strategies available in the literature.

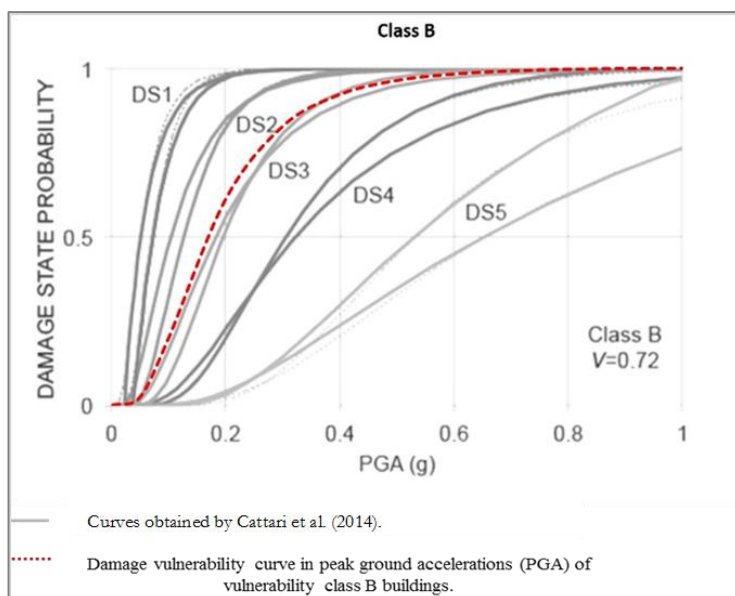


Fig. 83 Comparison between damage Vulnerability Curves of vulnerability Class B and the one obtained by Cattari et al (2014)

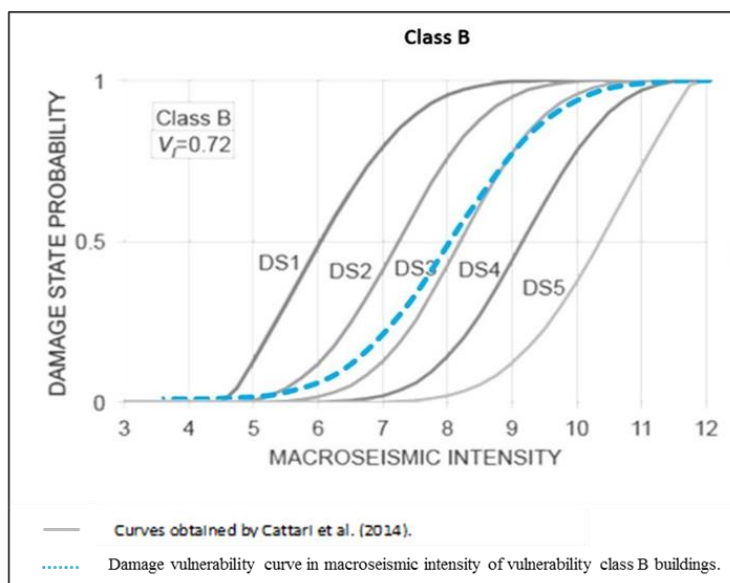


Fig. 84 Comparison between damage Vulnerability Curves of vulnerability Class B and the one obtained by Cattari et al, 2014.

The approach used by Cattari et al. (2014) which developed fragility curves for vulnerability class B then extrapolated to the other classes. Comparison with the proposed strategy are reported in **Fig. 83** and **Fig. 84** where probability curves have been plotted, respectively, with respect to the ground acceleration and the seismic intensity.

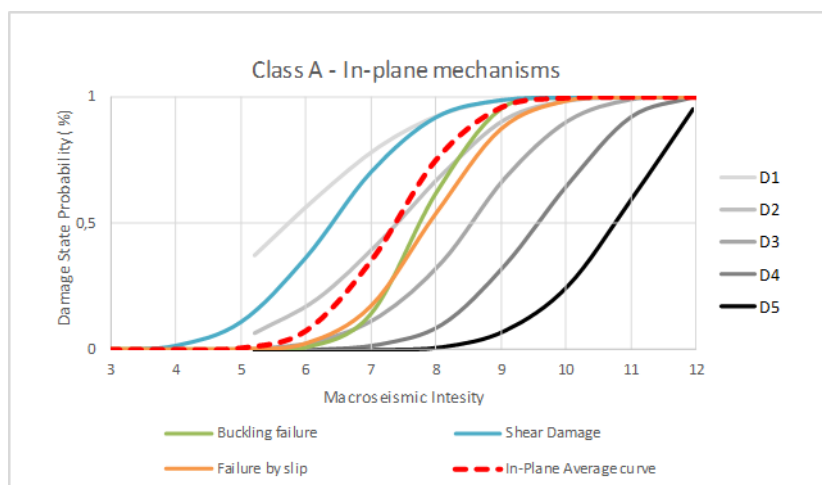
In both the cases, the proposed strategy presents a good matching with the curves esteemed for a damage level defined as D3 which denotes the first significant structural damage occurred in the structural elements which does not necessarily implies the contemporary collapse of several structural elements. This is consistent with the assumptions of the proposed strategy where vulnerability is function of the first limit state attainment. In fact, partial and total collapse of the structure, corresponding to damage levels D4 and D5, usually occur when more than a single structural element is collapsed, especially in presence of in-plane mechanisms.

In this sense, the proposed strategy proved to be encouragingly consistent with the benchmark data.

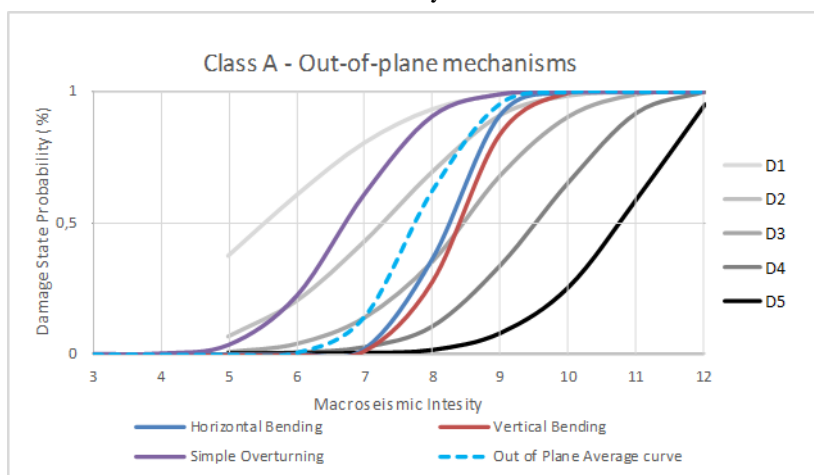
The partial or total collapse of the buildings (D4-D5), that generally requires not only the trigger of the first mechanism but the occurrence of more mechanisms and greater displacements, will be taken into account in the following development of the research.

The vulnerability curves are compared also with the empirical curves derived from the Damage Probability Matrices (DPM) (**Table 7**) (Zuccaro et al., 2015) obtained by statistical fitting of observed damages recorded of all the past seismic events in Italy from Irpinia 1980 earthquake up to L'Aquila event in 2009.

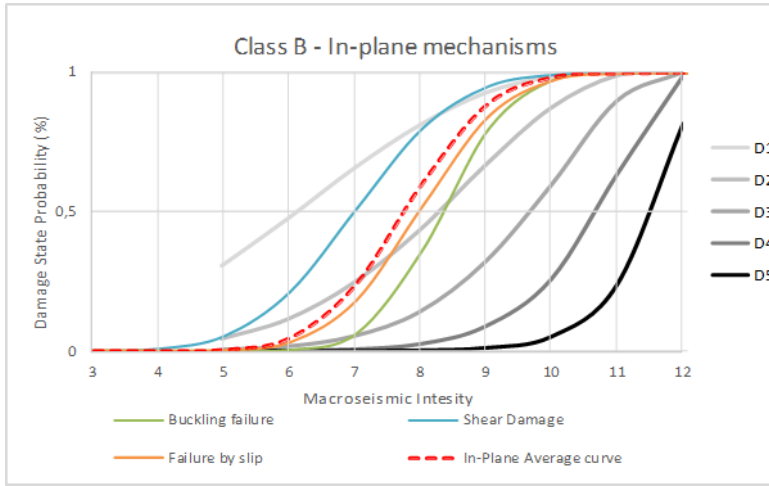
The set of statistical curves relevant to class A and B models, shown in Figures **Fig. 85 -Fig. 86**, encompasses the distributions esteemed by the proposed procedure. In particular, those latter span in between damage states D1 and D4. This is significant of the fact that, for the case of poor structural quality, even small damage mechanisms, incapable of producing significant damage for different structural typologies, could generate serious failures to vast parts of the structure. Moreover, it is worth to emphasize that, while in-plane mechanisms are limited to D1-D3 damage levels, out-of-plane curves reach the D4 level. This confirm the physical interpretation for which out-of-plane mechanisms are premonitory of serious and extended structural failures.



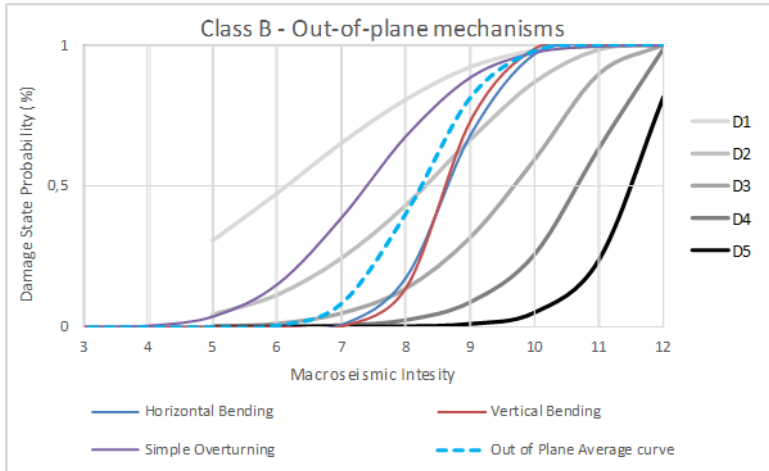
**Fig. 85** Comparison between the In-plane mechanisms vulnerability curves and vulnerability curves derived from DPM [Zuccaro and De Gregorio, 2015] for vulnerability class A



**Fig. 86** Comparison between the out of plane mechanisms vulnerability curves and vulnerability curves derived from DPM [Zuccaro and De Gregorio, 2015] for vulnerability class A



**Fig. 87** Comparison between the In-plane mechanisms vulnerability curves and vulnerability curves derived from DPM [Zuccaro and De Gregorio, 2015] for vulnerability class B.



**Fig. 88** Comparison between the out of plane mechanisms vulnerability curves and vulnerability curves derived from DPM [Zuccaro and De Gregorio, 2015] for vulnerability class B

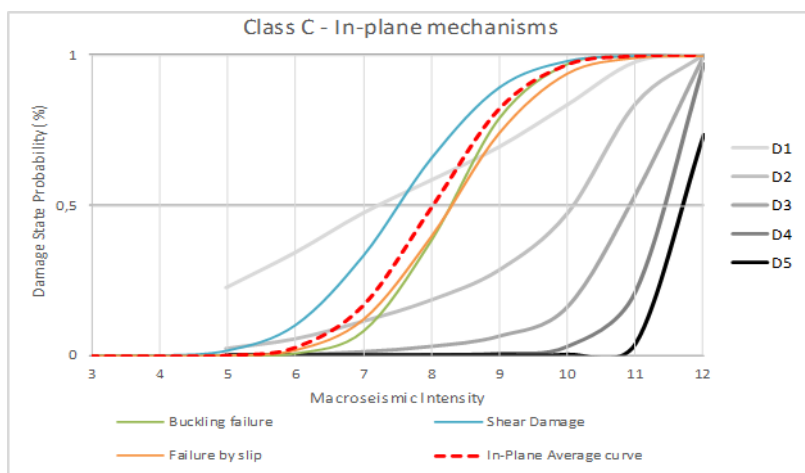
In vulnerability class C and D (Fig. 89-Fig. 90, Fig. 91-Fig. 92) the in-plane mechanism curves are representative of a level of damage D1-D2 and out of plane curves are representative of a level of damage D1-D3.

As long as the structural robustness is increased, as in the case of class B reported in Fig. 87 and Fig. 88 the proposed probability distributions shift to the left side of the graphs and are encompassed by statistical

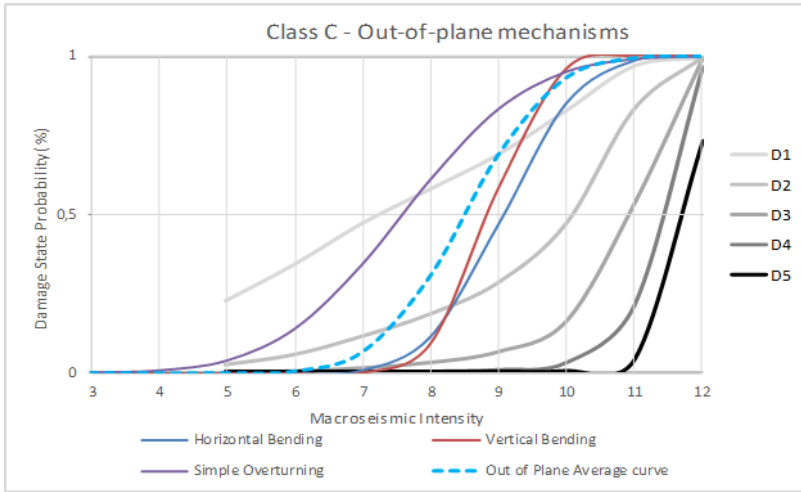


curves relevant to damage states D1 and D3. Results of vulnerability classes C and D provide similar probability distributions. For both the cases, probability relevant to in-plane mechanisms are encompassed by statistical curves of damage levels D1-D2 while the out-of-plane distributions attain at the D3 level. This is due to the fact that, in presence of connecting devices and sufficient ductility, damages induced by in-plane mechanisms are usually limited to a few structural elements and do not necessarily trigger global failure.

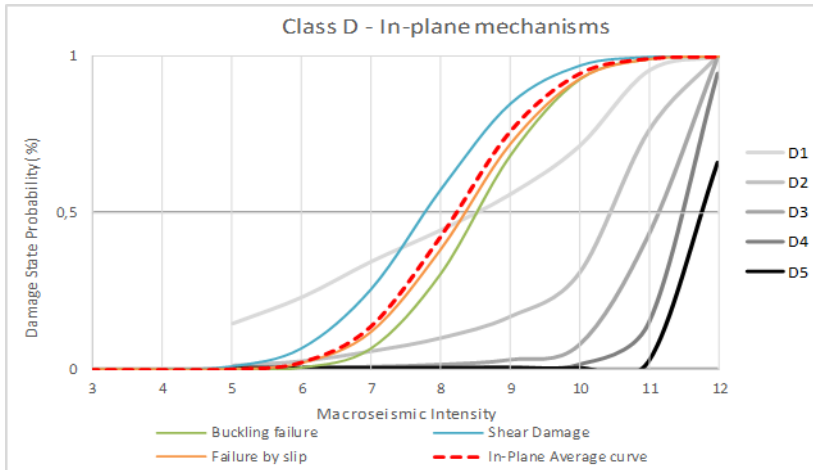
In conclusion, comparison with the different approaches, the derived vulnerability curves shows a good matching of the probability distributions computed by the proposed strategy, although further investigations are required. Nevertheless, the reported comparisons have shown a sufficient robustness of the proposed procedure and confirm the physical assumptions introduced in the computational framework.



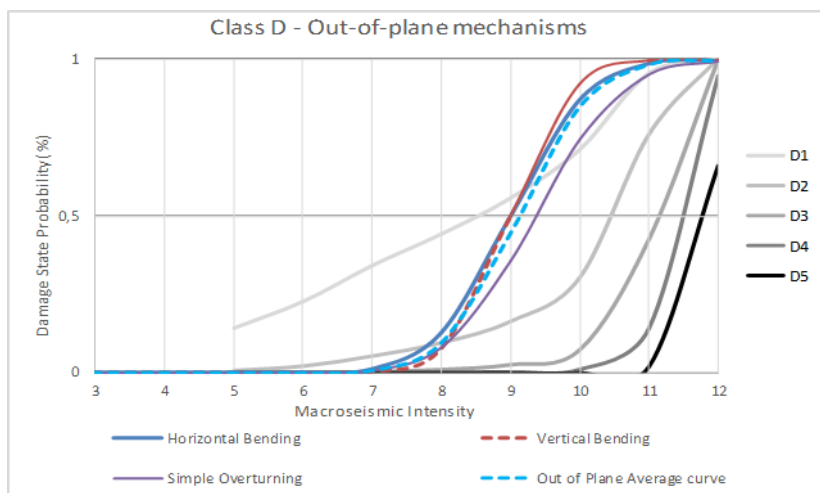
**Fig. 89** Comparison between the In-plane mechanisms vulnerability curves and vulnerability curves derived from DPM [Zuccaro and De Gregorio, 2015] for vulnerability class C



**Fig. 90** Comparison between the out of plane mechanisms vulnerability curves and vulnerability curves derived from DPM [Zuccaro and De Gregorio, 2015] for vulnerability class C



**Fig. 91** Comparison between the In-plane mechanisms vulnerability curves and vulnerability curves derived from DPM [Zuccaro and De Gregorio, 2015] for vulnerability class D



**Fig. 92 Comparison between the out of plane mechanisms vulnerability curves and vulnerability curves derived from DPM [Zuccaro and De Gregorio, 2015] for vulnerability class D**



## 7 CONCLUSIONS

In this dissertation, a hybrid methodology for determining the vulnerability curves as functions of the structural typology and of the seismic acceleration is presented.

It consists in determining a virtual set of structural models (about 100,000) representing the structural typologies of ordinary masonry buildings distributed on Italian territory. They have been derived through examination of structural characteristics (dimensions of structural elements, mechanical characteristics of material, typologies of horizontal structures and roofing, presence of vaults and/ or ties or ring beams, number of floors, etc.) collected by 'in situ' survey of about 250,000 buildings distributed along the Italian territory.

Each virtual structure is therefore analysed by a simplified procedure in which the structural performance is computed with respect of a limited set of in-plane (shear crack, failure by slip and buckling failure) and out-of-plane (simple overturning, vertical bending and horizontal bending) collapse mechanisms commonly observed in the experimental dataset.

Assuming a series system behaviour of each structural model, and in particular, setting as global failure condition the attainment of the first limit state, the probability distributions of global collapse with respect to the base acceleration have been derived and for each typological class (A, B, C, D), vulnerability curves are built, expressing the collapse probability as a function of the ground acceleration ( $a_g$ ).

Such distributions have been compared with benchmark vulnerability curves available in the literature and derived by Zuccaro et al. (2015) and Cattari et al. (2014).

The proposed methodology proved to be consistent with the benchmark results confirming physical interpretations commonly accepted in common practice, such as the high fragility induced by out-of-plane mechanisms. Nevertheless, some of the computed vulnerability curves turn out to be over-conservative with respect to the considered benchmarks.

Such an issue is due to the series system hypothesis assumed for the simplified structural analysis procedure. In fact, most of the considered

collapse mechanisms, although compromising the structural capacity of one or more structural elements, do not necessarily induce global failure phenomena.

For this reason, further investigations are required in order to account for the correlation of limit state conditions in different structural elements, ductility and more complex global kinematics. Such further information is oriented to determine failure probability distributions not only related to structural typologies, but also significant of different damage states.

The approach adopted constitutes a preliminary study to understand the basic seismic behavior of the ordinary masonry buildings.

Further developments of the research will include additional improvements also in dynamic state, able to identify a more accurate evaluation of collapse accelerations [Boothby, 2001; De Jong, 2009], considering micromechanical modelling of failure (effects of deformations in the mortar joints, detailed properties of the material, irregularity in the panels, etc.) and more detailed sensitivity analyses on the observed data used and on their reliability.

## 8 REFERENCES

- Addressi, D., Marfia, S., Sacco, E., Toti, J. (2014). Modeling Approaches for Masonry Structures. *The Open Civil Engineering Journal* 8, 288-300, 2014 (DOI: 10.2174/1874149501408010288).
- Alexandris, A., Protopapa, E., & Psycharis, I. 2004. Collapse mechanisms of masonry buildings derived by the distinct element method. In *13th World Conference on Earthquake Engineering*.
- Angelillo, M. (Ed.) 2014. *Mechanics of masonry structures*. Vienna: Springer.
- Augenti, N. (2000). *Il calcolo sismico degli edifici in muratura* Utet, Torino.
- Baratta, A. (1984). Il materiale non reagente a trazione come modello per il calcolo delle tensioni nelle pareti murarie. *Restauro*, p. 75.
- Baratta, A. (1991). Statics and reliability of masonry structures. In *General Principles Applications in Mechanics of Solids and Structures*. CISM, Udine: 205–235.
- Baratta, A., Corbi, O. (2005). On Variational Approaches In Nrt Continua, *International Journal Of Solids And Structures*.
- Barbat, A.H., Yépez Moya, F. and Canas, J.A. (1996). “Damage Scenarios Simulation for Seismic Risk Assessment in Urban Zones”, *Earthquake Spectra*, Vol. 12, No. 3, pp. 371-394.
- Benedetti and Petrini, 1984. A method for evaluating the seismic vulnerability of masonry buildings. *L'industria delle costruzioni*, 149 (1984), pp. 66-74.
- Bernardini, A., Giovinazzi S., Lagomarsino, S., Parodi, S. (2007a). Damage probability matrices implicit in scale EMS-98 by housing typologies. In Italian: Matrici di probabilità di danno implicite nella scala EMS-98 per tipologie di edilizia abitativa. XII Convegno ANIDIS L'ingegneria sismica in Italia, Pisa.
- Bernardini, A., Giovinazzi, S., Lagomarsino, S., Parodi, S. (2007b). Vulnerability and prediction of damage at regional scale using a methodology consistent with the EMS-98 macroseismic scale. In Italian: Vulnerabilità e previsione di danno a scala territoriale secondo una metodologia macrosismica coerente con la scala EMS-98. XII Convegno ANIDIS L'ingegneria sismica in Italia, Pisa.

- Betti, M., Galano, L., Petracchi, M., Vignoli A. (2012). Seismic Strength of Unreinforced Masonry Walls: Effects of the b Shape Factor of the Shear Failure Criterion with Diagonal Cracking. *Ingegneria Sismica* N. 4 – ottobre-dicembre 2012
- Boothby, T.E. (2001). Analysis of masonry arches and vaults, *Progress in Structural Engineering and Materials*, 3, 246-256.
- Braga, F., Dolce, M., Liberatore, D. (1986). Assessment of the relationships between macroseismic intensity, type of building and damage, based on the recent Italy earthquake data. *Proc. of the 8th European Conference on Earthquake Engineering*.
- Braga, F., Dolce, M., Liberatore, D. (1982). Southern Italy November 23, 1980 Earthquake: A Statistical Study on Damaged Buildings and an Ensuing Review of the M.S.K.-76 Scale. *CNR-PFG n.203, Roma.*
- Bramerini, F., Di Pascale, G., Orsini, G., Pugliese, A., Romeo, R. and Sabetta, F. (1995). Seismic risk in territory of Italy (in Italian). *Proceedings of 7th Convegno Nazionale di Ingegneria Sismica, Siena, Italy, September 25–28.*
- Bucchi, F., Arangio, S., & Bontempi, F. (2013). Seismic assessment of an historical masonry building using nonlinear static analysis.
- Calvi, G.M., Pinho, R., Magenes, G., Bommer, J.J., Restrepo-Vélez, L.F., Crowley, H. (2006). Development of seismic vulnerability assessment methodologies over the past 30 years. *ISET Journal of Earthquake Technology*, Paper No. 472, Vol. 43, No. 3, September 2006, pp. 75-104.
- Cattari, S., Lagomarsino, S., Ottonelli, D. (2014). Fragility curves for masonry buildings from empirical and analytical models. *Second European conference on earthquake engineering and seismology, Istanbul Aug. 25-29.*
- Cavalieri, L., Di Trapani, F., Ferrotto, M.F. (2017). A new hybrid procedure for the definition of seismic vulnerability in Mediterranean cross-border urban areas.”*Natural Hazards* 86(2), 517-541.
- Coburn, A.W and Spence R.J.S, 2002. *Earthquake Protection*, John Wiley and Sons
- Como, M. (1992). Equilibrium and Collapse Analysis Of Masonry Bodies. *Meccanica* 27: 184-194.
- Cornell, C.A. (1968). Engineering seismic risk analysis, *Bull. Seismol. Soc. Am.*, 58, p. 1,583–1,606.



- D'Ayala, D., and Speranza, E. (2003). Definition of Collapse Mechanisms and Seismic Vulnerability of Historic Masonry Buildings. *Earthquake Spectra*: August 2003, Vol. 19, No. 3, pp. 479-509.
- D'Ayala, D. and Tomasoni, E., 2008. Structural Behaviour of Masonry Vaults: Limit State Analysis with Finite Friction. In: D'Ayala, D. F. and Fodde, E., eds. *Structural Analysis of Historic Construction: Preserving Safety and Significance. Proceedings of the VI International Conference on Structural Analysis of Historic Construction, SAHC08, 2-4 July 2008, Bath, United Kingdom*. Vol. 1. London: Taylor & Francis, pp. 47-61.
- D'Ayala, D., Galasso, C., Minas, S., and Novelli, V. (2015). Review of methods to assess the seismic vulnerability of buildings, with particular reference to hospitals and medical facilities. Evidence on Demand, UK, 2015. iii + 28 pp. [DOI: 10.12774/eod\_hd.june2015.dayaladetal].
- Di Pasquale, S., (1984). Questioni Concernenti La Meccanica Dei Mezzi Non Reagenti A Trazione. Unilateral Problem In Structural Analysis, Ravelo, Pp 25-46.
- Dumova- Jovanoska, E. (2004). Fragility Curves for RC Structures in Skopje Region. *Proceedings of the 13<sup>th</sup>. World Conference on Earthquake Engineering, Vancouver, Canada, Paper No. 3 (on CD)*.2004.
- NTC (2008). New technical rules for constructions. In Italian: Nuove norme tecniche per le costruzioni. DM 14 gennaio 2008. *Gazzetta Ufficiale* n. 29 del 4 febbraio 2008 - Suppl. Ordinario n. 30.
- CM (2009). Instructions for applying the 'New Technical Standards for Construction'. In Italian: Istruzioni per l'applicazione delle 'Nuove norme tecniche per le costruzioni' di cui al decreto ministeriale 14 gennaio 2008. *CIRCOLARE* 2 febbraio 2009, n. 617 -. (GU n. 47 del 26-2-2009 - Suppl. Ordinario n.27).
- De Jong M. J. (2009). Seismic Assessment Strategies for Masonry Structures. Doctor of Philosophy in Architecture: Building Technology at the Massachusetts Institute of Technology (MIT). <https://dspace.mit.edu/handle/1721.1/49538>.
- Del Piero G., (1989). Constitutive Equation And Compatibility Of The External Loads For Linear Elastic Masonry-Like Materials, *Giornale Di Meccanica* 24 150-162.
- Faccioli, E. and Cauzzi, C. (2006). Macro seismic intensities for seismic scenarios estimated from instrumentally based correlations. *Proceeding First European Conference on Earthquake Engineering and Seismology*, Paper n. 569.

FEMA P-774/ (October 2009) Unreinforced Masonry Buildings and Earthquakes – Developing Successful Risk Reduction Programs.

Federal Emergency Management Agency (FEMA). (1994). "Reducing the risks of nonstructural earthquake damage, a practical guide." FEMA Publication 74. Washington, DC.

Franciosi, V. (1980). Friction in ultimate strength design of masonry". In Italian: L'attrito nel calcolo a rottura delle murature, *Giornale del Genio Civile* 8, 215-234.

Fuschi, P. , Giambianco G. And Rizzo S. (1995). Nonlinear Finite Element Analysys Od No-Tension Masonry Strucutres. *Meccanica* 233-249, 1995.

Gambarotta, L., Lagomarsino, S. (1997) Earthquake engineering & structural dynamics 26 (4), 441-462, 1997.

Giuffrè, A. (1991). Readings on Mechanics of Historic Masonry. In Italian: Letture sulla Meccanica delle Murature Storiche, Kappa, 1991.

GNDT, (1993). Rischio Sismico di Edifici Pubblici, Parte I: Aspetti Metodologici. *Tipografia Moderna*, Bologna.

Gómez Capera A.A., Albarello D., Gasperini P., (2007). Aggiornamento relazioni fra l'intensità macrosismica e PGA. Progetto DPC-INGV S1, Deliverable D11.

Grünthal, G. (1998). European Macroseismic Scale 1998.

Guagenti, E. & Petrini, V. (1989): Il caso delle vecchie costruzioni: verso una nuova legge danni-intensità, *Proceedings of the 4th Italian National Conference on Earthquake Engineering*, - Milan - (Italy), vol. I, pp. 145-153.

Heyman, J. (1966). The Stone Skeleton, *Journal Of Solids And Structures* 2, 269-279 ,1966.

Heyman, J., (1969). The Safety Of Masonry Arches, *Journal Of Mechanic Sciences* 2, 363-384.

Kooharian, A. (1952). Limit analysis of voussoir and concrete arches. *J. Amer concrete inst.* 24.

Lagomarsino S and Cattari S (2013) "Seismic vulnerability of existing buildings: Observational and mechanical.

approaches for application in urban areas," (Chapter 1), *Seismic Vulnerability of Structures*, P Gueguen

(ed), pp. 1-62. ISTE Ltd and John Wiley and Sons, ISBN 978-1-84821-524-5

- Lourenco, P., Rots, J. And Blaauwendraad, J.(1995). Two Approches For The Analysis Of Masonry Strcutres: Micro And Macro- Modeling, Heron, Vol 40, No.4, 1995.
- Lourenço, P., Milani, G., Tralli, A., Zucchini, A. (2007). Analysis of masonry structures: review of and recent trends in homogenization techniques. *Canadian Journal of Civil Engineering*, 2007, 34(11): 1443-1457.
- Maier, G. And Nappi, A. (1989). Theory Of No-Tension Discretized Structural Systems.
- Medvedev, S.V. and Sponheuer, W. (1969) Scale of seismic intensity. *Proceedings of the 5th World Conference Earthquake Engineering*, Santiago, 13-18 January 1969. 135-138.
- Milano, L., Mannella, A., Morisi, C., Martinelli, A. (2008). Illustrative forms of the main local collapse mechanisms in existing masonry buildings and their kinematic analysis models. In Italian: Schede illustrative dei principali meccanismi di collasso locali negli edifici esistenti in muratura e dei relativi modelli cinematici di analisi. Allegato alle Linee Guida per la Riparazione e il Rafforzamento di elementi strutturali, Tamponature e Partizioni - DPC-RELUIS - 2008 - Archivio Reluis.
- Navaratnarajah, Sathiparan. (2015). Mesh type seismic retrofitting for masonry structures: Critical issues and possible strategies. *European Journal of Environmental and Civil Engineering*, 19. 1136-1154.
- Park, Y.J. and Ang, A. H-S. and Wen, Y.K. (1987). Damage-limiting aseismic design of buildings". *Earthquake Spectra*, 3:1,1-26.
- Pitta A. (2000) Traditional stone masonry houses in Cyprus. Manual for post earthquake repairs.
- Nikosia 2000 (in Greek).
- POLIMI (2010). Inventory of earthquake-induced failure mechanisms related to construction types, structural elements, and materials, NIKER Grant Agreement n° 244123.
- POLIMI (2010). Critical review of methodologies and tools for assessment of failure mechanisms and interventions, NIKER Grant Agreement n° 244123.
- Masi, A. (2003). Seismic Vulnerability Assessment of Gravity Load Designed R/C Frames". *Bulletin of Earthquake Engineering*. November 2003, Volume 1, Issue 3, pp 371–395.

Novelli, V.I. and D'Ayala, D. (2012). Assessment of the most damaged historic centres of the Region Emilia Romagna due to the earthquake of the 20th and 29th of May 2012. *Ingegneria Sismica*, 29 (2-3), pp. 59-71.

J. Ochsendorf, "Collapse of Masonry Structures," Ph.D. Dissertation, University of Cambridge, Cambridge, 2002.

Porter, K., 2017. A Beginner's Guide to Fragility, Vulnerability, and Risk. University of Colorado Boulder, 98 pp.,

Reitherman, R. (1986). Background Paper on the Conversion of Damage Probability Matrices into Fragility Curves, Panel on Earthquake Loss Estimation National Research Council.

Reitherman, R. (2009). Unreinforced Masonry Buildings and Earthquakes. Prepared for Federal Emergency Management Agency (FEMA) Cathleen Carlisle, Project Monitor Washington, D.C.

Ricamato, M. 2007 Numerical and experimental analysis of masonry arches strengthened with FRP materials. PhD Thesis, University of Cassino, Italy.

Romano, G. And Sacco, E. (1983). Elastostatics Of Structures With Unilateral Conditions On Strains And Displacements. *Internat. Congr. On Unilateral Problem Of Structures*, Ravello.

Rossetto, T. and Elnashai, A. (2005). A new analytical procedure for the derivation of displacement-based vulnerability curves for populations of RC structures. *Engineering Structures* 27(3), 397-409.

Rossetto T., Ioannou I., Grant D.N., Maqsood T. Guidelines for empirical vulnerability assessment, GEM. Technical Report 2014-X, GEM Foundation, Pavia

Sandi, H. (1986). EAEE Working Group on Vulnerability and Risk Analysis or Individual Structures and for Systems. Report to the 8-th ECEE. *Proc. 8th European Conf. on Earthquake Engineering*, Lisbon. 1986.

Singhal, A. and Kiremidjian, A.S. (1996). Method for probabilistic evaluation of seismic structural damage. *Journal of Structural Engineering* 122:12, 1459-1467.

Spence, R., Coburn, A.W. and Pomonis, A. (1992). "Correlation of Ground Motion with Building

Damage: The Definition of a New Damage-Based Seismic Intensity Scale", *Proceedings of the Tenth*

World Conference on Earthquake Engineering, Madrid, Spain, Vol. 1, pp. 551-556.

- Tyagunov, S., Grunthal, G., Wahlstrom, R., Stempniewski, L., and Zschau, J. (2006). Seismic risk mapping for Germany. *Nat. Hazards Earth Syst. Sci.*, 6, 573–586, 2006
- Turnsek V. and Cacovic F. (1971). Some experimental result on the strength of brick masonry walls. *Proc. of the 2nd Intern. Brick Masonry Conference, Stoke-on-Trent.*
- Wang, Z. (2006). Understanding seismic hazard and risk: a gap between engineers and seismologists. University of Kentucky, Lexington, Kentucky, USA
- Whitman, R. V., (1973). Damage probability matrices for prototype buildings.
- Wood, H. O. and F. Neumann (1931). Modified Mercalli Intensity Scale of 1931, *Seismological Society of America Bulletin*, 21, 4, 277-283.
- Zuccaro, G., Bernardini, A., Gori, R., Muneratti, E., Paggiarin, C., Parisi, O. (2000). Vulnerability and probability of collapse for classes of masonry buildings. In: FACCIOLI E., PESSINAV. *The Catania Project: earthquake damage scenarios for high risk area in the Mediterranean.* p.146-158, ROMA: E. Faccioli e V. Pessina (Eds), CNR-GNDT, ISBN: 88-900449-0-X. 2000.
- Zuccaro, G. And Papa, F. (1996). *Modelli Tensionali In Pannelli Di Materiali Non Reagenti A Trazione.*
- Zuccaro, G. and Papa, F. (2004). MEDEA: A multimedia and didactic handbook for seismic damage evaluation. In: 29th European Seismological Commission General Assembly. p. 215-220, Potsdam (Germany), 12-17 September.
- Zuccaro, G., Cacace, F. (2006). Valutazione speditiva della Vulnerabilità per gli edifici strategici della Regione Campania, *Ingegneria Sismica*. n° 2.
- Zuccaro, G. and Papa, F. (2007). MEDEA Multimedia CD. Manual for Earthquake Damage Evaluation and safety Assessment for masonry and reinforced concrete buildings.
- Zuccaro, G., Cacace, F., Rauci M. (2009). Caratteristiche tipologiche degli edifici in muratura e meccanismi di collasso. *Atti XIII Convegno ANIDIS*, Bologna.
- Zuccaro, G., Cacace, F., Rauci, M. (2011). MEDEA: a multimedia and didactic handbook for structural damage and vulnerability assessment- L'Aquila case study. *Urban Habitat Constructions under Catastrophic Events (Proceedings)* – Mazzolani (Ed).© 2010 Taylor & Francis Group, London, ISBN 978-0-415-60685-1
- Zuccaro, G. and Cacace, F. (2012). Seismic vulnerability assessment of the masonry buildings based on the probability of occurrence of the main collapse

mechanism. Damage Vulnerability Curves vs. PGA. Proceeding 15th WCEE, Lisboa (Portugal).

Zuccaro, G. and Cacace, F. (2015). Seismic vulnerability assessment based on typological characteristics. The first level procedure SAVE. Soil Dynamics and Earthquake Engineering. Volume 69, February 2015, Pages 262-269.

Zuccaro, G. and De Gregorio, D. (2015). Vulnerability of exposed elements. In Italian: Vulnerabilità dei beni esposti. In: Urciuoli Gianfranco. (a cura di): Urciuoli Gianfranco, Gestione e mitigazione dei rischi naturali. p. 15-27, NAPOLI:Doppiavoce, ISBN: 978-88-89972-58-8.

Zuccaro, G., Dato, F., Cacace, F., De Gregorio, D., Sessa, S. (2017). Seismic Collapse Mechanisms Analyses And Masonry Structures Typologies A Possible Correlation. Ingegneria Sismica N4, Dicembre, 2017.

## **RINGRAZIAMENTI**

Desidero ricordare tutti coloro che mi hanno supportato durante la stesura della tesi, a loro va la mia gratitudine.

Ringrazio il Prof. Zuccaro per i suoi preziosi insegnamenti e per le opportunità di studio e di crescita che mi ha fornito durante questi anni di dottorato.

Ringrazio i collaboratori tutti del PLINIVS per avermi accompagnato in questo percorso e soprattutto ringrazio il Prof. Cacace e l'Ing. De Gregorio per il significativo supporto che mi hanno dato, indispensabile per il completamento della ricerca.

Ringrazio soprattutto mio marito Enzo per l'amore, la fiducia e la forza che mi ha dato in questi anni e mio figlio Giuseppe che inconsapevolmente ha partecipato alla stesura di questa tesi, addolcendo i lunghi periodi di studio. A loro è dedicato questo lavoro.

Ringrazio con affetto: mio padre, per avermi insegnato l'amore per lo studio e per essermi stato vicino in tutte le mie scelte, lasciando sempre per me un porto sicuro in cui ancorarsi in caso di tempesta; mia sorella, per aver gioito con me nei momenti felici e per avermi ascoltata nei momenti di difficoltà, dandomi consigli sinceri.

Ringrazio tutta la famiglia D'Abronzio-Toscano, mia famiglia acquisita, per l'aiuto, l'affetto e il sostegno che mi hanno dato in questi anni di importanti cambiamenti e soprattutto ringrazio Raffaella per aver creduto in me e per avermi fatto coraggio nei momenti più difficili.

Ringrazio infine le mie amiche e mia cugina, per avermi supportato e sopportato in questo percorso, mostrandomi che l'amicizia e l'affetto vanno oltre la distanza.

